Proceedings of 44th Sapporo Symposium on Partial Differential Equations

Edited by
S.-I. Ei, Y. Giga, N. Hamamuki, S. Jimbo, H. Kubo, H. Kuroda,
T. Ozawa, T. Sakajo, and K. Tsutaya

Series #177, 2019

HOKKAIDO UNIVERSITY
TECHNICAL REPORT SERIES IN MATHEMATICS

#158 Y. Giga, S. Jimbo, H. Terao, K. Yamaguchi, Proceedings of the 6th Pacific RIM Conference on Mathematics 2013, 154 pages. 2013.

#159 Y. Giga, S. Jimbo, T. Ozawa, K. Tsutaya, Y. Tonegawa, H. Kubo, T. Sakajo, and H. Takaoka, Proceedings of the 38th Sapporo Symposium on Partial Differential Equations, 76 pages. 2013.

#160 M. Kuroda, Y. Goto, K.Sasaki, S. Futakuchi, D. Funakawa, T. Yamashita, and K. Wada, 第 10 回数学総合若手研究集会, 335 pages. 2014.

#161 S. Ei, Y. Giga, S. Jimbo, H. Kubo, T. Ozawa, T. Sakajo, H. Takaoka, Y. Tonegawa, and K. Tsutaya, Proceedings of the 39th Sapporo Symposium on Partial Differential Equations, 147 pages. 2014.

#162 D. Funakawa, T. Kagaya, Y. Kabata, K. Sasaki, H. Takeda, Y. Chino, A. Tsuchida, T. Yamashita, and K. Wada, 第 11 回数学総合若手研究集会, 359 pages. 2015.

#163 S. Jimbo, S. Goto, Y. Kohsaka, H. Kubo, Y. Maekawa, and M. Ohnuma, Mathematics for Nonlinear Phenomena: Analysis and Computation - International Conference in honor of Professor Yoshikazu Giga on his 60th birthday- , 47 pages. 2015.

#164 S. Ei, Y. Giga, S. Jimbo, H. Kubo, T. Ozawa, T. Sakajo, H. Takaoka, Y. Tonegawa and K. Tsutaya, Proceedings of the 40th Sapporo Symposium on Partial Differential Equations, 122 pages. 2015.

#165 A. Tsuchida, Y. Aikawa, K. Asahara, M. Abe, Y. Kabata, H. Saito, F. Nakamura and S. Honda, 第 12 回数学総合若手研究集会, 373 pages. 2016.

#166 S.-I. Ei, Y. Giga, S. Jimbo, H. Kubo, T. Ozawa, T. Sakajo, H. Takaoka, Y. Tonegawa and K. Tsutaya, Proceedings of the 41st Sapporo Symposium on Partial Differential Equations, 110 pages. 2016.

#167 Kubo, Hideo and Ozawa, Tohru and Takamura, Hiroyuki, Mathematical Analysis for Stability in Nonlinear Dynamics - in honor of Professor Vladimir Georgiev on his 60th birthday -, 79 pages. 2016.

#168 F. Nakamura, Y. Aikawa, K. Asahara, M. Abe, D. Komori, H. Saito, S. Handa, K. Fujisawa, S. Honda, A. Rodrguez Mulet, 第 13 回数学総合若手研究集会, 501 pages. 2017.

#169 N. Tanaka (K. Kiyohara, T. Morimoto, K. Yamaguchi, Eds.), Geometric Theory of Systems of Ordinary Differential Equations I, 177 pages. 2017.

#170 N. Tanaka (K. Kiyohara, T. Morimoto, K. Yamaguchi, Eds.), Geometric Theory of Systems of Ordinary Differential Equations II, 519 pages. 2017.

#171 S.-I. Ei, Y. Giga, N. Hamamuki, S. Jimbo, H. Kubo, T. Ozawa, T. Sakajo, Y. Tonegawa, and K. Tsutaya, Proceedings of the 42nd Sapporo Symposium on Partial Differential Equations - In memory of Professor Taira Shirota - , 102 pages. 2017.

#172 Shigeru Kuroda, Takao Namiki, Akihiro Yamaguchi, Yutaka Yamaguchi, 複雑系数理の新展開：津田一郎教授退職記念研究集会報告集, 69 pages. 2018.

#173 S.Handa,D.Komori,K.Fujisawa,A.Rodriguez Mulet,M.Aoki,Y.kamijima,I.Fukuda,T.Yabu, 第 14 回数学総合若手研究集会, 580 pages. 2018.

#174 Yoshikazu Giga, Hideo Kubo, Tohru Ozawa, The 11th Mathematical Society of Japan - Seasonal Institute - The Role of Metrics in the Theory of Partial Differential Equations- , 160 pages. 2018.

#175 S.-I. Ei, Y. Giga, N. Hamamuki, S. Jimbo, H. Kubo, H. Kuroda, Proceedings of 43rd Sapporo Symposium on Partial Differential Equations, 99 pages. 2018.

#176 I.Fukuda, M.Aoki, Y.Ueda, Y.Kamijima, T.Yabu, T.Niimura, N.Satoh, H.Toyokawa, K.Matsuzaka, S.Yamagata, K.Yoshida 第 15 回数学総合若手研究集会, 657 pages. 2019.

Proceedings of 44th Sapporo Symposium on Partial Differential Equations

Edited by
S.-I. Ei, Y. Giga, N. Hamamuki, S. Jimbo, H. Kubo, H. Kuroda,
T. Ozawa, T. Sakajo, and K. Tsutaya

Sapporo, 2019

Partially supported by Core Research for Evolutional Science and Technology, Japan Science and Technology Agency

科学技術振興機構 戦略的創造研究 CREST （JTMJCR14D3）
日本学術振興会科学研究費補助金 （基盤研究 S 課題番号 26220702）
日本学術振興会科学研究費補助金 （基盤研究 B 課題番号 19H01795）

Preface

This volume is intended as the proceedings of Sapporo Symposium on Partial Differential Equations, held on August 5 through August 7 in 2019 at Faculty of Science, Hokkaido University.

Sapporo Symposium on PDE has been held annually to present the latest developments on PDE with a broad spectrum of interests not limited to the methods of a particular school. Late Professor Taira Shirota started the symposium more than 40 years ago. Professor Kôji Kubota and late Professor Rentaro Agemi made a large contribution to its organization for many years.

We always thank their significant contribution to the progress of the Sapporo Symposium on PDE.

S.-I. Ei (Hokkaido University)
Y. Giga (The University of Tokyo)
N. Hamamuki (Hokkaido University)
S. Jimbo (Hokkaido University)
H. Kubo (Hokkaido University)
H. Kuroda (Hokkaido University)
T. Ozawa (Waseda University)
T. Sakajo (Kyoto University)
K. Tsutaya (Hirosaki University)

Contents

The 44th Sapporo Symposium on Partial Differential Equations

第 44 回偏微分方程式論札幌シンポジウム

Period	August 5, 2019 – August 7, 2019
Venue	3-309, Faculty of Science Bld. No. 3, Hokkaido University
Organizers	Shin-Ichiro Ei, Nao Hamamuki
Program Committee	Shin-Ichiro Ei, Tohru Ozawa, Yoshikazu Giga, Hideo Kubo, Hirotoshi Kuroda, Takashi Sakajo, Shuichi Jimbo, Kimitoshi Tsutaya, Nao Hamamuki
URL	http://www.math.sci.hokudai.ac.jp/sympo/sapporo/program190805.html

Aug. 5, 2019 (Monday)

09:50-10:00 Opening

10:00-11:00 井口 達雄（慶應義塾大学）Tatsuo Iguchi (Keio University)
A mathematical analysis of the Isobe-Kakinuma model for water waves

11:00-11:30 *

11:30-12:30 Yaping Wu (Capital Normal University)
Existence and Stability of Traveling Waves and Steady States for SKT Competition model with Large Cross-diffusion

14:00-14:30 *

14:30-15:10 川上 竜樹（龍谷大学）Tatsuki Kawakami (Ryukoku University)
Critical exponent for the global existence of solutions to a semilinear heat equation with degenerate coefficients

15:10-15:40 *

15:40-16:10 Jan Brezina（Kyusyu University）
On the low stratification of the complete Euler system

16:10-16:40 梶原 直人（東京理科大学） Naoto Kajiwara (Tokyo University of Science)
Global solvability for the Cahn-Hilliard equations with dynamical boundary conditions

August 6, 2019 (Tuesday)

10:00-11:00 大塚 浩史（金沢大学） Hiroshi Ohtsuka（Kanazawa University）
On the linear response of equilibrium vortices

11:00-11:30 *

11:30-12:30 矢崎 成俊（明治大学） Shigetoshi Yazaki（Meiji University）
On an evolution equation of flame/smoldering combustion propagation of a paper sheet

14:00-14:30 *

14:30-15:10 松永 秀章（大阪府立大学） Hideaki Matsunaga（Osaka Prefecture University）
Asymptotic behavior of solutions of linear integral equations with two delays

15:10-15:40 *

15:40-16:20 上田 好寛（神戸大学） Yoshihiro Ueda（Kobe University）
Stability analysis for the system of linear differential equations

16:20-16:50 内免 大輔（室蘭工業大学）Daisuke Naimen (Muroran Institute of Technology)
Blow-up analysis for nodal radial solutions in Trudinger-Moser critical equations in $\mathbf{R}^2$

18:00-20:00 Reception Party

August 7, 2019 (Wednesday)

10:00-11:00 Yves van Gennip（Technische Universiteit Delft）
Graph Ginzburg-Landau: discrete dynamics, continuum limits, and applications

11:00-11:30 *

11:30-12:30 仙葉 隆（福岡大学）Takasi Senba (Fukuoka University)
Blowup of solutions to a system related to chemotaxis systems

12:30- Closing

(*: breaks/discussions)

A mathematical analysis of the Isobe–Kakinuma model for water waves

Tatsuo Iguchi

Department of Mathematics, Faculty of Science and Technology, Keio University

1 Basic equations for water waves

We consider the motion of a water filled in $(n+1)$-dimensional Euclidean space together with the motion of the water surface. The water wave problem is mathematically formulated as a free boundary problem for an irrotational flow of an inviscid and incompressible fluid under the gravitational field. Let t be the time, $x = (x_1, \dots, x_n)$ the horizontal spatial coordinates, z the vertical spatial coordinate, and $X = (x, z)$ the whole spatial variables. We assume that the water surface and the bottom are represented as $z = \eta(x,t)$ and $z = -h + b(x)$, respectively, where $\eta(x,t)$ is the surface elevation, h is the mean depth, and $b(x)$ represents the bottom topography. We denote by $\Omega(t)$, $\Gamma(t)$, and Σ the fluid region occupied by the water, water surface, and the bottom of the water at time t, respectively. Then, the motion of the water is described by the velocity potential $\Phi(X,t)$ satisfying Laplace's equation

$$\Delta_X \Phi = 0 \quad \text{in} \quad \Omega(t), \quad t > 0, \tag{1}$$

where Δ_X is the Laplacian with respect to X, that is, $\Delta_X = \Delta + \partial_z^2$ and $\Delta = \partial_{x_1}^2 + \cdots + \partial_{x_n}^2$. The boundary conditions on water surface are given by

$$\begin{cases} \partial_t \eta + \nabla\Phi \cdot \nabla\eta - \partial_z \Phi = 0 \quad \text{on} \quad \Gamma(t), \quad t > 0, \\ \partial_t \Phi + \dfrac{1}{2}|\nabla_X \Phi|^2 + g\eta = 0 \quad \text{on} \quad \Gamma(t), \quad t > 0, \end{cases} \tag{2}$$

where $\nabla = (\partial_{x_1}, \dots, \partial_{x_n})$ and $\nabla_X = (\partial_{x_1}, \dots, \partial_{x_n}, \partial_z)$ are the gradients with respect to x and to $X = (x, z)$, respectively, and g is the gravitational constant. The first equation is the kinematical condition and the second one is known as Bernoulli's law. The boundary condition on the bottom is given by

$$\nabla\Phi \cdot \nabla b - \partial_z \Phi = 0 \quad \text{on} \quad \Sigma, \quad t > 0, \tag{3}$$

which is the kinematical condition on the bottom Σ. These are the basic equations for water waves. Since η is a unknown function, the water wave problem is a free boundary problem. In fact, one of the principal subjects to the water wave problem is to clarify the behavior of the water surface, that is, the function η.

We put

$$\phi(x,t) = \Phi(x, \eta(x,t), t), \tag{4}$$

which is the trace of the velocity potential on the water surface. Then, the basic equations for the water waves (1)–(3) are transformed equivalently into

$$\begin{cases} \partial_t \eta - \Lambda(\eta, b)\phi = 0 & \text{for} \quad t > 0, \\ \partial_t \phi + g\eta + \dfrac{1}{2}|\nabla\phi|^2 - \dfrac{1}{2}\dfrac{\big(\Lambda(\eta,b)\phi + \nabla\eta\cdot\nabla\phi\big)^2}{1+|\nabla\eta|^2} = 0 & \text{for} \quad t > 0, \end{cases} \tag{5}$$

where $\Lambda(\eta, b)$ is the Dirichlet-to-Neumann map for Laplace's equation. More precisely, under appropriate assumptions on η and b, for any given function ψ the map $\Lambda(\eta, b)$ is defined by

$$\Lambda(\eta, b)\psi = (\partial_z \Psi - \nabla\eta \cdot \nabla\Psi)|_{z=\eta(x,t)},$$

where Ψ is the unique solution to the boundary value problem

$$\begin{cases} \Delta_X \Psi = 0 & \text{in} \quad -h + b(x) < z < \eta(x), \\ \Psi = \psi & \text{on} \quad z = \eta(x), \\ \nabla\Psi \cdot \nabla b - \partial_z \Psi = 0 & \text{on} \quad z = -h + b(x). \end{cases}$$

V. E. Zakharov [14] found that the water wave problem has a Hamiltonian structure and η and ϕ are the canonical variables. The Hamiltonian $\mathscr{H}$ is essentially the total energy, that is, $\mathscr{H} = \frac{1}{\rho}(E_{\text{kin}} + E_{\text{pot}})$, where ρ is a constant density of the water, E_{kin} is the kinetic energy

$$E_{\text{kin}} = \int_{\Omega(t)} \frac{1}{2}\rho |\nabla_X \Phi(X,t)|^2 \mathrm{d}X = \frac{1}{2}\rho \int_{\mathbf{R}^n} \phi(x,t)(\Lambda(\eta,b)\phi)(x,t)\mathrm{d}x,$$

and E_{pot} is the potential energy

$$E_{\text{pot}} = \frac{1}{2}\rho g \int_{\mathbf{R}^n} \eta(x,t)^2 \mathrm{d}x$$

due to the gravity. In fact, the water wave problem (5) is written in Hamilton's canonical form

$$\partial_t \eta = \frac{\delta \mathscr{H}}{\delta \phi}, \quad \partial_t \phi = -\frac{\delta \mathscr{H}}{\delta \eta}.$$

Therefore, nowadays (5) is called the Zakharov formulation or the Zakharov–Craig–Sulem formulation of the water wave problem.

As was shown by J. C. Luke [12], the water wave problem has also a variational structure. His Lagrangian density is of the form

$$\mathscr{L}(\Phi, \eta) = \int_{-h+b(x)}^{\eta(x,t)} \left(\partial_t \Phi(x,z,t) + \frac{1}{2}|\nabla_X \Phi(x,z,t)|^2 + gz \right) \mathrm{d}z \tag{6}$$

and the action function is given by

$$\mathscr{J}(\Phi, \eta) = \int_{t_0}^{t_1} \int_{\mathbf{R}^n} \mathscr{L}(\Phi, \eta) \mathrm{d}x \mathrm{d}t.$$

The first variation of this action function can be calculated as

$$\begin{aligned} \delta \mathscr{J}(\Phi, \eta) = &- \int_{t_0}^{t_1} \int_{\Omega(t)} (\Delta_X \Phi) \delta\Phi \, \mathrm{d}X \mathrm{d}t \\ &+ \int_{t_0}^{t_1} \int_{\mathbf{R}^n} \left(\partial_t \Phi + \frac{1}{2}|\nabla_X \Phi|^2 + g\eta \right)\Big|_{\Gamma(t)} \delta\eta \, \mathrm{d}x \mathrm{d}t \\ &- \int_{t_0}^{t_1} \int_{\mathbf{R}^n} \left(\partial_t \eta + \nabla\Phi \cdot \nabla\eta - \partial_z \Phi \right) \delta\Phi \big|_{\Gamma(t)} \, \mathrm{d}x \mathrm{d}t \\ &+ \int_{t_0}^{t_1} \int_{\mathbf{R}^n} (\nabla\Phi \cdot \nabla b - \partial_z \Phi) \delta\Phi \big|_{\Sigma} \, \mathrm{d}x \mathrm{d}t, \end{aligned}$$

so that the corresponding Euler–Lagrange equations are exactly the basic equations for water waves (1)–(3). We refer to J. W. Miles [13] for the relation between Zakharov's Hamiltonian and Luke's Lagrangian.

2 Isobe–Kakinuma model

M. Isobe [6, 7] and T. Kakinuma [8, 9, 10] approximated the velocity potential Φ in Luke's Lagrangian by

$$\Phi^{\mathrm{app}}(x,z,t)=\sum_{i=0}^{N}\Psi_i(z;b)\phi_i(x,t),$$

where $\{\Psi_i\}$ is an appropriate function system in the vertical coordinate z and may depend on the bottom topography b and $(\phi_0,\phi_1,\dots,\phi_N)$ are unknown variables, and derived an approximate Lagrangian density $\mathscr{L}^{\mathrm{app}}(\phi_0,\phi_1,\dots,\phi_N,\eta)=\mathscr{L}(\Phi^{\mathrm{app}},\eta)$. The Isobe–Kakinuma model is the corresponding Euler–Lagrange equation for the approximated Lagrangian. We have to choose the function system $\{\Psi_i\}$ carefully in order that the Isobe–Kakinuma model would be a good approximation for the water wave problem. One of the choices is obtained by the bases of a Taylor series of the velocity potential $\Phi(x,z,t)$ with respect to the vertical spatial coordinate z around the bottom. Such an expansion has been already used by J. Boussinesq [2] in the case of the flat bottom. From this point of view, one of the natural choices of the function system is given by

$$\Psi_i(z;b)=\begin{cases}(z+h)^{2i} & \text{in the case of the flat bottom,}\\ (z+h-b(x))^{i} & \text{in the case of the variable bottom.}\end{cases}$$

Here we note that the later choice is valid also for the case of the flat bottom. However, it turns out that the terms of odd degree do not play any important role in such a case so that the former choice economizes the computational resources in the numerical computations. In order to treat the both cases at the same time, we adopt the approximation

$$\Phi^{\mathrm{app}}(x,z,t)=\sum_{i=0}^{N}(z+h-b(x))^{p_i}\phi_i(x,t), \tag{7}$$

where $p_0,p_1,\dots,p_N$ are nonnegative integers satisfying $0=p_0<p_1<\cdots<p_N$. Then, the corresponding Isobe–Kakinuma model has the form

$$\begin{cases} H^{p_i}\partial_t\eta+\displaystyle\sum_{j=0}^{N}\left\{\nabla\cdot\left(\frac{1}{p_i+p_j+1}H^{p_i+p_j+1}\nabla\phi_j-\frac{p_j}{p_i+p_j}H^{p_i+p_j}\phi_j\nabla b\right)\right.\\ \qquad\left.+\,\frac{p_i}{p_i+p_j}H^{p_i+p_j}\nabla b\cdot\nabla\phi_j-\frac{p_ip_j}{p_i+p_j-1}H^{p_i+p_j-1}(1+|\nabla b|^2)\phi_j\right\}=0\\ \qquad\qquad\qquad\qquad\qquad\qquad\qquad\qquad\text{for}\quad i=0,1,\dots,N,\\ \displaystyle\sum_{j=0}^{N}H^{p_j}\partial_t\phi_j+g\eta+\frac{1}{2}\left\{\left|\sum_{j=0}^{N}(H^{p_j}\nabla\phi_j-p_jH^{p_j-1}\phi_j\nabla b)\right|^2+\left(\sum_{j=0}^{N}p_jH^{p_j-1}\phi_j\right)^2\right\}=0, \end{cases} \tag{8}$$

where $H(x,t)=h+\eta(x,t)-b(x)$ is the depth of the water. Here and in what follows we use the notational convention $0/0=0$. This system consists of $(N+1)$ evolution equations for η and only one evolution equation for $(N+1)$ unknowns $(\phi_0,\phi_1,\dots,\phi_N)$, so that this is an overdetermined and underdetermined composite system. However, the total number of the unknowns is equal to the total number of the equations.

3 Well-posedness

We consider the initial value problem to the Isobe–Kakinuma model (8) under the initial conditions

$$(\eta, \phi_0, \dots, \phi_N) = (\eta_{(0)}, \phi_{0(0)}, \dots, \phi_{N(0)}) \quad \text{at} \quad t = 0. \tag{9}$$

The Isobe–Kakinuma model (8) is written in the matrix form as

$$\begin{pmatrix} H^{p_0} & 0 & \cdots & 0 \\ \vdots & \vdots & & \vdots \\ H^{p_N} & 0 & \cdots & 0 \\ 0 & H^{p_0} & \cdots & H^{p_N} \end{pmatrix} \partial_t \begin{pmatrix} \eta \\ \phi_0 \\ \vdots \\ \phi_N \end{pmatrix} + \{\text{spatial derivatives}\} = \mathbf{0}.$$

Since the coefficient matrix always has the zero eigenvalue, the hypersurface $t = 0$ in the spacetime $\mathbf{R}^n \times \mathbf{R}$ is characteristic for the Isobe–Kakinuma model (8), so that the initial value problem to (8) is not solvable in general. In fact, if the problem has a solution $(\eta, \phi_0, \dots, \phi_N)$, then by eliminating the time derivative $\partial_t \eta$ from the equations we see that the solution has to satisfy the relation

$$\begin{aligned} & H^{p_i} \sum_{j=0}^{N} \nabla \cdot \left(\frac{1}{p_j + 1} H^{p_j+1} \nabla \phi_j - \frac{p_j}{p_j} H^{p_j} \phi_j \nabla b \right) \\ & = \sum_{j=0}^{N} \left\{ \nabla \cdot \left(\frac{1}{p_i + p_j + 1} H^{p_i+p_j+1} \nabla \phi_j - \frac{p_j}{p_i + p_j} H^{p_i+p_j} \phi_j \nabla b \right) \right. \\ & \qquad \left. + \frac{p_i}{p_i + p_j} H^{p_i+p_j} \nabla b \cdot \nabla \phi_j - \frac{p_i p_j}{p_i + p_j - 1} H^{p_i+p_j-1} (1 + |\nabla b|^2) \phi_j \right\} \end{aligned} \tag{10}$$

for $i = 1, \dots, N$. Therefore, as a necessary condition the initial date $(\eta_{(0)}, \phi_{0(0)}, \dots, \phi_{N(0)})$ and the bottom topography b have to satisfy the relation (10) for the existence of the solution.

It is well known that the well-posedness of the initial value problem to the water wave problem may be broken unless a generalized Rayleigh–Taylor sign condition $-\frac{\partial P}{\partial \boldsymbol{n}} \geq c_0 > 0$ on the water surface is satisfied, where P is the pressure and $\boldsymbol{n}$ is the unit outward normal on the water surface. This sign condition is equivalent to $-\partial_z P \geq c_0 > 0$ because the pressure P is equal to a constant atmospheric pressure P_{atm} on the water surface. By using Bernoulli's law

$$\partial_t \Phi + \frac{1}{2} |\nabla_X \Phi|^2 + \frac{1}{\rho} (P - P_{\text{atm}}) + gz \equiv 0,$$

the sign condition can be written in terms of the unknowns $(\eta, \phi_0, \dots, \phi_N)$ and b as $a(x, t) \geq c_0 > 0$, where

$$\begin{aligned} a = g & + \sum_{i=0}^{N} p_i H^{p_i-1} \partial_t \phi_i \\ & + \frac{1}{2} \sum_{i,j=0}^{N} \left\{ (p_i + p_j) H^{p_i+p_j-1} \nabla \phi_i \cdot \nabla \phi_j - 2p_i (p_i + p_j - 1) H^{p_i+p_j-2} \phi_i \nabla b \cdot \nabla \phi_j \right. \\ & \qquad \left. + p_i p_j (p_i + p_j - 2) H^{p_i+p_j-3} (1 + |\nabla b|^2) \phi_i \phi_j \right\}. \end{aligned} \tag{11}$$

In fact, we have $-\frac{1}{\rho}\partial_z P^{\rm app} = g + \partial_z\partial_t\Phi^{\rm app} + \nabla_X\partial_z\Phi^{\rm app}\cdot\nabla_X\Phi^{\rm app} = a$ on $z=\eta(x,t)$. Let $H^m = W^{m,2}(\mathbf{R}^n)$ be the L^2 Sobolev space of order m on $\mathbf{R}^n$ equipped with the norm $\|\cdot\|_m$. The following theorem guarantees the well-posedness locally in time of the initial value problem to the Isobe–Kakinuma model (8)–(9).

Theorem 1 ([11]) *Let g, h, c_0, M_0 be positive constants and m an integer such that $m > n/2+1$. There exists a time $T>0$ such that if the initial data $(\eta_{(0)}, \phi_{0(0)}, \dots, \phi_{N(0)})$ and the bottom topography b satisfy the relation* (10) *and*

$$\text{(12)}\qquad \begin{cases} \|\eta_{(0)}\|_m + \|\nabla\phi_{0(0)}\|_m + \|(\phi_{1(0)},\dots,\phi_{N(0)})\|_{m+1} + \|b\|_{W^{m+2,\infty}} \le M_0, \\ h+\eta_{(0)}(x) - b(x) \ge c_0, \quad a(x,0) \ge c_0 \qquad \textit{for} \quad x\in\mathbf{R}^n, \end{cases}$$

then the initial value problem (8)–(9) *has a unique solution $(\eta, \phi_0, \dots, \phi_N)$ satisfying*

$$\eta, \nabla\phi_0 \in C([0,T]; H^m), \quad \phi_1,\dots,\phi_N \in C([0,T]; H^{m+1}).$$

It is not so evident how we can prepare the initial data $(\eta_{(0)}, \phi_{0(0)}, \dots, \phi_{N(0)})$ to the Isobe–Kakinuma model so that they satisfy the relation (10). In order to clarify this point, we introduce a canonical variable ϕ to the Isobe–Kakinuma model (8) by

$$\text{(13)}\qquad \phi = \Phi^{\rm app}|_{z=\eta} = \sum_{i=0}^{N} H^{p_i}\phi_i,$$

which corresponds to Zakharov's canonical variable. In view of the Zakharov–Craig–Sulem formulation of the water wave problem (5), it is natural to specify the initial data to the canonical variables (η,ϕ). The following theorem implies that once the initial data to the canonical variables (η,ϕ) and the bottom topography b are given, the relations (10) and (13) determine uniquely the initial data $(\phi_{0(0)},\dots,\phi_{N(0)})$ to the variables of the Isobe–Kakinuma model.

Theorem 2 ([11]) *Let h, c_0, M_0 be positive constants and m an integer such that $m > n/2+1$. There exists a positive $C>0$ such that if (η,ϕ) and b are given such that*

$$\text{(14)}\qquad \begin{cases} \|\eta\|_m + \|b\|_{W^{m,\infty}} \le M_0, \quad \|\nabla\phi\|_{m-1} < \infty, \\ h+\eta(x)-b(x) \ge c_0 \qquad \textit{for} \quad x\in\mathbf{R}^n, \end{cases}$$

then the relations (10) *and* (13) *determine uniquely $(\phi_0,\dots,\phi_N)$, which satisfy*

$$\|\nabla\phi_0\|_{m-1} + \|(\phi_1,\dots,\phi_N)\|_m \le C\|\nabla\phi\|_{m-1}.$$

4 Hamiltonian structure

As in the case of the water wave problem, the Isobe–Kakinuma model (8) has a Hamiltonian structure. It is natural to expect that the Hamiltonian would be the total energy, which is given by

$$\begin{aligned} E^{\rm IK}(\eta,\boldsymbol{\phi}) &= \int_{\Omega(t)} \frac{1}{2}\rho|\nabla_X\Phi^{\rm app}(X,t)|^2 {\rm d}X + \frac{1}{2}\rho g\int_{\mathbf{R}^n}\eta(x,t)^2{\rm d}x \\ &= \frac{\rho}{2}\int_{\mathbf{R}^n}\Bigg\{\sum_{i,j=0}^{N}\Bigg(\frac{1}{p_i+p_j+1}H^{p_i+p_j+1}\nabla\phi_i\cdot\nabla\phi_j - \frac{2p_i}{p_i+p_j}H^{p_i+p_j}\phi_i\nabla b\cdot\nabla\phi_j \\ &\qquad + \frac{p_ip_j}{p_i+p_j-1}H^{p_i+p_j-1}(1+|\nabla b|^2)\phi_i\phi_j\Bigg) + g\eta^2\Bigg\}{\rm d}x \end{aligned}$$

for the Isobe–Kakinuma model, where $\boldsymbol{\phi} = (\phi_0, \phi_1, \dots, \phi_N)$. In fact, this energy function is a conserved quantity for any smooth solutions to the model (8). As in the case of the water wave problem, the canonical variables of the Isobe–Kakinuma model are the surface elevation η and the trace of the velocity potential on the water surface ϕ, which is given by (13) in terms of the variables of the Isobe–Kakinuma model $(\eta, \phi_0, \dots, \phi_N)$. Thanks of Theorem 2, for any fixed b and for any (η, ϕ) satisfying the conditions in (14), there exists a unique $\boldsymbol{\phi} = (\phi_0, \phi_1, \dots, \phi_N)$ satisfying (10) and (13), which will be denoted by $\boldsymbol{\phi}(\eta, \phi) = (\phi_0(\eta, \phi), \dots, \phi_N(\eta, \phi))$. Namely, the canonical variables η and ϕ determine uniquely the variables $(\phi_0, \phi_1, \dots, \phi_N)$ of the Isobe–Kakinuma model. Now, we put

$$\mathscr{H}^{\mathrm{IK}}(\eta, \phi) = \frac{1}{\rho} E^{\mathrm{IK}}(\eta, \boldsymbol{\phi}(\eta, \phi)), \tag{15}$$

which is essentially the total energy of the Isobe–Kakinuma model in terms of the canonical variables. The following theorem shows that the Isobe–Kakinuma model has a Hamiltonian structure.

Theorem 3 ([3]) *Under the conditions in* (14)*, the Isobe–Kakinuma model* (8) *is equivalent to Hamilton's canonical form*

$$\partial_t \eta = \frac{\delta \mathscr{H}^{\mathrm{IK}}}{\delta \phi}, \quad \partial_t \phi = -\frac{\delta \mathscr{H}^{\mathrm{IK}}}{\delta \eta}. \tag{16}$$

More precisely, for any smooth solution $(\eta, \phi_0, \dots, \phi_N)$ *to the Isobe–Kakinuma model* (8)*, if we define* ϕ *by* (13)*, then* (η, ϕ) *satisfy Hamilton's canonical form* (16)*. Conversely, for any smooth solution* (η, ϕ) *to Hamilton's canonical form* (16)*, if we define* $(\phi_0, \phi_1, \dots, \phi_N)$ *as a unique solution to* (10) *and* (13)*, then* $(\eta, \phi_0, \dots, \phi_N)$ *satisfy the Isobe–Kakinuma model* (8)*.*

In addition to the total energy, the Isobe–Kakinuma model (8) has another conserved quantity, that is, the mass given by

$$\text{Mass} = \int_{\mathbf{R}^n} \eta(x, t) \mathrm{d}x.$$

Moreover, in the case of the flat bottom, the momentum in the horizontal direction is also conserved and is given by

$$\begin{aligned} \text{Momentum} &= \int_{\Omega(t)} \rho \nabla \Phi^{\mathrm{app}}(X, t) \mathrm{d}X \\ &= \rho \int_{\mathbf{R}^n} \eta(x, t) \nabla \phi(x, t) \mathrm{d}x, \end{aligned}$$

where ϕ is the canonical variable given by (13).

5 Shallow water approximation

It turns out that the Isobe–Kakinuma model (8) is a higher order shallow water approximation to the water wave problem. To state this fact more precisely, we rewrite the equations in a nondimensional form and introduce a nondimensional parameter δ as a ratio of the mean depth h to the typical wavelength λ, that is, $\delta = h/\lambda$ which measures the shallowness of the water.

To begin with, we rewrite the Zakharov–Craig–Sulem formulation (5) of the water wave problem. We rescale the independent and the dependent variables by

$$x = \lambda\tilde{x}, \quad z = h\tilde{z}, \quad t = \frac{\lambda}{\sqrt{gh}}\tilde{t}, \quad \eta = h\tilde{\eta}, \quad b = h\tilde{b}, \quad \phi = \lambda\sqrt{gh}\tilde{\phi}. \tag{17}$$

Here we note that these rescaling of dependent variables are related to the strongly nonlinear regime of the wave. Plugging these into (5) and dropping the tilde sign in the notation we obtain the Zakharov–Craig–Sulem formulation in a nondimensional form

$$\begin{cases} \partial_t\eta - \Lambda(\eta, b, \delta)\phi = 0 & \text{for} \quad t > 0, \\ \partial_t\phi + \eta + \dfrac{1}{2}|\nabla\phi|^2 - \dfrac{1}{2}\delta^2\dfrac{\big(\Lambda(\eta, b, \delta)\phi + \nabla\eta\cdot\nabla\phi\big)^2}{1 + \delta^2|\nabla\eta|^2} = 0 & \text{for} \quad t > 0, \end{cases} \tag{18}$$

where $\Lambda(\eta, b, \delta)$ is the Dirichlet-to-Neumann map for a scaled Laplace's equation. More precisely, under appropriate assumptions on η and b, for any given function ψ the map $\Lambda(\eta, b, \delta)$ is defined by

$$\Lambda(\eta, b, \delta)\psi = (\delta^{-2}\partial_z\Psi - \nabla\eta\cdot\nabla\Psi)|_{z=\eta(x,t)},$$

where Ψ is the unique solution to the boundary value problem

$$\begin{cases} \Delta\Psi + \delta^{-2}\partial_z^2\Psi = 0 & \text{in} \quad -1 + b(x) < z < \eta(x), \\ \Psi = \psi & \text{on} \quad z = \eta(x), \\ \nabla\Psi\cdot\nabla b - \delta^{-2}\partial_z\Psi = 0 & \text{on} \quad z = -1 + b(x). \end{cases}$$

We impose the initial conditions

$$(\eta, \phi) = (\eta_{(0)}, \phi_{(0)}) \quad \text{at} \quad t = 0. \tag{19}$$

The existence of the solution to the initial value problem (18)–(19) on some time interval idependent of small δ was guaranteed by T. Iguchi [4] and B. Alvarez-Samaniego and D. Lannes [1].

We proceed to rewrite the Isobe–Kakinuma model (8) in a nondimensional form. In the following, according to the bottom topography, we restrict the choice of the approximation (7) as

$$\Phi^{\mathrm{app}}(x, z, t) = \begin{cases} \displaystyle\sum_{i=0}^{N}(z + h)^{2i}\phi_i(x, t) & \text{in the case of the flat bottom,} \\ \displaystyle\sum_{i=0}^{2N}(z + h - b(x))^i\phi_i(x, t) & \text{in the case of the variable bottom.} \end{cases} \tag{20}$$

Even in the case of the flat bottom, we can adopt the later choice of the above approximation. However, the number of the unknowns becomes nearly twice although the order of the approximation does not augment. In addition to the rescaling (17) we rescale $(\phi_0, \phi_1, \ldots, \phi_N)$ the variables of the Isobe–Kakinuma model by

$$\phi_i = \frac{\lambda\sqrt{gh}}{\lambda^{p_i}}\tilde{\phi}_i$$

to obtain the model in a nondimensional form. Moreover, it is more convenient to rescale ϕ_i again by

$$\phi_i = \delta^{-p_i}\tilde{\phi}_i.$$

Then, the Isobe–Kakinuma model in the nondimensional form has the form

(21)
$$\begin{cases} H^{p_i}\partial_t\eta + \displaystyle\sum_{j=0}^{N^*}\left\{\nabla\cdot\left(\frac{1}{p_i+p_j+1}H^{p_i+p_j+1}\nabla\phi_j - \frac{p_j}{p_i+p_j}H^{p_i+p_j}\phi_j\nabla b\right)\right. \\ \qquad\qquad \left. + \dfrac{p_i}{p_i+p_j}H^{p_i+p_j}\nabla b\cdot\nabla\phi_j - \dfrac{p_ip_j}{p_i+p_j-1}H^{p_i+p_j-1}(\delta^{-2}+|\nabla b|^2)\phi_j\right\} = 0 \\ \qquad\qquad\qquad\qquad\qquad\qquad\qquad\qquad \text{for} \quad i=0,1,\dots,N^*, \\ \displaystyle\sum_{j=0}^{N^*}H^{p_j}\partial_t\phi_j + \eta + \frac{1}{2}\left\{\left|\sum_{j=0}^{N^*}(H^{p_j}\nabla\phi_j - p_jH^{p_j-1}\phi_j\nabla b)\right|^2 + \delta^{-2}\left(\sum_{j=0}^{N^*}p_jH^{p_j-1}\phi_j\right)^2\right\} = 0, \end{cases}$$

where $H = 1+\eta-b$ and

$$\begin{cases} p_i = 2i, \quad N^* = N & \text{in the case of the flat bottom,} \\ p_i = i, \quad N^* = 2N & \text{in the case of the variable bottom.} \end{cases}$$

As before, we impose the initial conditions

$$(\eta,\phi_0,\dots,\phi_{N^*}) = (\eta_{(0)},\phi_{0(0)},\dots,\phi_{N^*(0)}) \quad \text{at} \quad t=0. \tag{22}$$

Corresponding to (10), as a necessary condition for the existence of the solution to the initial value problem for the Isobe–Kakinuma model (21), the initial data have to satisfy the relations

$$\begin{aligned} &H^{p_i}\sum_{j=0}^{N^*}\nabla\cdot\left(\frac{1}{p_j+1}H^{p_j+1}\nabla\phi_j - \frac{p_j}{p_j}H^{p_j}\phi_j\nabla b\right) \\ &= \sum_{j=0}^{N^*}\left\{\nabla\cdot\left(\frac{1}{p_i+p_j+1}H^{p_i+p_j+1}\nabla\phi_j - \frac{p_j}{p_i+p_j}H^{p_i+p_j}\phi_j\nabla b\right)\right. \\ &\qquad \left. + \frac{p_i}{p_i+p_j}H^{p_i+p_j}\nabla b\cdot\nabla\phi_j - \frac{p_ip_j}{p_i+p_j-1}H^{p_i+p_j-1}(\delta^{-2}+|\nabla b|^2)\phi_j\right\} \end{aligned} \tag{23}$$

for $i=1,\dots,N^*$. Moreover, corresponding to (13), the canonical variable ϕ is given by

$$\phi = \sum_{i=0}^{N^*}H^{p_i}\phi_i. \tag{24}$$

The following theorem gives a rigorous justification of the Isobe–Kakinuma model as a higher order shallow water approximation.

Theorem 4 ([5]) *Let c_0, M_0 be positive constants and m an integer such that $m > n/2+1$. There exist a time $T>0$ and constants $C, \delta_0 > 0$ such that the following statement holds true: Suppose that $0<\delta\le\delta_0$ and that the initial data $(\eta_{(0)},\phi_{(0)})$ and the bottom topography b satisfy*

$$\begin{cases} \|\eta_{(0)}\|_{m+4N+8} + \|\nabla\phi_{(0)}\|_{m+4N+7} + \|b\|_{W^{m+4N+8,\infty}} \le M_0, \\ 1+\eta_{(0)}(x) - b(x) \ge c_0 \qquad \textit{for} \quad x\in\mathbf{R}^n. \end{cases} \tag{25}$$

Then, (23) *and* (24) *determine uniquely the initial data $(\phi_{0(0)},\dots,\phi_{N^*(0)})$ to the Isobe–Kakinuma model and that there exist unique solutions $(\eta^{\mathrm{WW}},\phi^{\mathrm{WW}})$ and $(\eta^{\mathrm{IK}},\phi_0,\dots,\phi_{N^*})$ to the initial*

value problems for the water wave problem (18)–(19) *and the Isobe–Kakinuma model* (21)–(22)*, respectively, on the time interval* $[0,T]$*. Moreover, defining the canonical variable* ϕ^{IK} *of the Isobe–Kakinuma model by* (24) *we have an error bound*

$$\|\eta^{\mathrm{WW}}(t)-\eta^{\mathrm{IK}}(t)\|_{m+2}+\|\phi^{\mathrm{WW}}(t)-\phi^{\mathrm{IK}}(t)\|_{m+2}\le C\delta^{4N+2} \tag{26}$$

for $0\le t\le T$ *and* $0<\delta\le\delta_0$*.*

There are huge literatures devoted to modelization for the water wave problem and many approximate models were proposed and analyzed, especially, in weekly nonlinear regimes. Even in the strongly nonlinear regime, there are several model equations. Among them, the most famous model is the shallow water equations, which are also called Saint-Venant equations. The equations in the Zakharov–Craig–Sulem formulation of the water wave problem (18) can be expanded with respect to δ^2 and the shallow water equations are derived in the limit $\delta\to+0$, so that the shallow water equations are the approximation of the water wave problem with an error $O(\delta^2)$. This approximation of the equations leads to the approximation of the solution in the same order of the error as

$$|\eta^{\mathrm{WW}}(x,t)-\eta^{\mathrm{SW}}(x,t)|\lesssim\delta^2$$

for $0\le t\le T$ and $0<\delta\le\delta_0$, where η^{SW} is the solution to the shallow water equations. The other famous model in the strongly nonlinear regime is the Green–Naghdi equations, which are derived by introducing the vertically averaged horizontal velocity field and by retaining the terms of order δ^2 in the expansion of the equations. Therefore, the Green–Naghdi equations are the approximation of the water wave problem with an error $O(\delta^4)$. This approximation of the equations leads again to the approximation of the solution in the same order of the error as

$$|\eta^{\mathrm{WW}}(x,t)-\eta^{\mathrm{GN}}(x,t)|\lesssim\delta^4$$

for $0\le t\le T$ and $0<\delta\le\delta_0$, where η^{GN} is a solution to the Green–Naghdi equations.

On the other hand, the above error estimate (26) implies

$$|\eta^{\mathrm{WW}}(x,t)-\eta^{\mathrm{IK}}(x,t)|\lesssim\delta^{4N+2}$$

for $0\le t\le T$ and $0<\delta\le\delta_0$. Therefore, the Isobe–Kakinuma model is a much more precise approximate model than the well-known models in strongly nonlinear shallow water regime.

References

[1] B. Alvarez-Samaniego and D. Lannes, Large time existence for 3D water-waves and asymptotics, Invent. Math., **171** (2008), 485–541.

[2] J. Boussinesq, Théorie des ondes et des remous qui se propagent le long d'un canal rectangulaire horizontal, en communiquant au liquide contenu dans ce canal des vitesses sensiblement pareilles de la surface au fond, J. Math. Pure. Appl., **17** (1872), 55–108.

[3] V. Duchêne and T. Iguchi, A Hamiltonian structure of the Isobe–Kakinuma model for water waves, in preparation.

[4] T. Iguchi, A shallow water approximation for water waves, J. Math. Kyoto Univ., **49** (2009), 13–55.

[5] T. Iguchi, A mathematical justification of the Isobe–Kakinuma model for water waves with and without bottom topography, J. Math. Fluid Mech., **20** (2018), 1985–2018.

[6] M. Isobe, A proposal on a nonlinear gentle slope wave equation, Proceedings of Coastal Engineering, Japan Society of Civil Engineers, **41** (1994), 1–5 [Japanese].

[7] M. Isobe, Time-dependent mild-slope equations for random waves, Proceedings of 24th International Conference on Coastal Engineering, ASCE, 285–299, 1994.

[8] T. Kakinuma, 非線形緩勾配方程式の内部波への拡張, Proceedings of Coastal Engineering, Japan Society of Civil Engineers, **47** (2000), 1–5 [Japanese].

[9] T. Kakinuma, A set of fully nonlinear equations for surface and internal gravity waves, Coastal Engineering V: Computer Modelling of Seas and Coastal Regions, 225–234, WIT Press, 2001.

[10] T. Kakinuma, A nonlinear numerical model for surface and internal waves shoaling on a permeable beach, Coastal engineering VI: Computer Modelling and Experimental Measurements of Seas and Coastal Regions, 227–236, WIT Press, 2003.

[11] R. Nemoto and T. Iguchi, Solvability of the initial value problem to the Isobe–Kakinuma model for water waves, J. Math. Fluid Mech., **20** (2018), 631–653.

[12] J. C. Luke, A variational principle for a fluid with a free surface, J. Fluid Mech., **27** (1967), 395–397.

[13] J. W. Miles, On Hamilton's principle for surface waves, J. Fluid Mech., **83** (1977), 153–158.

[14] V. E. Zakharov, Stability of periodic waves of finite amplitude on the surface of a deep fluid, J. Appl. Mech. Tech. Phys., **9** (1968), 190–194.

Existence and Stability of Traveling Waves and Steady States for SKT Competition Model with Large Cross-diffusion

Yaping Wu
School of Mathematical Sciences, Capital Normal University,
Beijing 100048, China

1 Introduction

In this talk we focus on the following quasilinear reaction diffusion model with cross-diffusion, which was first proposed by Shigesada-Kawasaki-Teramoto [11] to describe the segregation of two competing species under the intra- and the inter specific population pressure,

$$\begin{cases} u_t = \Delta[(d_1 + \rho_{11}u + \rho_{12}v)u] + u(a_1 - b_1u - c_1v), & x \in \Omega, t > 0, \\ v_t = \Delta[(d_2 + \rho_{21}u + \rho_{22}v)v] + v(a_2 - b_2u - c_2v), & x \in \Omega, t > 0. \end{cases} \tag{1.1}$$

Here $u(x,t)$ and $v(x,t)$ represent the densities of two competing species at location x and time t. We always assume d_i, a_i, b_i, c_i are positive constants. The coefficients ρ_{11} and ρ_{22} denote the self-diffusion rates which represent intra-specific population pressures, ρ_{12} and ρ_{21} denote the cross diffusion coefficients which measure the population pressure from the competing species.

In the following if ρ_{12} or ρ_{21} is positive, the model (1.1) will be simply called the SKT competition model with cross diffusion, and in the following we denote $A = \dfrac{a_1}{a_2}, B = \dfrac{b_1}{b_2}$ and $C = \dfrac{c_1}{c_2}$.

From the macroscopic point of view for math modelling, according to Fick's law, the nonlinear diffusion term $\triangle S(u,v)$ with $S(u,v) = u(d_1 + \rho_{11}u + \rho_{12}v)$ means that the species u moves from the higher density of $S(u,v)$ to the lower density of $S(u,v)$, due to the intra-species population pressure ($\rho_{11} > 0$) and inter-species population pressure ($\rho_{12} > 0$). From microscopic point of view for math modelling, the selection of the transition probability for the individuals of a species also determines the form of the diffusion of the species.
In one dim-space, the corresponding microscopic scale model of two species (continuous in time and spatially discrete model) can be written as

$$\begin{cases} \frac{du_i}{dt} = \tau_{i-1}^{+}u_{i-1} + \tau_{i+1}^{-}u_{i+1} - (\tau_i^{+} + \tau_i^{-})u_i + f(u_i, v_i), \\ \frac{dv_i}{dt} = s_{i-1}^{+}v_{i-1} + s_{i+1}^{-}v_{i+1} - (s_i^{+} + s_i^{-})v_i + g(u_i, v_i), \end{cases} \tag{1.2}$$

here τ_i^+ (τ_i^-) is called the transition probability for the individuals of the species u per unit time for one-step jump moving from x_i to the neighboring site x_{i+1} (x_{i-1}). The SKT types of nonlinear diffusion terms are derived from the microscopic model (1.2) by choosing $\tau_i^+ = \tau_i^- = \tau(u_i, v_i) = (d_1 + \rho_{11}u_i + \rho_{12}v_i)/h^2$, $s_i^+ = s_i^- = (d_2 + \rho_{22}v_i + \rho_{21}u_i)/h^2$, which imply that the transition probability at (t, x_i) for the individuals of the species u and v depend only on the desire of the individual to leave the point $x = x_i$, and the repelling force is proportional to the value of $d_1 + \rho_{11}u + \rho_{12}v$ at the point $x = x_i$.

Choosing other types of transition probability for a species (or strategy of dispersal of a species) induces different forms of diffusion terms or dispersal, e.g. if $\tau_{i-1}^+ = [d + \gamma(v_i - v_{i-1})/2]/h^2$, $\tau_{i+1}^- = [d + \gamma(v_i - v_{i+1})/2]/h^2$ when the species u can detect the difference of density of another species v before moving and $s_i^{\pm} = \alpha/h^2$ (species v move randomly), then the macroscopic PDE model of u and v becomes the typical Keller-Segel chemotactic model with diffusion:

$$\begin{cases} u_t = d\triangle u - \gamma\nabla\cdot(u\nabla v)] + f(u,v), \\ v_t = \alpha\triangle v + g(u,v),\ \alpha > 0, \end{cases}$$

where $-\gamma\nabla\cdot(u\nabla v)$ is called the chemotactic term, which is another type of cross diffusion term, and γ is called chemotactic sensitivity.

If $\rho_{ij} = 0$ and $d_i > 0$ for $i, j = 1, 2$, (without self diffusion and cross diffusion), the SKT competition model (1.1) becomes the typical Lotka-Volterra competition model with random diffusion

$$\begin{cases} u_t = d_1\Delta u + u(a_1 - b_1u - c_1v), & x \in \Omega, t > 0, \\ v_t = d_2\Delta v + v(a_2 - b_2u - c_2v), & x \in \Omega, t > 0. \end{cases} \tag{1.3}$$

For the Lotka-Voltera competition model (1.3) with the random diffusion, based on comparison method there are a lot of works on the existence and stability of planar wave solution $(U(x-ct), V(x-ct))$ connecting two equilibrium points. For the Lotka-Voltera competition model (1.3) under zero Neumann boundary condition, it is also well known that based on comparison method for any fixed $d_1 > 0$, $d_2 > 0$ and any nonnegative initial data, there exists unique globally uniformly bounded solution and the asymptotic behaviour of solutions is nearly the same (except the case $B < A < C$) as that for Lotka-Voltera ODE systems (tending to some constant steady state eventually). While for the case $B < A < C$, it is also well known that if Ω is convex the system (1.3) has no stable non-constant positive steady state.

If ρ_{12} or $\rho_{21} > 0$, the SKT competition model with cross diffusion is a strongly coupled quasi-linear parabolic system, in the past three decades the SKT types of cross diffusion models (with a special type of negative taxis $\triangle(uv)$) and various types of chemotactic PDE models (with positive taxis $-\nabla\cdot(u\psi(v)\nabla v)$) have attracted tremendous attention of both mathematicians and ecologists, especially for the SKT competition model and some typical Keller-Segel chemotactic model, the global existence of solution in time, the existence and the stability of nontrivial steady states or traveling waves as well as the asymptotic behavior of solution have been widely and deeply investigated by many mathematicians, some interesting theoretical or numerical work also indicates that the aggregation phenomena,

some special wave phenomena, new pattern formation and finite time blow-up phenomena are induced by nonlinear cross diffusion.

In the following we shall just focus on the theoretical analysis on some several types of traveling waves and steady states of SKT competition model with cross diffusion.

2 The existence and stability of travelling waves with transition layers for some SKT competition models with cross diffusion

2.1 The existence and stability of travelling waves with transition layers for the non-degenerate SKT competition models with cross diffusion

Consider the following simplified SKT competition model with cross diffusion in one-dimensional case

$$\begin{cases} u_t = d_1 u_{xx} + (a_1 - b_1 u - c_1 v)u, \\ v_t = [(1+\gamma_2 u)v]_{xx} + (a_2 - b_2 u - c_2 v)v, \end{cases} \quad x \in \mathbb{R},\ t > 0; \tag{2.4}$$

with $a_i, b_i, c_i > 0$ and $d_i > 0$, $i = 1, 2$.

For the SKT model (2.4) without cross diffusion (i.e. $\gamma_2 = 0$), there are a lot of research works on the existence of travelling fronts. For each fixed $d_1 > 0$ and $B < A < C$ (strong competition), by applying the comparison method and spectral analysis, Y. Kan-on etc. (see[2] and the references therein) proved the existence and stability of travelling waves with a unique speed connecting $(0, a_2/c_2)$ and $(a_1/b_1, 0)$. For the cases $\max\{B, C\} < A$ and small enough $d_1 = \epsilon^2 > 0$, by applying the analytic singular perturbation method, Y. Hosono [1] proved the existence of traveling waves with transition layers $(U(x - c\epsilon t), V(x - c\epsilon t))$ connecting $(0, a_2/c_2)$ and $(a_1/b_1, 0)$ for any $c > c_*$.

For the strong competition case $B < A < C$, by applying the geometric singular perturbation method, Yaping Wu and Ye Zhao [16] proved that if the cross diffusion rate $\gamma_2 \geq \gamma_0 > 0$, then for small $d_1 = \epsilon^2 > 0$, there exists a family of travelling waves connecting $(0, a_2/c_2)$ and $(a_2/b_2, 0)$ with locally unique slow speed $c = \epsilon c_\epsilon$ and both components of the waves have transition layers.

Further by applying the Evan's function method and topological index method (estimates on the first Chern number) and the detailed spectral analysis, Yaping Wu and Y. Zhao [16] proved that the travelling waves with transition layers and with slow speed are locally asymptotically stable if $d_1 = \epsilon^2$ is sufficiently small.

Remark 2.1. For $B < A < C$ case and small $\gamma_2 \geq 0$ there are no results on the existence of waves with transition layers for small enough d_1, however for the case $\gamma_2 = 0$ it is known that (see [2]) for any $d_1 > 0$ there exist stable wave front connecting $(0, a_2/c_2)$

and $(a_1/b_1, 0)$. It is naturally guessed that for small $\gamma_2 \geq 0$ and small enough $d_1 > 0$ there still exist traveling waves with transition layers connecting $(0, a_2/c_2)$ and $(a_1/b_1, 0)$, but the detailed structure of the fast-slow structure of the wave may be different from the case when $\gamma_2 \geq \gamma_0 > 0$.

2.2 Existence of traveling waves with transition layers for the degenerate SKT system with cross diffusion

Consider the degenerate SKT competition models,

$$\begin{cases} u_t = \epsilon^2 (u^2)_{xx} + (a_1 - b_1 u - c_1 v)u, \\ v_t = [(1 + \gamma_2 u)v]_{xx} + (a_2 - b_2 u - c_2 v)v, \end{cases} \quad x \in \mathbb{R},\ t > 0. \tag{2.5}$$

For the strong competition case $B < A < C$, by applying the analytic singular perturbation method and the center manifold theorem, Yanxia Wu and Yaping Wu [13] proved that if γ_2 is large enough but $\epsilon > 0$ is small enough, then system (2.5) has a family of travelling wave solutions $(U^\epsilon(x - \epsilon c_\epsilon t), V^\epsilon(x - \epsilon c_\epsilon t))$ with transition layers connecting $(0, a_2/c_2)$ and $(a_1/b_1, 0)$, and $\lim\limits_{\epsilon \downarrow 0} c_\epsilon = c^*$, where the waves $(U^\epsilon(z), V^\epsilon(z))$ are smooth waves which decay exponentially at $\pm\infty$ for the case $c^* > 0$; while for the case $c^* < 0$ the waves $(U^\epsilon(z), V^\epsilon(z))$ are weak waves satisfying

$$U^\epsilon(z) \equiv 0, \ \text{ for } z \in (-\infty, -\epsilon l(\epsilon)]; \ \ U^\epsilon(z) > 0, \ \text{for } z > -\epsilon l(\epsilon).$$

and $l(\epsilon) \to l^*$ as $\epsilon \downarrow 0$.

Remark 2.2: Different from non-degenerate systems, for the degenerate SKT competition system without cross diffusion, it seems that there are no results on the existence of travelling waves, which also implies that for the degenerate systems the appearance of cross diffusion may induce new wave phenomena, however the stability of the waves for the degenerate model is still an open problem.

3 Existence and Stability of Nontrivial Positive Steady States for the SKT model with large cross diffusion

In this section we shall be more interested in the existence and stability of nontrivial positive steady states for a simplified SKT competition model with cross diffusion under the zero Neumann boundary condition

$$\begin{cases} u_t = \triangle[(d_1 + \rho_{12} v)u] + u(a_1 - b_1 u - c_1 v), & x \in \Omega, t > 0, \\ v_t = \triangle[(d_2 + \rho_{21} u)v] + v(a_2 - b_2 u - c_2 v), & x \in \Omega, t > 0 \\ \frac{\partial u}{\partial n} = \frac{\partial v}{\partial n} = 0, & x \in \partial\Omega, t > 0. \end{cases} \tag{3.6}$$

The first important theoretical work on the existence of nontrivial steady states for SKT model is due to M.Mimura,Y.Nishiura, A.Tesei,& A.Tsujikawa [9], in which it was shown that in some strong competition case $B < C$ if d_1 is large enough and and $\frac{\rho_{12}}{d_1} \geq 1$ but d_2 is small, (3.6) admits several types of positive steady states with interior or boundary transition layers; the stability/instability of such steady states was investigated by Y. Kanon [2] by applying SLEP method.

The existence and nonexistence of nontrivial positive steady states for SKT model (3.6) with cross diffusion were widely investigated by Y. Lou, W-M. Ni [5] [6]. In [6] the authors also proposed three types of limiting stationary problem of (3.6) to classify all the possible steady states as one of cross diffusion, say ρ_{12}, tends to infinity. By investigating the existence of steady states for some limiting systems in one dimensional case, Lou and Ni [6] also did some pioneering work on the existence of several types of spiky steady states for some related limiting systems and the original SKT cross diffusion system (3.6) when ρ_{12}/d_1 is large enough but d_2 is small.

For convenience of our later use, we shall restate the related results in [6] for the stationary SKT competition model of (3.6) as follows.

Consider the stationary SKT competition model of (3.6)

$$\begin{cases} \triangle[(d_1 + \rho_{12}v)u] + u(a_1 - b_1u - c_1v) = 0, & x \in \Omega, \\ \triangle[(d_2 + \rho_{21}u)v] + v(a_2 - b_2u - c_2v) = 0, & x \in \Omega, \\ \frac{\partial u}{\partial n} = \frac{\partial v}{\partial n} = 0, & x \in \partial\Omega. \end{cases} \tag{3.7}$$

Theorem. (see [6]) (**limiting behavior of positive steady states and three possible limiting systems of** (3.7) **as** $\rho_{12} \to \infty$)
Suppose that $N \leq 3$, $A \neq B$, $A \neq C$ and $\frac{a_2}{d_2}$ is not equal to any eigenvalue of $-\Delta$ with homogeneous Neumann boundary condition on $\partial\Omega$. Let $(u_i(x), v_i(x))$ be a sequence of positive nontrivial stationary solutions of (3.7) with $(d_1,\ \rho_{12}) = (d_{1,i}, \rho_{12,i})$ for the fixed $d_2 > 0$ and $\rho_{21} \geq 0$ then the following conclusions hold.

(1) If $\rho_{12,\,i}/d_{1,\,i} \to \infty$ and $d_{1,\,i} \to d_1 \in (0,\ \infty)$ as $i \to +\infty$, then by passing to a subsequence if necessary, the sequence of $\{(u_i(x), v_i(x))\}$ must satisfy either (i) or (ii) below;

(2) If $\rho_{12,\,i}/d_{1,\,i} \to \infty$ and $d_{1,\,i} \to \infty$ as $i \to +\infty$, then by passing to a subsequence if necessary, the sequence $\{(u_i(x), v_i(x))\}$ must satisfy either (i) or (iii) below, where

(i) $(u_i(x),\ v_i(x))$ converges uniformly to positive $(\frac{\xi}{\psi(x)}, \psi(x))$ as $i \to +\infty$, where ξ is a positive constant and $(\xi, \psi(x))$ satisfies

$$(I) \begin{cases} \displaystyle\int_\Omega \frac{1}{\psi}(a_1 - \frac{b_1\xi}{\psi} - c_1\psi) = 0, \\ d_2\Delta\psi + \psi(a_2 - c_2\psi) - b_2\xi = 0, \quad x \in \Omega, \\ \displaystyle\frac{\partial\psi}{\partial\nu} = 0, \ \ x \in \partial\Omega. \end{cases} \tag{3.8}$$

(ii) If $\|v_i(x)\|_{L_\infty(\Omega)} \to 0$ as $i \to +\infty$, then $(u_i(x),\ \rho_{12,i}\, v_i(x)/d_{1,\,i})$ converges uniformly to positive $(u(x), w(x))$ as $i \to +\infty$, where $(u(x), w(x))$ is a positive solution of

$$(II)\begin{cases} d_1\Delta[(1+w)u] + u(a_1 - b_1 u) = 0, & x \in \Omega, \\ d_2\Delta[(d_2 + \rho_{21}u(x))w(x)] + w(a_2 - b_2 u) = 0, & x \in \Omega, \\ \frac{\partial u}{\partial \nu} = \frac{\partial w}{\partial \nu} = 0, & x \in \partial\Omega. \end{cases} \tag{3.9}$$

(iii) If $\|v_i(x)\|_{L_\infty(\Omega)} \to 0$ as $i \to +\infty$, then $(u_i(x),\ \rho_{12,i}\, v_i(x)/d_{1,\,i})$ converges uniformly to positive $(\frac{\tau}{1+w(x)}, w(x))$, where τ is a positive constant and $(\tau, w(x))$ satisfies

$$(III)\begin{cases} \displaystyle\int_\Omega \frac{a_1}{(1+w(x))}\mathrm{d}x - \int_\Omega \frac{b_1\tau}{(1+w(x))^2}\mathrm{d}x = 0, \\ d_2\triangle[(d_2 + \rho_{21}\dfrac{\tau}{1+w(x)})w(x)] + w\left(a_2 - \dfrac{b_2\tau}{1+w}\right) = 0,\ x \in \Omega, \\ \dfrac{\partial w}{\partial \nu} = 0,\ \ x \in \partial\Omega. \end{cases} \tag{3.10}$$

For small enough $d_2 > 0$, under some assumption on A, B and C, Y. Lou and W-M. Ni [6] proved the existence of two types of nontrivial steady states with boundary spike layer in 1-dim for the limiting systems (3.8) and (3.10) and for the original cross diffusion model with large ρ_{12}, these two types of spiky steady states were proved to be unstable in [14] and [12].

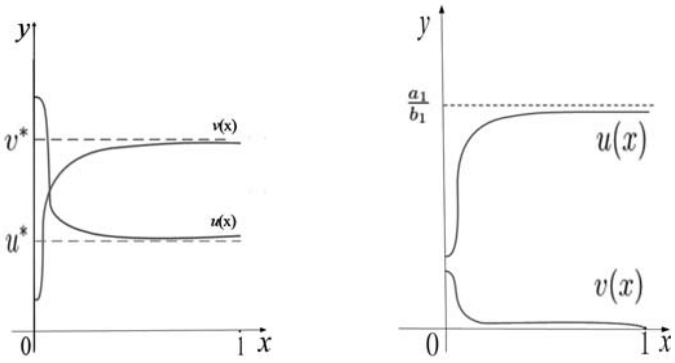

(a) (b)

Figure 1: (a): spiky steady state near (u^*, v^*) for small d_2, large enough ρ_{12} and ρ_{12}/d_1, (b) spiky steady state near $(a_1/b_1, 0)$ for $A > B$, when d_2 is small, d_1 and ρ_{12}/d_1 are large enough.

For 1-dim case e.g. $\Omega = (0,1)$, Y. Lou, W-M. Ni and S. Yostsutani [7] give a complete and nearly optimal results on the existence/nonexistence of monotone positive steady states $(v'(x) > 0)$ for the first limiting system (3.8) of SKT model as $\rho_{12}, \rho_{12}/d_1 \to \infty$; which can be briefly summarized as follows (see Figure 2):
If $d_2 \geqslant \frac{a_2}{\pi^2}$, then the limiting system (3.8) does not have any nonconstant solutions; while for $d_2 < \frac{a_2}{\pi^2}$, if $B < C$ and $A \in (0, B)$; or if $C < B$ and $A \in (0, \frac{B+3C}{4})$, then the limiting

system (3.8) has no non-trivial steady states; see also the part filled with slashes in Figure 2 in which the existence of positive monotone steady states are obtained.

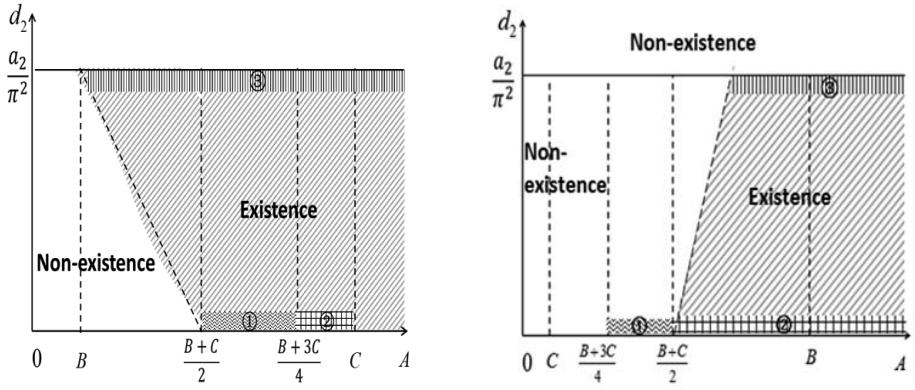

Figure 2: (a): $B < C$ i.e. strong competition; (b): $B > C$ i.e. weak competition.

It is also proved in [7] that for the cases:$(B + 3C)/4 < A$, if $B < C$ or $(B + C)/2 < A$, for $C < B$, (see region 2 in Figure 2) there exist a new type of positive spiky steady states $(\tau(d_2), V(x; d_2))$ for the first limiting system (3.8) when $d_2 > 0$ is small, which may correspond to large spiky steady states when ρ_{12} and ρ_{12}/d_1 are large enough and d_2 is small. Recently in [15] for any $A > \frac{B+3C}{4}$ by applying different approach we proved the existence and the detailed structure of the spiky steady states for the first limiting system (3.8) and existence of the corresponding large spiky steady states $(u(x), v(x))$(see Figure 3(a)) for the original SKT cross diffusion model with large enough ρ_{12} and small d_2.

In [7] it was proved that for any $A > B$ (see region 3 in Figure 2) the first limiting system (3.8) has a type of nontrivial positive steady states $(\xi_{d_2}, \psi_{d_2}(x))$ with a singular bifurcation structure when d_2 is near a_2/π^2, where $(\xi_{d_2}, \psi_{d_2}(x)) \to (0, 0)$ and $\xi_{d_2}/\psi_{d_2}(x) \to \frac{a_2}{b_2} \frac{1}{1-\sqrt{1-B/A}\cos(\pi x)}$ as $d_2 \to a_2/\pi^2$. The existence and stability of steady states $(u(x), v(x))$(see Figure 3(b)) perturbed from$(\xi_{d_2}/\psi_{d_2}(x), \psi_{d_2}(x))$ for the original SKT cross diffusion system were proved in [10]. Recently, similar existence and stability results for the shadow system (3.8) and the original SKT model in multidimensional case were proved in [8].

Focusing on the second limiting system (3.9) with the bounded d_1, fixed $d_2 \in (0, \frac{a_1 b_2}{b_1 \pi^2})$ and $\rho_{12} = 0$, recently K. Kuto [3] proved the existence of a local branch of positive steady states $(u(x, a_2), w(x, a_2))$ with bifurcating structure in multi-dimensional space when a_2 is near $a_1 b_2/b_2$; and proved the existence of a global branch of positive steady state $(u(x, a_2), w(x, a_2))$ in one dimensional case with $\Omega = (0, 1)$ for any $a_2 \in (d_2\pi^2, a_1 b_2/b_1)$, and the global branch of steady states in one dimensional space is proved to have special blowing up structure as $a_2 \to d_2\pi^2$, precisely speaking $w(x, a_2) \to +\infty$ but $u(x, a_2) \to \frac{a_2}{b_2} \frac{1}{1-\sqrt{1-B/A}\cos(\pi x)}$, as $a_2 \to d_2\pi^2$. Recently the local bifurcating steady states for the lim-

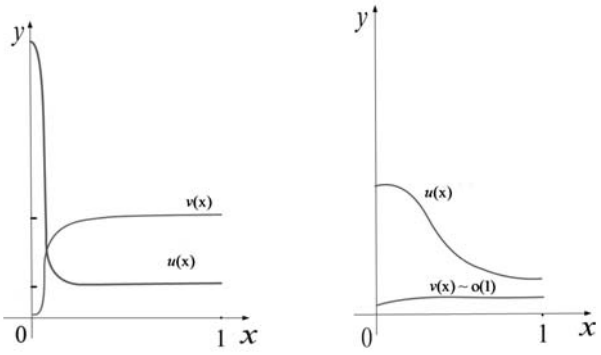

(a) (b)

Figure 3: (a): large spiky steady state for small d_2, large enough ρ_{12} and ρ_{12}/d_1, (b): positive steady state with singular bifurcation structure when d_2 is near a_2/π^2, ρ_{12} and ρ_{12}/d_1 are large enough.

iting system (3.9) were proved to be spectrally unstable in [4], in which it was also proved that there exists a local branch of the corresponding unstable positive steady states for the original SKT model when ρ_{12} is large enough for bounded fixed d_1.

In [3] it is remarked that in one dimensional case with $\Omega = (0,1)$ as $a_2 \to d_2\pi^2$ the w component of the nontrivial positive solution $(u(x),\ w(x))$ for the second limiting system (3.9) tends to infinity; while the u component tends to a bounded function, which is the same as the limit of $u-$ component of the another branch of steady states perturbed from the first limiting system (3.8) as $d_2 \to a_2/\pi^2$.

We shall also talk more details about our recent work on the existence and the stability analysis of the nontrivial positive steady states for the third limiting system (3.10) with bounded $\rho_{21} \geq 0$ and for the SKT cross diffusion system when both d_1 and ρ_{12}/d_1 are large enough, which includes the existence of a global branch of positive steady states to the third limiting system (3.10) in 1-dim $\Omega = (0,1)$ for $A > B$ and $0 < d_2 < a_2/\pi^2$ with bifurcation parameter d_2, bifurcating from infinity at $d_2 = a_2/\lambda_1$ and connecting the small spiky steady state as $d_2 \to 0^+$; and our work on the existence and instability of blowing up steady state to the limiting system (3.10) for d_2 near a_2/λ_1 in multi-dim case, as well as the existence and instability of the perturbed positive steady states for the original SKT model with large d_1 and large enough ρ_{12}/d_1.

Let $\lambda_1 > 0$ be the second eigenvalue (and assume it is simple, with eigenfunction denoted by $\phi_1(x)$) of

$$\begin{cases} -\Delta\varphi = \lambda\varphi, \ \ x \in \ \Omega, \\ \dfrac{\partial\phi}{\partial\nu} = 0, \ \ x \in \ \partial\Omega. \end{cases}$$

For $n = 1$ and $\Omega = (0,1)$, $\lambda_1 = \pi^2$ is simple.

Here we just state our recent work on the existence and instability of the large positive

steady states for the limiting system (3.10) with bounded $\rho_{21} \geq 0$ when $A > B$ and d_2 near a_2/λ_1 in multi-dim case, the method of proof is based on rescaling, higher order expansion, detailed spectral analysis and Lyapunov-Schmitz decomposition method.

Theorem 3.1 (Existence and blowing up structure of steady states for the limiting system) *Assume $A > B$, $\rho_{12} \geq 0$, $N \leq 4$ and λ_1 is simple, then for each fixed small $\epsilon = a_2/\lambda_1 - d_2 > 0$, the limiting system* (3.10) *has two non-constant positive solutions $(\tau_\epsilon^{\pm},\ w_\epsilon^{\pm}(x))$ satisfying*

$$\lim_{\epsilon \downarrow 0} \epsilon \tau_\epsilon^{\pm} = k_0 > 0,\ \lim_{\epsilon \downarrow 0} \epsilon w_\epsilon^{\pm}(x) = k_0 l(x),\ l(x) = \frac{b_2}{a_2}(1 + \mu_{\pm}\varphi_1(x)) > 0.$$

Theorem 3.2 (Spectral instability of large steady states of the limiting system) *Assume $A > B$, $\rho_{12} \geq 0$, $N \leqslant 4$ and λ_1 is simple. If $\epsilon = \frac{a_2}{\lambda_1} - d_2 > 0$ is small enough, then the large positive steady state $(\tau_\epsilon^{\pm},\ w_\epsilon^{\pm}(x))$ to the limiting system* (3.10) *are spectrally unstable, and the linearized operator has a positive eigenvalue $\sigma_\epsilon = \epsilon\lambda_1 + o(\epsilon)$.*

The talk is based on the joint work with Prof. Wei-Ming Ni, Dr. Ye Zhao, Dr. Qian Xu, Dr. Yanxia Wu, Dr. Qing Li and Zhibao Tang.

Acknowledgements

The work is supported by NNSF of China (11471221,11501031) and Beijing Municipal Education Commission (KZ201310028030).

References

[1] Y.Hosono, Traveling waves for a diffusive Lotka-Volterra competition model I-singular perturbation approach, *Discrete Contin. Dyn. Syst. Ser. B*, **3**: 79–95 (2003).

[2] Y. Kan-on and Q.Fang, Stability of monotone traveling waves for competition-diffusion equation, *Japan, J. Indust. Appl. Math.* **13**: 343–349 (1996).

[3] K. Kuto, Limiting structure of shrinking solutions to the stationary Shigesada–Kawasaki–Teramoto model with large cross-Diffusion, *SIAM J. Math. Anal.*, 47 (2015), 5, 3993-4024.

[4] Q. Li and Y. Wu, Stability analysis on a type of steady state for the SKT competition model with large cross diffusion, *J. Math. Anal. Appl.*, 462 (2018), 1048-1072.

[5] Y. Lou and W. Ni, Diffusion, self-diffusion and cross-diffusion, *J. Differential Equations*, 131 (1996), 79-131.

[6] Y. Lou and W. Ni, Diffusion vs cross-diffusion: an elliptic approach, *J. Differential Equations*, 131 (1999), 157-190.

[7] Y. Lou, W. M. Ni and S. Yotsutani, On a limiting system in the Lotka-Volterra competition with cross diffusion, *Discrete and Contin. Dyn. Syst.*, 10 (2004), 435-458.

[8] Y. Lou, W. M. Ni, and S. Yotsutani, Pattern formation in a cross-diffusion system, *Discrete and Contin. Dyn. Syst.*, 35(2015), 1589-1607.

[9] M. Mimura, Y. Nishiura, A. Tesei and T. Tsujikawa, Coexistence problem for two competing species models with density-dependent diffusion, *Hiroshima Math. J.*, 14 (1984), 425-449.

[10] W. M. Ni, Y. Wu and Q. Xu, The existence and stability of nontrivial steady states for S-K-T competition model with cross-diffusion, *Discrete and Contin. Dyn. Syst.*, 34 (2014), 5271-5298.

[11] N. Shigesada, K. Kawasaki, E. Teramoto, Spatial segregation of interacting species, *J. Theor. Biol.* **79**: 83–99 (1979).

[12] L. Wang, Y. Wu and Q. Xu, Instability of spiky steady states for S-K-T biological competing model with cross-diffusion, preprint, *Nonlinear Anal.*, 159 (2017), 424-457.

[13] Yanxia Wu and Yaping Wu, Existence of traveling waves with transition layers for Some Degenerate Cross-Diffusion Systems, *Comm. Pure Appl. Anal.*, 11 (2012), 911-934.

[14] Y. Wu, The instability of spiky steady states for a competing species model with cross-diffusion, *J. Differential Equations*, 213 (2005), 289-340.

[15] Y. Wu and Q. Xu, The Existence and structure of large spiky steady states for S-K-T competition system with cross-diffusion, *Discrete Contin. Dyn. Syst.*, 29 (2011), 367-385.

[16] Y. Wu and Y. Zhao, The existence and stability of traveling waves with transition layers for the S-K-T competition model with cross-diffusion, *Science China*, 53(2010), 1161-1184.

Critical exponent for the global existence of solutions to a semilinear heat equation with degenerate coefficients

Tatsuki Kawakami*
Department of Applied Mathematics and Informatics,
Ryukoku University
Seta Otsu 520-2194, Japan

1 Introduction

We consider the problem

$$\begin{cases} \partial_t u - \mathrm{div}(w(x)\nabla u) = u^p, & x \in \mathbb{R}^N, \ t > 0, \\ u(x,0) = u_0(x) \geq 0, & x \in \mathbb{R}^N, \end{cases} \tag{1.1}$$

where the coefficient w is either $w(x) = |x_1|^a$ with $a \in [0,1)$, or $w(x) = |x|^b$ with $b \in [0,N)$. Here one has $N \geq 1$, $\partial_t := \partial/\partial t$ and $p > 1$. The aim of the present work is to develop a global-in-time existence theory of mild solutions for the problem (1.1). We prove that there is a critical exponent for the global existence of positive solutions of problem (1.1), the so-called Fujita exponent.

We give first the definition of a solution to (1.1). Let $\Gamma = \Gamma(x,y,t)$ be the fundamental solution of

$$\partial_t v - \mathrm{div}(w(x)\nabla v) = 0, \qquad x \in \mathbb{R}^N, \quad t > 0,$$

with a pole at $(y,0)$. Under the condition either $w(x) = |x_1|^a$ with $a \in [0,1)$, or $w(x) = |x|^b$ with $b \in [0,1)$, this fundamental solution Γ satisfies the mass conservation property, the semigroup one and suitable Gaussian estimates (see (K1)–(K3) in Section 3). Using Γ, we define the solution of (1.1) as follows.

Definition 1.1 *Let u_0 be a nonnegative measurable function in $\mathbb{R}^N$. Let $T \in (0,\infty]$ and u be a nonnegative measurable function in $\mathbb{R}^N \times (0,T)$ such that $u \in L^\infty(0,T : L^\infty(\mathbb{R}^N))$. Then we call u a solution of (1.1) in $\mathbb{R}^N \times (0,T)$ if u satisfies*

$$u(x,t) = \int_{\mathbb{R}^N} \Gamma(x,y,t)u_0(y)\,dy + \int_0^t \int_{\mathbb{R}^N} \Gamma(x,y,t-s)u(y,s)^p\,dy\,ds < \infty \tag{1.2}$$

for almost all $x \in \mathbb{R}^N$ and $t \in (0,T)$. In particular, we call u a global-in-time solution of (1.1) if u is a solution of (1.1) in $\mathbb{R}^N \times (0,\infty)$.

*kawakami@math.ryukoku.ac.jp
This is a joint work with Y. Fujishima (Shizuoka University) and Y. Sire (Johns Hopkins University).

The previous definition is the well-known class of *mild solutions* and is natural to tackle parabolic problems. A main point of the previous definition is that it involves the fundamental solution of the operator under consideration. It is important to notice that in our context, due to the non-homogeneity of the operator, the fundamental solution is not translation-invariant. Furthermore, there is no explicit expression of it, though bounds are known. This makes the theory harder.

Remark 1.1 (i) *For the case of the semilinear heat equation, namely* (1.1) *with either* $a = 0$ *or* $b = 0$*, if* $u_0 \in L^\infty(\mathbb{R}^N)$*, then there exists a local-in-time solution* u *of* (1.1) *in* $\mathbb{R}^N \times (0, T)$ *for some* $T > 0$ *satisfying* (1.2)*. See e.g.* [19].

(ii) *In oder to prove the regularity of the solution satisfying* (1.2)*, even for the case of the semilinear heat equation, we need suitable bounds for the derivatives and the translation-invariant property of the fundamental solution.* (*See e.g.* [5, 9].) *However, unfortunately, it seems that they have been still left open.* (*See also Remark* 2.2 (iii).) *On the other hand, under our definition, in order to prove the existence/nonexistence of global-in-time solutions of* (1.1)*, we only need properties* (K1)–(K3) *and decay estimates, which are given in Lemma* 3.2*.*

We discuss now the features of the weight $w(x)$. In both cases under consideration, the weights belong to the class A_2 of Muckenhoupt functions [15]. This class of functions is very important in harmonic analysis for the boundedness of Maximal Functions. From the PDE point of view, elliptic equations and potential theory involving these weights have been studied in [2, 3, 4]. See also [1, 8] for the parabolic counterpart. In the present work, we do not consider general weights since it is very complicated in this case to give precise results as our aim is. We will consider two types of weights. The first one is $|x_1|^a$ which is A_2 if and only if $a \in (-1, 1)$ and exhibits singularities along the line $x_1 = 0$. The other weight under consideration is $|x|^b$ which is A_2 for $b \in (-N, N)$ and exhibits a singularity at the origin $x = 0$.

2 Main results

Now we state our main results but several explanations are in order. In most of the parabolic problem dealing with homogeneous equations, a crucial role is played by the fundamental solution. It happens that one can deduce several strong results as soon as one has an explicit form of the fundamental solution, allowing to get estimates for the function and its derivatives (see e.g. [10, 18]). In our problems, even if the coefficients are rather simple, such an explicit form is unavailable. On the other hand, bounds on the solution are known (see e.g. [12]). In order to apply known bounds one has to impose additional properties on the weights under consideration. More precisely, the weights have to belong to the $A_{1+\frac{2}{N}}$ class additionally to being A_2 and $w^{-N/2}$ has to satisfy a reverse doubling condition. We refer the reader to Section 4 for a discussion of these fact. In what follows, we put

$$p_*(\alpha) := 1 + \frac{2-\alpha}{N} \qquad \text{for} \quad \alpha \in \{a, b\}\,.$$

Furthermore, we assume either

(A) $w(x) = |x_1|^a$ with $a \in [0, 1)$ if $N = 1, 2$ and $a \in [0, 2/N)$ if $N \geq 3$,

or

(B) $w(x) = |x|^b$ with $b \in [0, 1)$.

Before treating main results, we introduce some notations. For any $1 \leq r \leq \infty$ and $a \leq \sigma \leq \infty$, we denote by $\|\cdot\|_r$ and $\|\cdot\|_{r,\sigma}$ the usual norm of the Lebesgue space $L^r := L^r(\mathbb{R}^N)$ and the Lorentz space $L^{r,\sigma} := L^{r,\sigma}(\mathbb{R}^N)$, respectively. (For the definition of the Lorentz space, see e.g. [11].)

The first theorem is concerned with the nonexistence of global-in-time solutions of (1.1).

Theorem 2.1 ([6]) *Assume either* (A) *or* (B). *Let* α *be such that* $\alpha = a$ *for the case* (A) *and* $\alpha = b$ *for the case* (B). *Assume* $1 < p \leq p_*(\alpha)$. *Then problem* (1.1) *has no nontrivial global-in-time solutions.*

In second theorem we give a sufficient condition for the existence of nontrivial global-in-time solutions of (1.1).

Theorem 2.2 ([6]) *Assume either* (A) *or* (B). *Let* α *be such that* $\alpha = a$ *for the case* (A) *and* $\alpha = b$ *for the case* (B). *Assume* $p > p_*(\alpha)$. *Put*

$$r_* := \frac{N}{2-\alpha}(p-1) > 1.$$

Then the following holds:

(i) *There exists a positive constant* δ *such that, for any* $u_0 \in L^\infty \cap L^{r_*,\infty}$ *with*

$$\|u_0\|_{r_*,\infty} < \delta,$$

a unique global-in-time solution u *of* (1.1) *exists and it satisfies*

$$\sup_{t>0} (1+t)^{\frac{N}{2-\alpha}(\frac{1}{r_*}-\frac{1}{q})} \|u(t)\|_{q,\infty} < \infty, \qquad r_* \leq q \leq \infty. \tag{2.1}$$

(ii) *Let* $1 \leq r \leq r_*$. *Then there exists a positive constant* δ *such that, for any* $u_0 \in L^\infty \cap L^r$ *with*

$$\|u_0\|_r^{\frac{r}{r_*}} \|\varphi\|_\infty^{1-\frac{r}{r_*}} < \delta,$$

a unique global-in-time solution u *of* (1.1) *exists and it satisfies*

$$\sup_{t>0} (1+t)^{\frac{N}{2-\alpha}(\frac{1}{r}-\frac{1}{q})} \|u(t)\|_q < \infty, \qquad r \leq q \leq \infty.$$

Remark 2.1 *As far as the regularity of the mild solutions constructed in this theorem is concerned, Chiarenza and Serapioni* [1] *considered degenerate parabolic equations with* A_2*-weights. However, their starting point are weak solutions. To upgrade our mild solutions to weak solutions one needs gradient bounds on the fundamental solution* Γ*, which are not available.*

As a direct consequence of Theorem 2.2, we have:

Corollary 2.1 *Let $\alpha \in \{a, b\}$. Assume $p > p_*(\alpha)$. Then there exists a positive constant δ such that, if*

$$|u_0(x)| \le \frac{\delta}{1+|x|^{(2-\alpha)/(p-1)}}, \qquad x \in \mathbb{R}^N, \tag{2.2}$$

then a unique global-in-time solution u of (1.1) *exists and it satisfies* (2.1).

Remark 2.2 (i) *For the case $\alpha = 0$, it is well known that the decay rate for initial data, which is given by* (2.2)*, at spatial infinity is optimal to obtain the global existence of solutions for* (1.1) (*see e.g.* [14]). *If $u_0(x)$ satisfies* (2.2)*, then it holds that $u_0 \in L^{r_*,\infty}$. On the other hand, if $u_0(x) = O(|x|^{-(2-\alpha)/(p-1)})$ as $|x| \to \infty$, then $u_0 \notin L^{r_*}$. This is a clear advantage in using $L^{r,\infty}$ spaces instead of the classical L^r spaces.*

(ii) *Beginning with the classical paper by Fujita* [7]*, critical exponents for the global existence of solutions* (*not only positive ones but also sign-changing ones*) *were established for many classes of evolution problems* (*see e.g.* [17]). *By Theorems* 2.1 *and* 2.2 *we see that $p_*(\alpha)$ is the Fujita exponent for problem* (1.1). *In fact, if $\alpha = 0$, then $p_*(0) = 1 + 2/N$, which is the Fujita exponent for* (1.1) *with $w(x) \equiv 1$.*

(iii) *If we have suitable bounds for the derivatives of the fundamental solution, then, applying the arguments in* [9]*, we can obtain the asymptotic behavior of solutions for* (1.1). *However, unfortunately, it seems that they have been still left open.*

(iv) *By Theorem* 2.2*, for suitable small initial data, the solution exists globally in time and it is bounded. On the other hand, in general, it seems difficult to prove the boundedness of solutions even if the solution exists globally in time. In fact, for the case $\alpha = 0$, if $p < p_S := (N+2)/(N-2)$ and u_0 belongs to a weighted H^1 space, then global-in-time solutions are bounded* (*see e.g.* [13])*, and if p is critical or supercritical in the sense of Joseph-Lundgren, then there exists a continuous function u_0 such that solution u is global and $\lim_{t\to\infty} \|u(t)\|_\infty = \infty$* (*see* [16, Theorem 1.3]).

3 Estimates of the fundamental solution

A crucial tool in our arguments is based on the use of the fundamental solution of the operator $\partial_t - \mathrm{div}(w(x)\nabla\cdot)$. As already mentioned due to the inhomogeneity of the operator, an explicit formula is not known but bounds are available (see below). In order to check these bounds, following [12], one has to check that the coefficient $w(x)$ is a $A_{1+\frac{2}{N}}$ weight in the sense of Muckenhoupt class and that the function $w^{-N/2}$ satisfies a doubling and reverse doubling condition of order μ with $\mu > 1/2$. Here we say that the function $w^{-N/2}$ satisfies doubling and a reverse doubling conditions if there exist positive constants C_1 and C_2 such that

$$\int_{B_{sR}(x)} w(y)^{-\frac{N}{2}}\,dy \le C_1 s^{\mu N} \int_{B_R(x)} w(y)^{-\frac{N}{2}}\,dy$$

and

$$\int_{B_{sR}(x)} w(y)^{-\frac{N}{2}}\,dy \ge C_2 s^{\mu N} \int_{B_R(x)} w(y)^{-\frac{N}{2}}\,dy$$

for all $x \in \mathbb{R}^N$, $s \geq 1$ and $R > 0$, respectively. It is a direct computation to check that under condition (A) or (B) depending on the case, the weight $w(x)$ is an $A_{1+\frac{2}{N}}$ weight in the sense of Muckenhoupt class. Furthermore, the function $w^{-N/2}$ satisfies a doubling condition and reverse doubling condition of order μ with $\mu > 1/2$.

Under condition either (A) or (B), the fundamental solution $\Gamma = \Gamma(x, y, t)$ has the following properties (see [12]):

(K1) $\displaystyle\int_{\mathbb{R}^N} \Gamma(x, y, t)\, dx = \int_{\mathbb{R}^N} \Gamma(x, y, t)\, dy = 1$ for $x, y \in \mathbb{R}^N$ and $t > 0$;

(K2) $\displaystyle\Gamma(x, y, t) = \int_{\mathbb{R}^N} \Gamma(x, \xi, t - s)\, \Gamma(\xi, y, s)\, d\xi$ for $x, y \in \mathbb{R}^N$ and $t > s > 0$;

(K3) Put

$$c_0 := \sup_Q \left(\frac{1}{|Q|} \int_Q w(x)\, dx \right) \left(\frac{1}{|Q|} \int_Q w(x)^{-1}\, dx \right) < \infty,$$

where the supremum is taken over all cubes Q in $\mathbb{R}^N$. Then there exist positive constants c_* and C_* depending only on N and c_0 such that

$$\begin{aligned} c_*^{-1} \left(\frac{1}{[h_x^{-1}(t)]^N} + \frac{1}{[h_y^{-1}(t)]^N} \right) e^{-c_* \left(\frac{h_x(|x-y|)}{t} \right)^{\frac{1}{1-\alpha}}} &\leq \Gamma(x, y, t) \\ &\leq C_*^{-1} \left(\frac{1}{[h_x^{-1}(t)]^N} + \frac{1}{[h_y^{-1}(t)]^N} \right) e^{-C_* \left(\frac{h_x(|x-y|)}{t} \right)^{\frac{1}{1-\alpha}}} \end{aligned}$$

for $x, y \in \mathbb{R}^N$ and $t > 0$, where $\alpha \in \{a, b\}$. Here

$$h_x(r) = \left(\int_{B_r(x)} w(y)^{-\frac{N}{2}}\, dy \right)^{\frac{2}{N}} \tag{3.1}$$

and h_x^{-1} denotes the inverse function of h_x.

By (A), (B) and (3.1) we state a lemma on upper and lower estimates of $h_x(r)$. In what follows, by the letters C and C' we denote generic positive constants (independent of x and t) and they may have different values also within the same line.

Lemma 3.1 *The following hold.*

(i) *Let $w(x) = |x_1|^a$ and assume condition (A). There exist positive constants C and C' depending only on N and a such that*

$$h_x(r) \leq C r^{2-a} \tag{3.2}$$

and

$$h_x(r) \geq C' \begin{cases} r^2 |x_1|^{-a} & \text{if} \quad 0 < r \leq |x_1|, \\ r^{2-a} & \text{if} \quad r \geq |x_1|, \end{cases} \tag{3.3}$$

for all $x \in \mathbb{R}^N$ and $r > 0$.

(ii) *Let $w(x) = |x|^b$ and assume condition (B). There exist positive constants C and C' depending only on N and b such that*

$$h_x(r) \le Cr^{2-b}$$

and

$$h_x(r) \ge C' \begin{cases} r^2|x|^{-b} & \text{if} \quad 0 < r \le |x|, \\ r^{2-b} & \text{if} \quad r \ge |x|, \end{cases}$$

for all $x \in \mathbb{R}^N$ and $r > 0$.

For any $x \in \mathbb{R}^N$, since $w(x) \ge 0$, by (3.1) we can easily obtain that

$$\frac{d}{dr} h_x(r) > 0 \tag{3.4}$$

for all $r > 0$. Then, in the case (A), by (3.2) and (3.4) we have

$$h_x^{-1}(t) \ge Ct^{\frac{1}{2-a}} \tag{3.5}$$

for all $x \in \mathbb{R}^N$ and $t > 0$. Similarly, by (3.3) we see that

$$h_x^{-1}(t) \le C \begin{cases} |x_1|^{\frac{a}{2}} t^{\frac{1}{2}} & \text{if} \quad 0 < t \le |x_1|^{2-a}, \\ t^{\frac{1}{2-a}} & \text{if} \quad t \ge |x_1|^{2-a}, \end{cases}$$

for all $x \in \mathbb{R}^N$ and $t > 0$. This together with Lemma 3.1, (K3) and (3.5) implies that

$$\begin{aligned} & d^{-1} \left(\min\{|x_1|^{-\frac{aN}{2}}, t^{-\frac{aN}{2}\frac{1}{2-a}}\} + \min\{|y_1|^{-\frac{aN}{2}}, t^{-\frac{aN}{2}\frac{1}{2-a}}\} \right) t^{-\frac{N}{2}} e^{-d\left(\frac{|x-y|^{2-a}}{t}\right)^{\frac{1}{1-a}}} \\ & \qquad \le \Gamma(x,y,t) \le D^{-1} t^{-\frac{N}{2-a}} \begin{cases} e^{-D\left(\frac{|x-y|^2}{t|x_1|^a}\right)^{\frac{1}{1-a}}} & \text{if} \quad |x-y| \le |x_1|, \\ e^{-D\left(\frac{|x-y|^{2-a}}{t}\right)^{\frac{1}{1-a}}} & \text{if} \quad |x-y| > |x_1|, \end{cases} \end{aligned} \tag{3.6}$$

for $x, y \in \mathbb{R}^N$ and $t > 0$. Here D and d are positive constant depending only on N and a. Similarly to (3.6), in the case (B), we see that

$$\begin{aligned} & d^{-1} \left(\min\{|x|^{-\frac{bN}{2}}, t^{-\frac{bN}{2}\frac{1}{2-b}}\} + \min\{|y|^{-\frac{bN}{2}}, t^{-\frac{bN}{2}\frac{1}{2-b}}\} \right) t^{-\frac{N}{2}} e^{-d\left(\frac{|x-y|^{2-b}}{t}\right)^{\frac{1}{1-b}}} \\ & \qquad \le \Gamma(x,y,t) \le D^{-1} t^{-\frac{N}{2-b}} \begin{cases} e^{-D\left(\frac{|x-y|^2}{t|x|^b}\right)^{\frac{1}{1-b}}} & \text{if} \quad |x-y| \le |x|, \\ e^{-D\left(\frac{|x-y|^{2-b}}{t}\right)^{\frac{1}{1-b}}} & \text{if} \quad |x-y| > |x|, \end{cases} \end{aligned} \tag{3.7}$$

for $x, y \in \mathbb{R}^N$ and $t > 0$. Here D and d are positive constant depending only on N and b. By (3.6) and (3.7) we obtain

$$\Gamma(x, y, t) \le D^{-1} t^{-\frac{N}{2-\alpha}}$$

for $x, y \in \mathbb{R}^N$ and $t > 0$. This together with (K1) implies that

$$\|\Gamma(\cdot, y, t)\|_r \le C t^{-\frac{N}{2-\alpha}(1-\frac{1}{r})}, \qquad \|\Gamma(x, \cdot, t)\|_r \le C t^{-\frac{N}{2-\alpha}(1-\frac{1}{r})}, \tag{3.8}$$

for any $1 \le r \le \infty$, where we can take the constant C so that it depends only on N and $\alpha \in \{a, b\}$. Furthermore, we have the following.

Lemma 3.2 *Assume either* (A) *or* (B). *Let* α *be such that* $\alpha = a$ *for the case* (A) *and* $\alpha = b$ *for the case* (B). *Then, for any* $1 \le r < \infty$, *there exists a positive constant* C *depending only on* α, r *and* N *such that*

$$\|\Gamma(x, \cdot, t)\|_{r,1} \le C t^{-\frac{N}{2-\alpha}(1-\frac{1}{r})}, \tag{3.9}$$

for $x \in \mathbb{R}^N$ *and* $t > 0$.

For any measurable function φ, we put

$$[S(t)\varphi](x) := \int_{\mathbb{R}^N} \Gamma(x, y, t)\varphi(y)\, dy$$

for all $x \in \mathbb{R}^N$ and $t > 0$. Since the fundamental solution Γ is not translation-invariant, we can not apply the usual Young inequality and weak Young inequality to get these estimates. However, modifying the proof of L^q–L^r and $L^{q,\infty}$–$L^{r,\infty}$ estimates for the solution of the heat equation with (3.8) and (3.9), we can prove the following estimates.

(G1) For any $\varphi \in L^q$ and $1 \le q \le r \le \infty$, it holds that

$$\|S(t)\varphi\|_r \le c_1 t^{-\frac{N}{2-a}(\frac{1}{q}-\frac{1}{r})} \|\varphi\|_q, \qquad t > 0.$$

Here c_1 can be taken so that it depends only on N and $\alpha \in \{a, b\}$.

(G2) For any $\varphi \in L^{q,\infty}$ with $1 < q \le \infty$ and $q \le r \le \infty$, it holds that

$$\|S(t)\varphi\|_{r,\infty} \le c_2 t^{-\frac{N}{2-\alpha}(\frac{1}{q}-\frac{1}{r})} \|\varphi\|_{q,\infty}, \qquad t > 0.$$

Here c_2 can be taken so that it depends only on q, N and $\alpha \in \{a, b\}$. In particular, the constant c_2 is bounded in $q \in (1 + \epsilon, \infty)$ for any fixed $\epsilon > 0$ and $c_2 \to \infty$ as $q \to 1$.

(G3) For $\varphi \in L^\infty$ with $\varphi \ge 0$ in $\mathbb{R}^N$, it holds that

$$[S(t)\varphi](x) \ge c_3 t^{-\frac{N}{2-\alpha}} \int_{|y| \le t^{\frac{1}{2-\alpha}}} \varphi(y)\, dy$$

for $|x| \le t^{\frac{1}{2-\alpha}}$ and $t > 0$. Here c_3 can be taken so that it depends only on α and N.

Applying these estimates, we can prove our main results.

Acknowledgment. This research is partially supported by JSPS KAKENHI Grant Number JP16K17629.

References

[1] F. Chiarenza and R. Serapioni, Degenerate parabolic equations and Harnack inequality, Ann. Mat. Pura Appl. (4) **137** (1984), 139–162.

[2] E. Fabes, C. Kenig and R. Serapioni, The local regularity of solutions of degenerate elliptic equations, Comm. Partial Differential Equations 7 (1982), **1**, 77–116.

[3] E. Fabes, D. Jerison and C. Kenig, The Wiener test for degenerate elliptic equations, Ann. Inst. Fourier (Grenoble) 32 (1982), **3**, vi, 151–182.

[4] E. Fabes, C. Kenig and D. Jerison, Boundary behavior of solutions to degenerate elliptic equations, Conference on harmonic analysis in honor of Antoni Zygmund, Vol. I, II (Chicago, Ill., 1981), 577–589.

[5] A. Friedman, *Partial Differential Equations of Parabolic Type*, Prentice-Hall, Inc., Englewood Cliffs, N. J. 1964.

[6] Y. Fujishima, T. Kawakami and Y. Sire, Critical exponent for the global existence of solutions to a semilinear heat equation with degenerate coefficients, Calc. Var. Partial Differential Equations **58** (2019), Art. 62.

[7] H. Fujita, On the blowing up of solutions of the Cauchy problem for $u_t = \Delta u + u^{1+\alpha}$, J. Fac. Sci. Univ. Tokyo Sec. 1A Math. **16** (1966), 105–113

[8] K. Ishige, On the behavior of the solutions of degenerate parabolic equations, Nagoya Math. J. **155** (1999), 1–26.

[9] K. Ishige, T. Kawakami and K. Kobayashi, Global solutions for a nonlinear integral equation with a generalized heat kernel, Discrete Contin. Dyn. Syst. Ser. S. **7** (2014), 767–783.

[10] K. Ishige, T. Kawakami and H. Michihisa, Asymptotic expansions of solutions of fractional diffusion equations, SIAM J. Math. Anal. **49** (2017), 2167–2190.

[11] L. Grafakos, Classical Fourier Analysis, Springer-Verlag, 2008.

[12] C.E. Gutiérrez, G.S. Nelson, Bounds for the fundamental solution of degenerate parabolic equations, Comm. Partial Differential Equations **13** (1988) 635–649.

[13] T. Kawanago, Asymptotic behavior of solutions of a semilinear heat equation with subcritical nonlinearity, Ann. Inst. H. Poincaré Anal. Non Linéaire **13** (1996), 1–15.

[14] T. Y. Lee and W. M. Ni, Global existence, large time behavior and life span of solutions of a semilinear parabolic Cauchy problem, Trans. Amer. Math. Soc. **333** (1992), 365–378.

[15] B. Muckenhoupt, Weighted norm inequalities for the Hardy maximal function, Trans. Amer. Math. Soc. **165** (1972), 207-226.

[16] P. Poláčik and E. Yanagida, On bounded and unbounded global solutions of a supercritical semilinear heat equation, Math. Ann. **327** (2003), 745–771.

[17] P. Quittner and P. Souplet, Superlinear Parabolic Problems, Blow-up, Global Existence and Steady States, Birkhäuser Advanced Texts: Basler Lehrbücher, Birkhäuser Verlag, Basel, 2007.

[18] S. Sugitani, On nonexistence of global solutions for some nonlinear integral equations, Osaka J. Math. **12** (1975), 45–51.

[19] F.B. Weissler, Semilinear evolution equations in Banach spaces, J. Funct. Anal. **32** (1979), 277-296.

On the low stratification of the complete Euler system

Jan Březina*, Václav Mácha†

1 Introduction

In this talk we will show how to obtain the Euler-Boussinesq (E-B) system as a singular limit of the complete Euler system. The concept of dissipative measure-valued solutions will allow us to derive E-B in a rigorous way.

Firstly, we introduce complete Euler system

$$\begin{aligned}
\partial_t \varrho + \operatorname{div}(\varrho \mathbf{u}) &= 0 \\
\partial_t(\varrho \mathbf{u}) + \operatorname{div}(\varrho \mathbf{u} \otimes \mathbf{u}) + \frac{1}{\mathrm{Ma}^2} \nabla p(\varrho, \theta) &= \frac{1}{\mathrm{Fr}^2} \varrho \nabla F \\
\partial_t \left(\frac{1}{2} \varrho |\mathbf{u}|^2 + \frac{1}{\mathrm{Ma}^2} \varrho e(\rho, \theta) \right) + \operatorname{div} \left[\left(\frac{1}{2} \varrho |\mathbf{u}|^2 + \frac{1}{\mathrm{Ma}^2} \varrho e(\varrho, \theta) \right) \mathbf{u} \right] & \\
+ \frac{1}{\mathrm{Ma}^2} \operatorname{div}(p(\varrho, \theta) \mathbf{u}) &= \frac{1}{\mathrm{Fr}^2} \varrho \nabla F \cdot \mathbf{u}
\end{aligned} \tag{1}$$

on a time-space domain $(0, T) \times \Omega$, where $T > 0$ and $\Omega \subseteq \mathbb{R}^3$. The unknowns are scalar quantities ϱ and θ standing for the density and the temperature, and a vector quantity $\mathbf{u}$ representing the velocity. Further, we assume that the right-hand side F, expressing the potential forces, is independent of time, i.e. $F : \Omega \mapsto \mathbb{R}$. The quantities Ma and Fr denote Mach and Froude numbers, respectively.

Secondly, we investigate the *low stratification regime*, i.e. we assume that

*Kyushu University, 744 Motooka, Nishi-ku, Fukuoka, 819-0395, Japan; E-mail: brezina@artsci.kyushu-u.ac.jp

†Institute of Mathematics CAS, Žitná 25, 115 67 Praha 1, Czechia; E-mail: macha@math.cas.cz

$\mathrm{Ma} = \varepsilon$ and $\mathrm{Fr} = \sqrt{\varepsilon}$ as $\varepsilon \to 0$. This formally leads to the E-B system

$$\begin{aligned} \operatorname{div} \mathbf{U} &= 0 \\ \partial_t \mathbf{U} + \mathbf{U} \cdot \nabla \mathbf{U} + \nabla \Pi &= \frac{r}{\overline{\varrho}} \nabla F \\ \partial_t \Theta + \mathbf{U} \cdot \nabla \Theta &= \frac{1}{1 + c_v} \mathbf{U} \cdot \nabla F \\ r + \frac{\overline{\varrho}}{\overline{\theta}} \Theta &= \frac{\overline{\varrho}}{\overline{\theta}} F \end{aligned} \tag{2}$$

which is of great importance in modeling flows of air in the atmosphere (see [8]).

The low Mach number limit of a system of Euler equations has been already studied. The isentropic system has been discussed in [6], where the authors deal with both well and ill-prepared initial data. They consider the case $F = 0$. The complete system has been treated in [4] and [5] – both papers focus on the *strong stratification*, i.e. $\mathrm{Ma} = \mathrm{Fr} = \varepsilon$ as $\varepsilon \to 0$, for well-prepared initial data. Unlike in the isentropic case, the target system for the complete system case is not uniquely determined and it depends on the choice of the initial data – the isothermal case has been studied in [5] and the isentropic case in [4].

In this talk we aim to derive the E-B equations from the complete Euler system under the state equations of a *perfect gas*, i.e. we assume

$$p(\varrho, \theta) = \varrho\theta, \qquad e(\varrho, \theta) = c_v \theta,$$

where $c_v > 0$ is the specific heat at constant volume. Since the existence of weak solutions to the complete Euler system is currently a difficult task, we take advantage of a more general concept of dissipative measure-valued solutions whose existence and properties were discussed recently by Březina and Feireisl (see e.g. [2], [3]). In particular, our result holds for finite energy weak solutions as well.

Depending on the type of initial data we deal with the following two cases of domains. Either $\Omega \subset \mathbb{R}^3$ is a bounded domain or $\Omega \subset \mathbb{R}^3$ is an exterior domain with compact and smooth boundary – the regularity of this domain is motivated by an existence of dispersive estimates. In both situations we assume the impermeability boundary conditions

$$\mathbf{u} \cdot \mathbf{n}|_{\partial\Omega} = 0 \text{ for (1) and } \mathbf{U} \cdot \mathbf{n} = 0 \text{ for (2).} \tag{3}$$

In the case of an exterior domain, we further impose the far field boundary conditions, i.e.

$$\varrho \to \overline{\varrho},\ \theta \to \overline{\theta} \text{ and } \mathbf{u} \to \mathbf{0} \text{ as } |x| \to \infty, \tag{4}$$

where $\overline{\varrho}$ and $\overline{\theta}$ are some positive constants specified later.

As for the potential force F we consider the following situations

$$\begin{aligned} &\Omega \text{ bounded: } F \in W^{k,2}(\Omega) \text{ for some } k > 5/2, \\ &\Omega \text{ exterior: } F(x) = \int_{\mathbb{R}^3} \frac{1}{x - y} m(y)\, \mathrm{d}y \text{ for some } m \text{ with supp } m \subseteq \mathbb{R}^3 \setminus \Omega. \end{aligned} \tag{5}$$

Note that in the case of an exterior domain the relation in (5) expresses the fact that the flow of the fluid is driven by the gravitational force of an object lying outside of the fluid.

To avoid any problems stemming from the possibility of vacuum we reformulate the Euler system in the conservative variables:

$$\varrho,\ \mathbf{m} = \varrho\mathbf{u},\ p = \varrho\theta.$$

Here, ϱ is the density, $\mathbf{m}$ is the momentum and p is the pressure of the fluid.

The system (1) is then equivalent to

$$\begin{aligned} \partial_t \varrho + \operatorname{div} \mathbf{m} &= 0 \\ \partial_t \mathbf{m} + \operatorname{div}\left(\frac{\mathbf{m}\otimes\mathbf{m}}{\varrho}\right) + \frac{1}{\varepsilon^2}\nabla p &= \frac{1}{\varepsilon}\varrho\nabla F \\ \frac{\mathrm{d}}{\mathrm{d}t}\int_\Omega \left[\frac{1}{2}\frac{|\mathbf{m}|^2}{\varrho} + \frac{c_v}{\varepsilon^2}p\right]\,\mathrm{d}x &\le \int_\Omega \frac{1}{\varepsilon}\nabla F\cdot\mathbf{m}\,\mathrm{d}x \\ \partial_t\left(\varrho\chi\left(\log\left(\frac{p}{\varrho^\gamma}\right)\right)\right) + \operatorname{div}\left(\chi\left(\log\left(\frac{p}{\varrho^\gamma}\right)\right)\mathbf{m}\right) &\ge 0,\ \gamma = 1 + \frac{1}{c_v} \end{aligned} \tag{6}$$

for a certain set of cut-off functions χ. Here, (3) changes into $\mathbf{m}\cdot\mathbf{n}|_{\partial\Omega} = 0$ and (4) into $\varrho \to \overline{\varrho}$, $p \to \overline{\varrho}\overline{\theta}$ and $\mathbf{m} \to \mathbf{0}$ as $|x| \to 0$. Here, we generalized the problem by including energy inequality and a regularized form of the transport equation of the entropy production rate.

1.1 Measure-valued solutions to the primitive system

We establish the set

$$\mathcal{Q} \equiv \left\{(\varrho, \mathbf{m}, p)|\ \varrho \ge 0,\ \mathbf{m}\in\mathbb{R}^3,\ p \ge 0\right\}.$$

Definition 1.1. *We define a* renormalized dissipative measure–valued *(rDMV)* solution *to* (1) *with the initial conditions* $U_0 \in L^\infty_{w^*}(\Omega; \mathcal{P}(\mathcal{Q}))$ *as a parameterized family of probability measures*

$$U \in L^\infty_{w^*}((0,T)\times\Omega; \mathcal{P}(\mathcal{Q}))$$

that has the following properties:

- $\langle U_{t,x}; \varrho\rangle - \overline{\varrho} \in L^\infty(0,T,L^1(\Omega))$ *for some* $\overline{\varrho}$ *positive and*

$$\int_0^T\int_\Omega \left[\langle U_{t,x};\varrho\rangle\partial_t\varphi + \langle U_{t,x};\mathbf{m}\rangle\cdot\nabla\varphi\right]\,\mathrm{d}x\mathrm{d}t = \int_\Omega \langle U_{t,x};\varrho\rangle\varphi(T,\cdot)\,\mathrm{d}x - \int_\Omega \langle U_{0,x};\varrho\rangle\varphi(0,\cdot)\,\mathrm{d}x$$

  for any $\varphi \in C_c^\infty([0,T]\times\overline{\Omega})$*;*

- $$\int_0^T \int_\Omega \left[\langle U_{t,x}; \mathbf{m} \rangle \cdot \partial_t \boldsymbol{\varphi} + \left\langle U_{t,x}; \frac{\mathbf{m} \otimes \mathbf{m}}{\varrho} \right\rangle : \nabla \boldsymbol{\varphi} + \frac{1}{\varepsilon^2} \langle U_{t,x}; p \rangle \operatorname{div} \boldsymbol{\varphi} \right] \mathrm{d}x\mathrm{d}t$$
$$= \int_\Omega \langle U_{T,x}; \mathbf{m} \rangle \cdot \boldsymbol{\varphi}(T, \cdot) \, \mathrm{d}x - \int_\Omega \langle U_{0,x}; \mathbf{m} \rangle \cdot \boldsymbol{\varphi}(0, \cdot) \, \mathrm{d}x$$
$$- \frac{1}{\varepsilon} \int_0^t \int_\Omega \langle U_{t,x}; \varrho \rangle \nabla F \cdot \boldsymbol{\varphi} \, \mathrm{d}x\mathrm{d}t + \int_0^T \int_{\overline{\Omega}} \nabla \boldsymbol{\varphi} : \mathrm{d}\mu_C$$

  for any $\boldsymbol{\varphi} \in C_c^\infty([0,T] \times \overline{\Omega}; \mathbb{R}^3)$, $\boldsymbol{\varphi} \cdot \mathbf{n}|_{\partial\Omega} = 0$, *where* μ_C *is a vectorial signed measure on* $[0,T] \times \overline{\Omega}$*;*

- $\langle U_{t,x}; \rho(s(\rho,p) - s(\overline{\varrho}, \overline{\varrho}\overline{\theta})) \rangle \in L^\infty(0,T, L^1(\Omega))$ *for some* $\overline{\theta}$ *positive and*

$$\int_0^T \int_\Omega \left[\langle U_{t,x}; \varrho \chi(s(\varrho,p)) \rangle \partial_t \varphi + \langle U_{t,x}; \chi(s(\varrho,p)) \mathbf{m} \rangle \cdot \nabla \varphi \right] \mathrm{d}x\mathrm{d}t$$
$$\leq \int_\Omega \langle U_{T,x}; \varrho \chi(s(\varrho,p)) \rangle \varphi \, \mathrm{d}x - \int_\Omega \langle U_{0,x}; \varrho \chi(s(\varrho,p)) \rangle \varphi \, \mathrm{d}x$$

  for any $\varphi \in C_c^\infty([0,T] \times \overline{\Omega})$, $\varphi \geq 0$, *and any increasing concave function* χ *satisfying* $\chi(s) \leq \chi_\infty$ *for all* $s \in \mathbb{R}$*;*

- *The inequality*

$$\int_\Omega \left[\left\langle U_{t,x}; \frac{1}{2} \frac{|\mathbf{m}|^2}{\varrho} + \frac{1}{\varepsilon^2} c_v p \right\rangle \right]_{t=0}^{t=\tau} \mathrm{d}x \leq \frac{1}{\varepsilon} \int_0^\tau \int_\Omega \langle U_{t,x}; \mathbf{m} \rangle \cdot \nabla F \, \mathrm{d}x\mathrm{d}t$$

  holds for a.a. $\tau \in [0,T]$.

- $$\int_0^\tau \int_{\overline{\Omega}} |\mathrm{d}\mu_C| \lesssim \int_0^\tau \mathcal{D}(t) \, \mathrm{d}t \tag{7}$$

  for a.a. $\tau \in [0,T]$, *where*

$$\mathcal{D}(\tau) = \int_\Omega \left[\left\langle U_{0,x}; \frac{1}{2} \frac{|\mathbf{m}|^2}{\varrho} + \frac{1}{\varepsilon^2} c_v p \right\rangle \right]_{t=\tau}^{t=0} \mathrm{d}x + \frac{1}{\varepsilon} \int_0^\tau \int_\Omega \langle U_{t,x}; \mathbf{m} \rangle \cdot \nabla F \, \mathrm{d}x\mathrm{d}t.$$

  Here and hereafter, the symbol $a \lesssim b$ *means* $a \leq cb$ *for a certain constant* $c > 0$ *independent of* $\varepsilon > 0$, *which may vary from line to line.*

We refer to [1] and [2] for details about the existence of rDMV solutions.

1.2 Initial data

For the complete Euler system (6) we consider the initial data in the form

$$\varrho_{0,\varepsilon} = \overline{\varrho} + \varepsilon \varrho_{0,\varepsilon}^{(1)}, \quad \mathbf{u}_{0,\varepsilon}, \quad \theta_{0,\varepsilon} = \overline{\theta} + \varepsilon \theta_{0,\varepsilon}^{(1)}, \tag{8}$$

where $\overline{\varrho}$, $\overline{\theta}$ are positive constants and

$$\|\varrho_{0,\varepsilon}^{(1)}\|_{L^\infty(\Omega)} + \|\mathbf{u}_{0,\varepsilon}\|_{L^\infty(\Omega)} + \|\theta_{0,\varepsilon}^{(1)}\|_{L^\infty(\Omega)} \leq c. \tag{9}$$

Moreover, we assume that

$$\begin{aligned} &\mathbf{u}_{0,\varepsilon} \to \mathbf{u}_0 \ \text{ strongly in } L^2(\Omega), \\ &\varrho_{0,\varepsilon}^{(1)} \to \varrho_0^{(1)} \ \text{ strongly in } L^2(\Omega), \\ &\theta_{0,\varepsilon}^{(1)} \to \theta_0^{(1)} \ \text{ strongly in } L^2(\Omega). \end{aligned} \tag{10}$$

The initial conditions for (2) have the form

$$\mathbf{U}(0,\cdot) = \mathbf{U}_0, \ \operatorname{div} \mathbf{U}_0 = 0, \ \Theta(0,\cdot) = \Theta_0, \tag{11}$$

and $r(0,\cdot)$ is given by $(2)_4$ and Θ_0.

Following the nowadays standard theory of well-posedness for hyperbolic systems, see e.g. Kato [7], we can assume that the Euler-Boussinesq system (2) with the initial data

$$\begin{aligned} (\mathbf{U}_0, \Theta_0) \in W^{k,2}(\Omega; \mathbb{R}^4), \quad \|(\mathbf{U_0}, \Theta_0)\|_{W^{k,2}(\Omega,\mathbb{R}^4)} \leq C, \\ \operatorname{div} \mathbf{U}_0 = 0, \quad \mathbf{U}_0 \cdot \mathbf{n}|_{\partial\Omega} = 0, \ k > \frac{5}{2}, \end{aligned} \tag{12}$$

has a regular solution $(r, \mathbf{U}, \Theta)$ defined on a maximal time interval $[0, T_{max}(C))$ with the regularity

$$(r, \mathbf{U}, \Theta) \in C([0, T_{max}); W^{k,2}(\Omega; \mathbb{R}^5)), \ (\partial_t \mathbf{U}, \nabla \Pi) \in C([0, T_{max}); W^{k-1,2}(\Omega, \mathbb{R}^6)),$$

where F was specified in (5).

1.2.1 Well-prepared data

By well-prepared initial data we mean the case when $\operatorname{div} \mathbf{u}_0 = 0$ and $\varrho_0^{(1)}$, $\theta_0^{(1)}$ satisfy the Boussinesq relation $(2)_{(4)}$, i.e.

$$\varrho_0^{(1)} + \frac{\overline{\varrho}}{\overline{\theta}} \theta_0^{(1)} = \frac{\overline{\varrho}}{\overline{\theta}} F. \tag{13}$$

We then take

$$r_0 = \varrho_0^{(1)}, \quad \mathbf{U}_0 = \mathbf{u}_0, \quad \Theta_0 = \theta_0^{(1)} \tag{14}$$

as the initial data for the Euler-Boussinesq system (2).

1.2.2 Ill-prepared data

The ill-prepared initial data refer to the general case when neither $\operatorname{div} \mathbf{u}_0 = 0$ nor (13) need to be satisfied. In order to tackle this problem one has to take into account the acoustic analogy. It can be shown that this discrepancy between

the initial data decays very quickly to 0 on the exterior domain. In this case we take

$$r_0 = \varrho_0^{(1)}, \quad \mathbf{U}_0 = \mathbf{H}[\mathbf{u}_0], \quad \Theta_0 = \frac{\overline{\theta}}{c_v + 1} \left(c_v \frac{1}{\overline{\theta}} \theta_0^{(1)} - \frac{1}{\overline{\varrho}} \varrho_0^{(1)} + \frac{1}{\overline{\theta}} F \right) \tag{15}$$

as the initial data for (2). Here, $\mathbf{H}$ denotes the standard *Helmholtz projection* on the space of solenoidal functions.

2 Main results

We begin with a result for the case of well-prepared initial data.

Theorem 2.1. *Let Ω be a regular bounded domain in $\mathbb{R}^3$, F satisfy (5) and $\overline{\varrho}, \overline{\theta}$ be positive constants. Assume that there is a smooth solution r, $\mathbf{U}$ and Θ to the Euler-Boussinesq system (2) on $[0, T_{max})$, $T_{max} > 0$ emanating from the initial data*

$$\mathbf{U_0}, \quad \Theta_0$$

satisfying (12). Assume further that $U^\varepsilon_{t,x}$ is a family of rDMV solutions to (1) with the initial data

$$U^\varepsilon_{0,x} = \delta_{\varrho_{0,\varepsilon}, (\varrho_{0,\varepsilon} \mathbf{u}_{0,\varepsilon}), (\varrho_{0,\varepsilon} \theta_{0,\varepsilon})},$$

where $(\varrho_{0,\varepsilon}, \mathbf{u}_{0,\varepsilon}, \theta_{0,\varepsilon})$ satisfy

$$\varrho_{0,\varepsilon} > 0, \quad \theta_{0,\varepsilon} > 0, \quad \log \left(\frac{\theta_{0,\varepsilon}^{c_v}}{\varrho_{0,\varepsilon}} \right) \geq s_0 > -\infty$$

together with (8)–(14). Moreover, suppose that the constant in (7) is independent of $\{U^\varepsilon\}$.

Then for any $0 < T < T_{max}$ there holds $\mathcal{D}^\varepsilon \to 0$ in $L^\infty(0,T)$ and

$$\begin{aligned} \langle U^\varepsilon_{t,x}; \varrho \rangle &\to \overline{\varrho} \text{ strongly in } L^\infty(0,T,L^1(\Omega)), \\ \langle U^\varepsilon_{t,x}; p \rangle &\to \overline{\varrho}\overline{\theta} \text{ strongly in } L^\infty(0,T,L^1(\Omega)), \\ \left\langle U^\varepsilon_{t,x}; \frac{\mathbf{m}}{\sqrt{\varrho}} \right\rangle &\to \sqrt{\overline{\varrho}} \mathbf{U} \text{ strongly in } L^\infty(0,T,L^2(\Omega)). \end{aligned}$$

Moreover,

$$\left\langle U^\varepsilon_{t,x}; \frac{\varrho - \overline{\varrho}}{\varepsilon} \right\rangle \to r \text{ and } \left\langle U^\varepsilon_{t,x}; \frac{p - \overline{\varrho}\overline{\theta}}{\varepsilon} \right\rangle \to \overline{\theta} r + \overline{\varrho} \Theta = \overline{\varrho} F$$

strongly in $L^\infty(0,T,L^1(\Omega))$.

Next we formulate the result for ill-prepared initial data.

Theorem 2.2. *Let $\Omega \subset \mathbb{R}^3$ be a regular exterior domain, F satisfy* (5) *and $\overline{\varrho}, \overline{\theta}$ be positive constants. Assume that there is a smooth solution r, $\mathbf{U}$ and Θ to the Euler-Boussinesq system* (2) *on $[0, T_{max})$, $T_{max} > 0$ emanating from the initial data*

$$\mathbf{U_0}, \quad \Theta_0$$

satisfying (12). *Assume further that $U^\varepsilon_{t,x}$ is a family of rDMV solutions to* (1) *with the initial data*

$$U^\varepsilon_{0,x} = \delta_{\varrho_{0,\varepsilon}, (\varrho_{0,\varepsilon}\mathbf{u}_{0,\varepsilon}), (\varrho_{0,\varepsilon}\theta_{0,\varepsilon})},$$

where $(\varrho_{0,\varepsilon}, \mathbf{u}_{0,\varepsilon}, \theta_{0,\varepsilon})$ satisfy

$$\varrho_{0,\varepsilon} > 0, \quad \theta_{0,\varepsilon} > 0, \quad \log\left(\frac{\theta^{c_v}_{0,\varepsilon}}{\varrho_{0,\varepsilon}}\right) \geq s_0 > -\infty$$

together with (8)–(10) *and* (15). *Moreover, suppose that the constant in* (7) *is independent of $\{U^\varepsilon\}$.*

Then for any $0 < T < T_{max}$ there holds $\mathcal{D}^\varepsilon \to 0$ in $L^\infty(0,T)$ and

$$\langle U^\varepsilon_{t,x}; \varrho \rangle \to \overline{\varrho} \text{ in strongly } L^\infty(0,T,L^1(\Omega)),$$
$$\langle U^\varepsilon_{t,x}; p \rangle \to \overline{\varrho}\overline{\theta} \text{ in strongly } L^\infty(0,T,L^1(\Omega)),$$
$$\left\langle U^\varepsilon_{t,x}; \frac{\mathbf{m}}{\sqrt{\varrho}} \right\rangle \to \sqrt{\overline{\varrho}}\mathbf{U} \text{ in strongly } L^\infty_{loc}((0,T],L^2(\Omega)).$$

Moreover,

$$\left\langle U^\varepsilon_{t,x}; \frac{\varrho - \overline{\varrho}}{\varepsilon} \right\rangle \to r \text{ and } \left\langle U^\varepsilon_{t,x}; \frac{p - \overline{\varrho}\overline{\theta}}{\varepsilon} \right\rangle \to \overline{\theta} r + \overline{\varrho}\Theta = \overline{\varrho} F$$

strongly in $L^\infty_{loc}((0,T], L^1_{loc}(\overline{\Omega}))$.

The idea of the proofs is to compare $U^\varepsilon_{t,x}$ with the smooth solution $r,\ \mathbf{U},\ \Theta$ using the *relative energy inequality*

$$\begin{aligned}
&\left[\int_\Omega \langle U^\varepsilon_{t,x}; \mathcal{E}^\varepsilon_\chi(\varrho, \mathbf{m}, p | \tilde{\varrho}, \tilde{\mathbf{U}}, \tilde{\theta})\rangle \,\mathrm{d}x\right]_{t=0}^{t=\tau} + \mathcal{D}^\varepsilon(\tau) \\
&\quad \leq -\frac{1}{\varepsilon^2}\int_0^\tau \int_\Omega \langle U^\varepsilon_{t,x}; \varrho\chi(s(\varrho,p))\rangle \partial_t\tilde{\theta} + \langle U^\varepsilon_{t,x}; \chi(s(\varrho,p))\mathbf{m}\rangle \cdot \nabla\tilde{\theta} \,\mathrm{d}x\mathrm{d}t \\
&\quad + \int_0^\tau \int_\Omega \langle U^\varepsilon_{t,x}; \varrho\tilde{\mathbf{U}} - \mathbf{m}\rangle \cdot \partial_t\tilde{\mathbf{U}} + \left\langle U^\varepsilon_{t,x}; \frac{(\varrho\tilde{\mathbf{U}} - \mathbf{m}) \otimes \mathbf{m}}{\varrho} \right\rangle : \nabla\tilde{\mathbf{U}} \,\mathrm{d}x\mathrm{d}t \\
&\qquad\qquad - \frac{1}{\varepsilon^2}\int_0^\tau \int_\Omega \langle U^\varepsilon_{t,x}; p\rangle \operatorname{div}\tilde{\mathbf{U}} \,\mathrm{d}x\mathrm{d}t \\
&\qquad + \frac{1}{\varepsilon^2}\int_0^\tau \int_\Omega \langle U^\varepsilon_{t,x}; \varrho\rangle \partial_t\tilde{\theta} s(\tilde{\varrho},\tilde{p}) + \langle U^\varepsilon_{t,x}; \mathbf{m}\rangle \cdot \nabla\tilde{\theta} s(\tilde{\varrho},\tilde{p}) \,\mathrm{d}x\mathrm{d}t \\
&\qquad + \frac{1}{\varepsilon^2}\int_0^\tau \int_\Omega \langle U^\varepsilon_{t,x}; \tilde{\varrho} - \varrho\rangle \frac{1}{\tilde{\varrho}}\partial_t\tilde{p} - \langle U^\varepsilon_{t,x}; \mathbf{m}\rangle \cdot \frac{1}{\tilde{\varrho}}\nabla\tilde{p} \,\mathrm{d}x\mathrm{d}t \\
&\qquad\quad + \frac{1}{\varepsilon}\int_0^\tau \int_\Omega \langle U^\varepsilon_{t,x}; \mathbf{m} - \varrho\tilde{\mathbf{U}}\rangle \cdot \nabla F \,\mathrm{d}x\mathrm{d}t + \int_0^\tau \int_\Omega \nabla\tilde{\mathbf{U}} : \mathrm{d}\mu^\varepsilon_C,
\end{aligned}$$

for a.a. $\tau \in (0,T)$, where we use the notation $\tilde{p} = \tilde{\varrho}\tilde{\theta}$ and

$$\mathcal{E}^\varepsilon_\chi\left(\varrho, \mathbf{m}, p | \tilde{\varrho}, \tilde{\mathbf{U}}, \tilde{\theta}\right) := \frac{1}{2}\frac{|\mathbf{m}|^2}{\varrho} - \mathbf{m}\tilde{\mathbf{U}} + \frac{1}{2}\varrho|\tilde{\mathbf{U}}|^2 + \frac{1}{\varepsilon^2}\left(c_v p - \varrho\tilde{\theta}\chi(s(\varrho,p)) + \tilde{p} - c_v\varrho\tilde{\theta} + \varrho\tilde{\theta}s(\tilde{\varrho},\tilde{p}) - \varrho\tilde{\theta}\right).$$

In short: Following the ideas introduced in [3, Section 3.2] we split every function into its *essential* and *residual* part and obtain coercive estimates on $\mathcal{E}^\varepsilon$. Observing that once the initial entropy is bounded below it remains bounded below for all times $t > 0$ allows us to remove χ from the picture. We then give a series of estimates leading to

$$\int_\Omega \langle U^\varepsilon_{\tau,x}; \mathcal{E}^\varepsilon(\varrho, \mathbf{m}, p | \tilde{\varrho}_{\varepsilon,\eta}, \tilde{\mathbf{U}}_{\varepsilon,\eta}, \tilde{\theta}_{\varepsilon,\eta})\rangle \,\mathrm{d}x + \mathcal{D}^\varepsilon(\tau) \leq \int_0^\tau \int_\Omega \langle U^\varepsilon_{t,x}; \mathcal{E}^\varepsilon(\varrho, \mathbf{m}, p | \tilde{\varrho}_{\varepsilon,\eta}, \tilde{\mathbf{U}}_{\varepsilon,\eta}, \tilde{\theta}_{\varepsilon,\eta})\rangle \,+ \int_0^\tau \mathcal{D}^\varepsilon(t)\,\mathrm{d}t + \omega(\varepsilon,\eta)$$

for a.a. $\tau \in (0,T)$. The Gronwall inequality concludes the proof.

The case of ill-prepared initial data is more complex as we need to get rid of acoustic waves that need to disperse on the unbounded domain.

References

[1] Jan Březina Existence of a measure-valued solutions to a complete Euler system for a perfect gas, arXiv:1805.05570v1

[2] Jan Březina and Eduard Feireisl Maximal dissipation principle for the complete Euler system, RIMS Kôkyûroku No.2070 (2018) 44–68

[3] Jan Březina and Eduard Feireisl Measure-valued solutions to the complete Euler system, J. Math. Soc. Japan 70 (2018), no. 4, 1227–1245

[4] Gabriele Bruell and Eduard Feireisl On a singular limit for the stratified compressible fluids

[5] Eduard Feireisl, Christian Klingenberg, Ondřej Kreml and Simon Markfelder On oscillatory solutions to the complete Euler system, arXiv:1710.10918

[6] Eduard Feireisl, Christian Klingenberg and Simon Markfelder On the low Mach number limit for the compressible Euler system, arXiv:1804.09509v1

[7] Tosio Kato Remarks on zero viscosity limit for nonstationary Navier-Stokes flows with boundary. Seminar on nonlinear partial differential equations, Math. Sci. Res. Inst. Publ., 2, Springer, New York, 1984

[8] Joseph Pedlosky Geophysical fluid dynamics, Springer, New York, 1987

Global solvability for the Cahn–Hilliard equations with dynamical boundary conditions

Naoto Kajiwara*

1. Introduction

Let $0 < T < \infty$ be a fixed time and $\Omega \subset \mathbb{R}^n$ $(n \geq 2)$ be a bounded domain whose boundary $\Gamma := \partial\Omega$ is smooth. Denote $J := (0, T)$, $Q := J \times \Omega$ and $\Sigma := J \times \Gamma$. We consider the following Cahn-Hilliard equation

$$\partial_t u - \Delta\mu = 0 \qquad \text{in } Q, \tag{1}$$

$$\mu = -\Delta u + F'(u) \qquad \text{in } Q. \tag{2}$$

Here u is the unknown order parameter, μ and F are the chemical and physical potentials, respectively. In this talk we improve one of following two boundary conditions:

$$\Delta\mu + b\partial_\nu\mu + c\mu = 0 \qquad \text{on } \Sigma, \tag{3}$$

$$-\alpha\Delta_\Gamma u + \partial_\nu u + G'(u) = \mu/b \qquad \text{on } \Sigma, \tag{4}$$

or

$$\Delta\mu + b\partial_\nu\mu - c\Delta_\Gamma\mu = 0 \qquad \text{on } \Sigma, \tag{5}$$

$$-\alpha\Delta_\Gamma u + \partial_\nu u + G'(u) = \mu/b \qquad \text{on } \Sigma. \tag{6}$$

The first one appears the case that the domain has porous (permeable) walls and the second one corresponds to non-permeable walls.

In the boundary conditions, α, b, c are positive constants, Δ_Γ is the Laplace-Beltrami operator on Γ, ν is the unit outward normal vector to Γ and G is the nonlinear term which comes from the surface energy. A typical example of F and G are $F(u) = \frac{1}{4}(u^2-1)^2$ and $G(u) = \frac{g_s}{2}u^2 - h_s u$ with $g_s > 0, h_s \neq 0$. Our method can treat the case $c = 0$. Since the method to get global well-posedness is the same for three types of boundary conditions, we focus on the first boundary conditions (3) (4) with $c > 0$.

The Cahn-Hilliard equation is known as describing the spinodal decomposition of binary mixtures, which we can see in the cooling processes of alloys, glasses or polymer mixtures (See [1,12]). For the study of the Cahn-Hilliard equation, various boundary conditions has been considered. At first, we would like to mention the following usual boundary conditions:

$$\partial_\nu\mu = 0 \qquad \text{on } \Sigma, \tag{7}$$

$$\partial_\nu u = 0 \qquad \text{on } \Sigma. \tag{8}$$

* Department of Mathematics, Faculty of Science and Technology, Tokyo University of Science.
e-mail: kajiwara_naoto@ma.noda.tus.ac.jp

The condition (7) derives that the mass $\int_\Omega u dx$ does not change for all time $t > 0$. The other condition (8) is called the variational boundary condition since it derives $\frac{d}{dt}E_\Omega(u) = -\|\nabla\mu\|_2^2$, where $E_\Omega(u)$ is the bulk free energy

$$E_\Omega(u) := \int_\Omega \left(\frac{1}{2}|\nabla u|^2 + F(u)\right) dx. \tag{9}$$

For the Cahn-Hilliard equation (1)-(2) with (7)-(8), the global well-posedness result and large time behavior were constructed. See [5,11,12].

However, it was proposed by physicists that one should add the following surface free energy

$$E_\Gamma(u|_\Gamma) := \int_\Gamma \left(\frac{\alpha}{2}|\nabla_\Gamma u|_\Gamma|^2 + G(u|_\Gamma)\right) dS \tag{10}$$

to the bulk free energy $E_\Omega(u)$, where ∇_Γ is the surface gradient. Together with the no-flux boundary condition (7), the total energy $E(u) = E_\Omega(u) + E_\Gamma(u|_\Gamma)$ satisfies $\frac{d}{dt}(E_\Omega(u) + E_\Gamma(u|_\Gamma)) = -\|\nabla\mu\|_2^2 - \|\mu_\Gamma\|_2^2$ when the dynamical boundary condition

$$\alpha\Delta_\Gamma u|_\Gamma - \partial_\nu u + G'(u) = u_t \qquad \text{on } \Sigma, \tag{11}$$

is posed. For this problem, see e.g. [2,8,9,10,13]. We would like to mention the paper [9]. The authors obtained results on the maximal L_p regularity and asymptotic behavior.

The so-called Wentzell boundary condition (3) was proposed in the paper [6]. Thanks to the boundary condition (4), the total energy $E(u)$ is non-increasing:

$$\frac{d}{dt}E(u(t)) = -\int_\Omega |\nabla\mu|^2 dx - \frac{c}{b}\int_\Gamma \mu^2 dS \le 0 \quad (t > 0). \tag{12}$$

Under these boundary conditions, volume conservation ($\frac{d}{dt}\int_\Omega u dx = 0$) no longer holds. Since $\frac{d}{dt}(\int_\Omega u dx + \int_\Gamma u\frac{dS}{b}) = -c\int_\Gamma \mu\frac{dS}{b}$, the case $c = 0$ corresponds to the case of the conservation of the total mass in the bulk and on the boundary. Moreover we have that the total mass decreases when $\int_\Gamma \mu dS$ is positive and vice verse. In the paper [6] the existence and uniqueness of a global solution were proved via the Caginalp type equation, which is the similar method in [10]. Later in [13] it was shown that each solution of this model converges to a steady state as time goes to infinity and their convergence rate by using Łojasiewics-Simon inequality.

In contrast to permeable walls, the Cahn-Hilliard equation (1)-(2) with (5)-(6) in the non-permeable walls was considered, e.g. [7]. The first boundary condition (5) represents the Cahn-Hilliard equation on the boundary Γ. The second boundary condition (6), which is also called the variational boundary condition, leads non-increasing for the total energy $E(u)$:

$$\frac{d}{dt}(E_\Omega(u) + E_\Gamma(u_\Gamma)) = -\|\nabla\mu\|_2^2 - \frac{c}{b}\|\nabla_\Gamma\mu_\Gamma\|_2^2. \tag{13}$$

In this system, $\int_\Omega u dx + \int_\Gamma u\frac{dS}{b}$ is a constant. The existence and uniqueness of weak solutions and their asymptotic behavior were shown in [7].

In this talk we show the global existence and uniqueness of the Cahn-Hilliard equation on permeable walls in maximal L_p regularity spaces. The strategy is as follows. First we prove the maximal L_p regularity for the linear equation which was treated by Denk-Prüss-Zacher [3]. The theorem states that the maximal L_p regularity of the linear equations is equivalent to the solvability for the corresponding ordinary differential equations. This is so-called Lopatinskii-Shapiro condition or complementing condition, and we are able to solve uniquely it. Then we give local well-popsedness of original non-linear Cahn–Hilliard equations by using fixed point argument as usual. At last, we extend this local solution to the global solution by a energy estimate and a priori estimate.

2. Linear theory

Before we study the linear Cahn-Hilliard equation, we would like to mention about the equations. We distinguish u, μ in the domain and u_Γ, μ_Γ on the boundary, but $u|_\Gamma = u_\Gamma, \mu|_\Gamma = \mu_\Gamma$, where "$|_\Gamma$" is the trace operator on the boundary Γ. Moreover for the boundary condition (3) and (5), we replace $(\Delta\mu)|_\Gamma$ with $\partial_t u_\Gamma$ since $\partial_t u = \Delta\mu$ in the domain Ω. The linear equations with inhomogeneous terms is as follows

$$(*)\begin{cases} \partial_t v + \Delta^2 v = f & \text{in} \quad Q, \\ \partial_t v_\Gamma - b\partial_\nu \Delta v + bc\partial_\nu v - \alpha bc\Delta_\Gamma v_\Gamma = g & \text{on} \quad \Sigma, \\ v|_\Gamma = v_\Gamma, \quad -(\Delta v)|_\Gamma - b\partial_\nu v + \alpha b\Delta_\Gamma v_\Gamma = h & \text{on} \quad \Sigma, \\ v(0) = v_0 \quad \text{in } \Omega, \quad v_\Gamma(0) = v_{0\Gamma} \quad \text{on } \Gamma. \end{cases}$$

Here the functions $f, g, h, v_0, v_{0\Gamma}$ are given and (v, v_Γ) are unknown functions defined on Ω and Γ.

Throughout this talk, let $1 < p < \infty$. From the maximal L_p regularity class $\mathbb{E}_1(J) := W_p^1(J; L_p(\Omega)) \cap L_p(J; W_p^4(\Omega))$, we characterize the spaces on data (f, g, h), solution v_Γ and initial data $(v_0, v_{0\Gamma})$. By considering the differential operator $\partial_t + \Delta^2, \partial_\nu\Delta, \Delta \cdot |_\Gamma$ to $\mathbb{E}_1(J)$, we have that

$$\begin{aligned} &(f, g, h) \in \mathbb{F}(J) := \mathbb{F}_1(J) \times \mathbb{F}_2(J) \times \mathbb{F}_3(J) \\ &:= L_p(J; L_p(\Omega)) \times \left(W_p^{\kappa_0}(J; L_p(\Gamma)) \cap L_p(J; W_p^{4\kappa_0}(\Gamma))\right) \times \left(W_p^{\kappa_1}(J; L_p(\Gamma)) \cap L_p(J; W_p^{4\kappa_1}(\Gamma))\right) \end{aligned}$$

with $\kappa_0 = 1/4 - 1/(4p), \kappa_1 = 1/2 - 1/(4p)$. This is based on a trace theorem for parabolic spaces. Moreover, from the structure on the equations, the optimal class for v_Γ is

$$v_\Gamma \in \mathbb{E}_2(J) := W_p^{1+\kappa_0}(J; L_p(\Gamma)) \cap W_p^1(J; W_p^{4\kappa_0}(\Gamma)) \cap L_p(J; W_p^{2+4\kappa_1}(\Gamma)).$$

The initial data is

$$(v_0, v_{0\Gamma}) \in \pi\mathbb{E}_1 \times \pi\mathbb{E}_2 := B_{p,p}^{4-4/p}(\Omega) \times B_{p,p}^{4-4/p}(\Gamma)$$

by operating the initial trace on $\mathbb{E}_1(J), \mathbb{E}_2(J)$. The details will be in the talk.

To see Lopatinskii-Shapiro condition, we need to solve the ordinary differential equation

$$\begin{cases} \left((\lambda + (-|\xi'|^2 + \partial_y^2)^2\right) v(y) = 0 \quad (y > 0), & (14) \\ -b(-\partial_y)(-|\xi'|^2 + \partial_y^2)v(0) + \left((\lambda - \alpha bc(-|\xi'|^2)\right) \sigma = 0, & (15) \\ v(0) - \sigma = 0, & (16) \\ -(-|\xi'|^2 + \partial_y^2)v(0) + \alpha b(-|\xi'|^2)\sigma = 0. & (17) \end{cases}$$

This ODE is uniquely solved by $(v, \sigma) = (0, 0) \in C_0^4([0, \infty); \mathbb{C}) \times \mathbb{C}$. Therefore based on the paper [DHP], we have the following linear theory.

Theorem 2.1. *Let $\Omega \subset \mathbb{R}^n$ be a bounded domain of class C^4 and $1 < p < \infty$ be $p \neq 5/4, 5/2, 5$. Then the linearized Cahn-Hilliard equation $(*)$ admits a unique solution $(v, v_\Gamma) \in \mathbb{E}_1(J) \times \mathbb{E}_2(J)$ if and only if $(f, g, h) \in \mathbb{F}(J)$, $(v_0, v_{0\Gamma}) \in \pi\mathbb{E}_1 \times \pi\mathbb{E}_2$ and the compatibility conditions*

$$\begin{aligned} &v_0|_\Gamma = v_{0\Gamma} && \text{on } \Gamma \quad \text{if} \quad p > 5/4, \\ &-(\Delta v_0)|_\Gamma - b\partial_\nu v_{0\Gamma} + \alpha b \Delta_\Gamma v_{0\Gamma} = h|_{t=0} && \text{on } \Gamma \quad \text{if} \quad p > 5/2, \\ &g|_{t=0} + b\partial_\nu \Delta v_0 - bc\partial_\nu v_0 + \alpha bc \Delta_\Gamma v_{0\Gamma} \in B^{1-5/p}_{p,p}(\Gamma) && \quad \text{if} \quad p > 5. \end{aligned}$$

are satisfied.

For the eliminated exponent $p = 5/4, 5/2, 5$, it is hard to characterize the compatibility conditions. However in these cases above condition is a sufficient condition to make a unique solution.

3. Non-linear theory

3.1. Local well-posedness

We prove the local well-posedness for the Cahn-Hilliard equations on permeable walls

$$(\mathrm{CH})_{\mathrm{per.}} \begin{cases} \partial_t u + \Delta^2 u = \Delta F'(u) + f & \text{in} \quad Q, \\ \partial_t u_\Gamma - b\partial_\nu \Delta u + bc\partial_\nu u - \alpha bc \Delta_\Gamma u_\Gamma = -b\partial_\nu F'(u) - bcG'(u_\Gamma) + g & \text{on} \quad \Sigma, \\ u|_\Gamma = u_\Gamma, \quad -(\Delta u)|_\Gamma - b\partial_\nu u + \alpha b \Delta_\Gamma u_\Gamma = -F'(u)|_\Gamma + bG'(u_\Gamma) & \text{on} \quad \Sigma, \\ u(0) = u_0 \quad \text{in } \Omega, \quad u_\Gamma(0) = u_{0\Gamma} \quad \text{on } \Gamma. \end{cases}$$

Here $F \in C^{4-}(\mathbb{R}), G \in C^{2-}(\mathbb{R})$, i.e. $F \in C^3(\mathbb{R})$ and $F''' \in \mathrm{Lip}(\mathbb{R})$ and G is also defined that way. The original equation we explained in the introduction is the case $f = g = 0$, but we are able to add non-homogeneous terms f, g. We will prove existence and uniqueness of this solution. First we need to consider the compatibility conditions for the boundary. Let $(g, u_0, u_{0\Gamma}) \in \mathbb{F}_2(J) \times \pi\mathbb{E}_1 \times \pi\mathbb{E}_2$ satisfy the following compatibility conditions

$$u_0|_\Gamma = u_{0\Gamma} \quad \text{on } \Gamma \quad \text{if } p > 5/4, \tag{18}$$

$$-(\Delta u_0)|_\Gamma - b\partial_\nu u_{0\Gamma} + \alpha b \Delta_\Gamma u_{0\Gamma} = -F'(u_0)|_\Gamma + bG'(u_{0\Gamma}) \quad \text{on } \Gamma \quad \text{if } p > 5/2, \tag{19}$$

$$g|_{t=0} + b\partial_\nu \Delta u_0 - bc\partial_\nu u_0 + \alpha bc \Delta_\Gamma u_{0\Gamma} - b\partial_\nu F'(u_0) - bcG'(u_{0\Gamma}) \in B^{1-5/p}_{p,p}(\Gamma) \text{ if } p > 5. \tag{20}$$

We use the notation $J_a := (0, a) \subset J$, $\mathbb{F}(a)$ and $\mathbb{E}_i(a)(i = 1, 2)$ to indicate the time interval under consideration.

The local well-posedness is as follows.

Theorem 3.1. *Let $1 < p < \infty$ be $p > (n+4)/4$ and $p \neq 5/2, 5$, and let $(f, g, u_0, u_{0\Gamma}) \in \mathbb{F}_1(J) \times \mathbb{F}_2(J) \times \pi\mathbb{E}_1 \times \pi\mathbb{E}_2$ satisfy the compatibility conditions* (18)-(20) *and $F \in C^{4-}(\mathbb{R}), G \in C^{2-}(\mathbb{R})$. Then there is an $a \in (0, T]$ and a unique solution $(u, u_\Gamma) \in \mathbb{E}_1(a) \times \mathbb{E}_2(a)$ of $(\mathrm{CH})_{\mathrm{per.}}$.*

The proof is based on the contraction mapping principle. Since we restrict the time interval. we are able to control the non-linear terms.

3.2. Global well-posedness

In this section we consider the global solution for the equation with non-homogeneous terms f, g;

$$\begin{cases} \partial_t u = \Delta\mu + f, \quad \mu = -\Delta u + F'(u) & \text{in} \quad Q, \\ \partial_t u_\Gamma + b\partial_\nu \mu + c\mu_\Gamma = g, \quad -\alpha\Delta_\Gamma u_\Gamma + \partial_\nu u + G'(u_\Gamma) = \frac{\mu_\Gamma}{b} & \text{on} \quad \Sigma, \\ u|_\Gamma = u_\Gamma, \quad \mu|_\Gamma = \mu_\Gamma & \text{on} \quad \Sigma, \\ u(0) = u_0 \quad \text{in } \Omega, \quad u_\Gamma(0) = u_{0\Gamma} \quad \text{on } \Gamma. \end{cases}$$

As we explained in introduction, the unknown functions are only u and u_Γ though we use μ and μ_Γ. By the previous subsection there is a unique solution on some maximal time interval $J_{\max} = (0, a_{\max})$. We fix some arbitrary J_a for $0 < a \leq a_{\max} (\leq T)$ and show the boundedness near the point $t = a$ from a priori estimate derived from energy estimate.

From the energy structure of the equations we have

$$\frac{d}{dt}E(u, u_\Gamma) + C_1(|\nabla\mu|_2^2 + |\mu_\Gamma|_{2,\Gamma}^2) \leq C_2 \left(\frac{1}{2}|u|_2^2 + \frac{1}{2}|\nabla u|_2^2 + \frac{1}{2b}|u_\Gamma|_{2,\Gamma}^2\right) + C_3(|f|_2^2 + |g|_{2,\Gamma}^2)$$

for some $C_i > 0$ $(i = 1, 2, 3)$.
We assume that F and G satisfy the following condition:

$$\begin{cases} F(s) \geq -c_1, & c_1 > 0, \ s \in \mathbb{R}, \\ G(s) \geq -\frac{1}{2b}s^2 - c_2, & c_2 > 0, \ s \in \mathbb{R}. \end{cases} \tag{21}$$

Under these assumptions we have

$$E(u, u_\Gamma) \leq C \left(E(u_0, u_{0\Gamma}) + \int_0^T (|f|_2^2 + |g|_{2,\Gamma}^2 + 1)\right)$$

and

$$(u, u_\Gamma) \in L_\infty(J_{a_{\max}}, W_2^1(\Omega) \times W_2^1(\Gamma)) \tag{22}$$

when $(f, g, u_0, u_{0\Gamma}) \in \mathbb{F}_1(T) \times \mathbb{F}_2(T) \times \pi\mathbb{E}_1 \times \pi\mathbb{E}_2$ with $p \geq 2$ and $p > (n+4)/4$. Here the constant C depends only on $T > 0$ and is independent of $a_{\max}$.
To get the global solution we have to assume that the dimension $n = 2, 3$ and some growth condition on F and G:

$$\begin{cases} |F'''(s)| \leq C(1 + |s|^\beta), & s \in \mathbb{R}, \\ |G'(s)| \leq C(1 + |s|^{\beta+2}), & s \in \mathbb{R}, \end{cases} \quad \text{with} \quad \begin{cases} \beta < 3 \text{ in the case } n = 3, \\ \beta > 0 \text{ in the case } n = 2. \end{cases} \tag{23}$$

Lemma 3.2. *Suppose $2 \le p < \infty$, $n = 2, 3$, the function F and G satisfy (21) and (23) and let $(u, u_\Gamma) \in \mathbb{E}(a)$ be the solution of $(\mathrm{CH})_{\mathrm{per.}}$. Then there exist constants $m, C > 0$ and $\delta \in (0, 1)$, independent of $a > 0$, such that*

$$\begin{aligned}&\|\Delta F'(u)\|_{\mathbb{F}_1(a)} + \|\partial_\nu F'(u)\|_{\mathbb{F}_2(a)} + \|G'(u_\Gamma)\|_{\mathbb{F}_2(a)} + \|F'(u)|_\Gamma\|_{\mathbb{F}_3(a)} + \|G'(u_\Gamma)\|_{\mathbb{F}_3(a)}\\ \le& C(1 + \|u\|^\delta_{\mathbb{E}_1(a)}\|u\|^m_{L_\infty(J_a, W^1_2(\Omega))}).\end{aligned}$$

Combining maximal L_p regularity estimate,

$$\begin{aligned}&\|(u, u_\Gamma)\|_{\mathbb{E}(a)}\\ \le& C(\|\Delta F'(u)\|_{\mathbb{F}_1(a)} + \|\partial_\nu F'(u)\|_{\mathbb{F}_2(a)} + \|G'(u_\Gamma)\|_{\mathbb{F}_2(a)} + \|F'(u)|_\Gamma\|_{\mathbb{F}_3(a)}\\ &\qquad + \|G'(u_\Gamma)\|_{\mathbb{F}_2(a)} + \|f\|_{\mathbb{F}_1(T)} + \|g\|_{\mathbb{F}_2(T)} + \|(u_0, u_{0\Gamma})\|_{\pi\mathbb{E}_1\times\pi\mathbb{E}_2})\\ \le& \widetilde{C}(1 + \|u\|^\delta_{\mathbb{E}_1(a)}), \qquad (24)\end{aligned}$$

where the constant $\widetilde{C}$ is independent of a. Hence $\|u\|_{\mathbb{E}_1(a)}$ is bounded and it derives the boundedness of $\|u_\Gamma\|_{\mathbb{E}_2(a)}$. Therefore the solution $(u, u_\Gamma) \in \mathbb{E}_1(a) \times \mathbb{E}_2(a)$ is global solution, i.e. $a_{\max} = T$. We obtain the following main theorem of this paper.

Theorem 3.3. *Suppose $2 \le p < \infty$, $p \ne 5/2, 5$, $n = 2, 3$ and that the function F and G satisfy (21) and (23). Then for any $(f, g, u_0, u_{0\Gamma}) \in \mathbb{F}_1(T) \times \mathbb{F}_2(T) \times \pi\mathbb{E}_1 \times \pi\mathbb{E}_2$ satisfying the compatibility conditions (18)-(20), there exists a unique global solution $(u, u_\Gamma) \in \mathbb{E}_1(T) \times \mathbb{E}_2(T)$ of $(\mathrm{CH})_{\mathrm{per.}}$.*

References

[1] J. W. Cahn, J. E. Hilliard, Free energy of a nonuniform system. I. interfacial free energy. The Journal of Chemical physics, **28** No.2 (1958) 258–267.

[2] R. Chill, E. Fašangová, J. Prüss. Convergenec to steady state of solutions of the Cahn–Hilliard and Caginalp equations with dynamic boundary conditions. Math. Nachr., **279** No.13-14 (2006) 1448–1462.

[3] R. Denk, J. Prüss, R. Zacher, Maximal L_p-regularity of parabolic problems with boundary dynamics of relaxation type, J. Funct. Anal. ,**255** No.11 (2008) 3149–3187.

[4] C. G. Gal, A Cahn–Hilliard model in bounded domains with permeable walls, Math. Methods Appl. Sci. , **29** No.17 (2006) 2009–2036.

[5] C. Elliiott, S. Zheng. On the Cahn–Hilliard equation. Arch. Rational Mech. Anal., **96** No.4 (1986) 339–357.

[6] C. G. Gal. A Cahn-Hilliard model in bounded domains with permeable walls. Math. Methods Appl. Sci., **29** No.17 (2006) 2009–2036.

[7] G. R. Goldstein, A. Miranville, G. Schimperna. A Cahn-Hilliard model in a domain with non-permeable walls. Phys. D, **240**, No.8, (2011) 754–766.

[8] J. Prüss, R. Racke, S. Zheng. Maximal regularity and asymptotic behavior of solutions for the Cahn-Hilliard equation with dynamic boundary conditions. Ann. Mat. Pura Appl. (4), Vol. 185, No. 4, (2006) 627–648.

[9] J. Prüss, M. Wilke, Maximal L_p-regularity and long-time behaviour of the non-isothermal Cahn–Hilliard equation with dynamic boundary conditions, Oper. Theory Adv. Appl., **168** (2006) 209–236.

[10] R. Racke, S. Zheng. The Cahn-Hilliard equation with dynamic boundary con- ditions. Adv. Diff. Eq., **8**, No. 1 (2003) 83–110.
[11] P. Rybka, K. Hoffmann. Convergence of solutions to Cahn-Hilliard equation. Comm. PDE, **24**, No. 5-6 (1999) 1055–1077.
[12] R. Temam. Infinite-dimensional dynamical systems in mechanics and physics, Vol. 68 of Applied Mathematical Sciences. Springer-Verlag, New York, second edition, 1997.
[13] H. Wu, S. Zheng. Convergence to equilibrium for the Cahn-Hilliard equation with dynamic boundary conditions. J. Diff. Eq., **204**, No. 2 (2004) 511–531.

On the linear response of equilibrium vortices [1] [2]

Hiroshi Ohtsuka[3]
Faculty of Mathematics and Physics,
Institute of Science and Engineering,
Kanazawa University

This is a joint work with Y. Yatsuyanagi (Shizuoka University) and T. Hatori (National Institute for Fusion Science).

1 Introduction

Motivated by the ring hole phenomenon observed in a confined non-neutral plasma (electron gas), we are interested in *the linear response* for equilibrium vortices. The motion of guiding centers of electrons composing the plasma are known to be described by the Hamiltonian of vortices in two dimensional non-viscous incompressible fluid and the system of vortices is a famous simplyfied model describing the motion of the fluid, which we will review below briefly. The system of vortices is also know to be a stage of *self-organization* of large scale structure since Onsager pointed it out by the possibility of the *negative* temperature equilibrium state [11], see also [3]. We note that the Jupiter's great red spot is considered to be the most famous example of the large scale structure in the fluid motion. On the other hand, the ring hole is observed around a clump of electrons, which corresponds to the large scale structure in the system of vortices, that is, the ring hole will be described by the detailed study around the large scale structure appearing in the equilibrium vortices. Our strategy to describe the ring hole is to study *the correlation function* of vortices via *the linear response theory* à la Green-Kubo. Unfortunately we get, up to now, only a story to reach the conclusion, but we think it contains a plenty of mathematically interesting problems. In this talk we will present the story and answers to some of the problem in it. For more information on the background materials, see [4] for non-neutral plasmas, [13] for ring hole phenomenon, [1, 9, 5] for fluid motions and vortices, and [7] for the linear response theory, for example.

2 System of vortices

Let Λ be a bounded domain in $\mathbf{R}^2$ with smooth boundary $\partial\Lambda$. To simplify the presentation, we assume Λ is simply connected throughout this talk. Then the motion of nonviscous incompressible fluid in Λ is described by the equation for the vorticity field $\omega = \operatorname{curl} \boldsymbol{v} := \frac{\partial v_2}{\partial x_1} - \frac{\partial v_1}{\partial x_2}$:

$$\frac{\partial \omega}{\partial t} + (\boldsymbol{v} \cdot \nabla)\, \omega = 0, \tag{1}$$

where $\boldsymbol{v} = (v_1(x,t), v_2(x,t))$ is the velocity field satisfying the incompressible condition and the usual slip boundary condition:

$$\operatorname{div} \boldsymbol{v} := \frac{\partial v_1}{\partial x_1} + \frac{\partial v_2}{\partial x_2} = 0, \quad \boldsymbol{v} \cdot \boldsymbol{\nu} = 0 \quad \text{on } \partial\Lambda.$$

[1] "The 44th Sapporo Symposium on Partial Differential Equations" at Hokkaido University (August 5–7, 2019).

[2] This work is supported by Grant-in-Aid for Scientific Research (A)26247013 and (C)15K04951, Japan Society for the Promotion of Science.

[3] 大塚浩史 (金沢大学理工研究域数物科学系), e-mail:ohtsuka@se.kanazawa-u.ac.jp

Using the solution ψ of the Poisson equation

$$-\Delta\psi = \omega \quad \text{in } \Lambda, \qquad \psi = 0 \quad \text{on } \partial\Lambda,$$

the velocity field $\boldsymbol{v}$ is represented as follows:

$$\boldsymbol{v} = \nabla^{\perp}\psi = \left(\frac{\partial\psi}{\partial x_2}, -\frac{\partial\psi}{\partial x_1}\right).$$

The function ψ is called *the stream function* of the velocity field $\boldsymbol{v}$ and is uniquely determined by ω under appropriate assumptions.

The N-points *vortices* are nothing but the set $\{(x_j(t), \Omega_j)\}_{j=1,\cdots,N} \subset \Lambda \times \mathbf{R}$ that composes the vorticity field $\omega(x,t) = \sum_{j=1}^{N} \Omega_j \delta_{x_j(t)}$ satisfying the vorticity equation (1), where δ_p is the Dirac measure supported at $p \in \Lambda$. We call Ω_j the intensity of j-th vortex. From Kelvin's circulation law, the intensity Ω_j and the form $\sum_{j=1}^{N} \Omega_j \delta_{x_j}$ are considered to be preserved during the time evolution. However, it still seems to exist a problem how to recognize the vortices as a solution of vorticity equation (1) since the singularity of vorticity field like $\sum_{j=1}^{N} \Omega_j \delta_{x_j}$ is too strong to assume $\omega(x,t) = \sum_{j=1}^{N} \Omega_j \delta_{x_j(t)}$ to be a solution of (1) even in a weak sense.

Nevertheless, vortices are considered to obey the following system of ordinary differential equations:

$$\Omega_j \frac{dx_j}{dt} = \nabla_j^{\perp} H^N(x_1, \cdots, x_N) \left(:= \left(\frac{\partial H^N}{\partial x_{i,2}}, -\frac{\partial H^N}{\partial x_{i,1}}\right)\right), \tag{2}$$

where H^N is the following funtion on $\Lambda^N \subset \mathbf{R}^{2N}$:

$$H^N(x_1, \cdots, x_N) := \frac{1}{2}\sum_{j=1}^{N} \Omega_j^2 K(x_j, x_j) + \frac{1}{2} \sum_{1 \le j,k \le N,\, j \ne k} \Omega_j \Omega_k G(x_j, x_k).$$

Here $G(x,y)$ is the Green function of $-\Delta$ with the Dirichlet boundary condition, i.e., $G(\cdot, y)$ satisfies

$$-\Delta G(\cdot, y) = \delta_y \quad \text{in } \Lambda, \qquad G(\cdot, y) = 0 \quad \text{on } \partial\Lambda,$$

and $K(x,y)$ is it's regular part defined as follows:

$$G(x,y) = \frac{1}{2\pi} \log |x-y|^{-1} + K(x,y).$$

In this talk, we will not take care of the validity of the theory of the vortices and we will start with the system (2).

3 Equilibrium statistical mechanics of vortices

H^N is usually called *the Kirchhoff-Routh path function* and the value of H^N is preserved under the time evolution. Therefore, we are able to assume that the system of vortices (2) forms a Hamiltonian system with the Hamiltonian H^N and consequently we are able to develop the statistical mechanics for equilibrium vortices. To this purpose, we introduce the canonical (Gibbs) distribution function for equilibrium vortices:

$$\mu^N(x_1, \cdots, x_N) := \frac{e^{-\beta H^N(x_1, \cdots, x_N)}}{\int_{\Lambda^N} e^{-\beta H^N(x_1, \cdots, x_N)}},$$

where $\beta \in \mathbf{R}$ is a parameter called *the inverse temperature*. We are interested in the *negative temperature case* $\beta < 0$ according to the Onsager's observation [11].

Here we define *1 and 2 body distribution functions*:

$$P_1^N(x_1) := \int_{\Lambda^{N-1}} \mu^N(x_1, x_2, \cdots, x_N) dx_2 \cdots dx_N,$$
$$P_2^N(x_1, x_2) := \int_{\Lambda^{N-2}} \mu^N(x_1, x_2, x_3, \cdots, x_N) dx_3 \cdots dx_N,$$

which represent the probability density functions for a vortex at $x_1 \in \Lambda$ or vortices at $(x_1, x_2) \in \Lambda^2$ in the equilibrium N-vortices. Now we define the *2-body correlation function* $g^N(x, y)$ from the following relation:

$$P_2^N(x_1, x_2) = P_1^N(x_1) P_2^N(x_2)(1 + g^N(x_1, x_2))$$

The conditional probability $P(x|y)$ of a vorex at x when the second vortex is at y is given by

$$P^N(x_1|x_2) = P_1^N(x_1)(1 + g^N(x_1, x_2)).$$

Therefore $g^N(x, y)$ will represent the deformation (*responce*) of the vortex density by the existence of one vortex at y.

We are interested in the study of the pure electron plasma and in this case the intensity Ω_j, which corresponds to the electric charge of an electron, is constant. Therefore we assume $\Omega_j \equiv \Omega > 0$. Then the Hamiltonian $H^N(x_1, \cdots, x_N)$ is invariant under the permutation of $(x_1, \cdots, x_N)$. Using this symmetry, Caglioti et al. [2] and Kiessling[6], see also [8], proved the following facts:

Fact 1 (Caglioti et al.[2] and Kiessling[6])**.** Suppose $\Omega = \widetilde{\Omega}/N$ for some $\widetilde{\Omega} > 0$ and $\beta/N := \widetilde{\beta} \in (-8\pi, \infty)$, we get

$$P_1^N(x) \longrightarrow P(x), \quad P_2^N(x, y) \longrightarrow P(x)P(y) \quad \text{as } N \longrightarrow \infty$$

weakly in the sense of measures, where $P(x)$ satisfies *the self-consistency equation*

$$P(x) = \frac{e^{-\widetilde{\beta}\widetilde{\Omega}^2 GP(x)}}{\int_\Lambda e^{-\widetilde{\beta}\widetilde{\Omega}^2 GP(x)} dx} \tag{3}$$

where $GP(x) := \int_\Omega G(x, y)P(y)dy$.

We note that here also we used the fact that Λ is simply connected implicitly in order to use the famous result of Suzuki [14].

From Fact 1, we are able to observe that

$$g^N(x_1, x_2) \longrightarrow 0$$

at least formally. In order to see the fine asymptotic behavior of the correlation function $g^N(x_1, x_2)$ as $N \longrightarrow \infty$, we study *the linear response* of equilibrium vortices.

4 The linear response of equiriblium vortices

To get information of $P_2^N(x,y)$, we slightly perturb the Hamiltonian H^N:

$$H_c^N(x_1,\cdots,x_N) := H^N(x_1,\cdots,x_N) + \Omega c\sum_{j=1}^N \psi_e(x_j),$$

where $c \in \mathbf{R}$ is a parameter representing the strength of the perturbation and $\psi_e(x)$ is an arbitrary function that represents the profile of the external potential field. We set

$$\mu_c^N(x_1,\cdots,x_N) = \frac{e^{-\beta H_c^N(x_1,\cdots,x_N)}}{\int_{\Lambda^N} e^{-\beta H_c^N(x_1,\cdots,x_N)}}$$

and also set $P_{c,1}^N(x)$, $P_{c,2}^N(x,y)$ similarly. We note that $\mu^N = \mu_0^N$, $P_1^N(x) = P_{0,1}^N(x)$, and $P_2^N(x,y) = P_{0,2}^N(x,y)$.

From the symmetry of H^N and H_c^N, we get the following formula

$$\begin{aligned}\frac{\partial}{\partial c}P_{c,1}^N\Big|_{c=0}(x_1) = (-\beta\Omega)\left\{P_1^N(x_1)\psi_e(x) + (N-1)\int_{\Lambda^2} P_2^N(x_1,x_2)\psi_e(x_2)dx_2\right\}\\ + \beta\Omega P_1^N(x_1)N\int_\Lambda P_1^N(x_2)\psi_e(x_2)dx_2,\end{aligned}$$

which is expressed as *a fluctuation-response formulra* à la Green-Kubo:

$$\frac{\partial}{\partial c}\omega_c^N\Big|_{c=0} = -\beta\int_\Omega <\delta\omega(x)\delta\omega(y)>\psi_e(y)dy. \tag{4}$$

Here *the mean vorticity field* ω^N (and ω_c^N similarily), *the fluctuation* $\delta\omega$, and *the mean correlation* $<\delta\omega(x)\delta\omega(y)>$ of fluctuation corresponding to the vortices $\sum_{j=1}^N \Omega\delta_{x_j}$ are defined as follows:

$$\begin{aligned}\omega^N(x) &:= \left\langle\sum_{j=1}^N \Omega\delta_{x_j}(x)\right\rangle = \int_{\Lambda^N}\mu^N(x_1,\cdots,x_N)\sum_{j=1}^N\Omega\delta_{x_j}(x)dx_1\cdots dx_N = N\Omega P_1^N(x).\\ \delta\omega(x) &:= \sum_{j=1}^N\Omega\delta_{x_j}(x) - \left\langle\sum_{j=1}^N\Omega\delta_{x_j}(x)\right\rangle = \sum_{j=1}^N\Omega\delta_{x_j}(x) - \omega^N(x),\\ <\delta\omega(x)\delta\omega(y)> &:= \int_{\Lambda^N}\mu^N(x_1,\cdots,x_N)\delta\omega(x)\delta\omega(y)dx_1\cdots dx_N.\end{aligned}$$

Unfortunately we must assume here, up to now, a physical assumption

$$<\delta\omega(x)\delta\omega(y)> = \Omega\omega^N(x)\delta(y-x) + \omega^N(x)\omega^N(y)g^N(x,y),$$

which is call *the Ornstein-Zernike formula*. Then we get

$$\frac{\partial}{\partial c}\omega_c^N\Big|_{c=0} = -\beta\Omega\omega^N(x)\psi_e(x) - \beta\omega^N(x)\int_\Lambda g^N(x,y)\omega^N(y)\psi_e(y)dy.$$

Here we set $\Omega = \widetilde{\Omega}/N$、$\beta/N = \widetilde{\beta}$ and take $N\longrightarrow\infty$. Then we get, at least formally,

$$\frac{\partial}{\partial c}\omega_c\Big|_{c=0} = -\widetilde{\beta}\widetilde{\Omega}\omega(x)\psi_e(x) - \widetilde{\beta}\omega(x)\int_\Lambda g(x,y)\omega(y)\psi_e(y)dy, \tag{5}$$

where

$$\omega_c(x) := \lim_{N\longrightarrow\infty} \omega_c^N(x) = \widetilde{\Omega} P_{c,1}(x),$$
$$g(x,y) := \lim_{N\longrightarrow\infty} N g^N(x,y).$$

Of course this is only an observation but we think this $g(x,y)$, not $\lim_{N\longrightarrow\infty} g^N(x,y)$, would describe our target phenomenon.

In order to get the infromation of $g(x,y)$, we observe another linear response. Actually we observe the linear response of the mean field, that is, the solution of the self-consistency equation (3). According to the procedure of Caglioti et al. and Kiessling, the origin of which goes back to Messer-Sphon [10], we reach the self-consistency equation at $N \longrightarrow \infty$ for the perturbed Hamiltonian system:

$$P_{c,1}(x) = \frac{e^{-\widetilde{\beta}\left(\widetilde{\Omega}^2 G P_{c,1}(x) + \widetilde{\Omega} t \psi_e(x)\right)}}{\int_\Lambda e^{-\widetilde{\beta}\left(\widetilde{\Omega}^2 G P_{c,1}(x) + \widetilde{\Omega} t \psi_e(x)\right)} dx}. \tag{6}$$

Differentiating this with respect to c, we get

$$\left.\frac{\partial}{\partial c}\omega_c\right|_{c=0} = -\widetilde{\beta}\widetilde{\Omega}\omega(x)\left(G\left.\frac{\partial \omega_c}{\partial c}\right|_{c=0} + \psi_e(x)\right) + \widetilde{\beta}\omega(x)\int_\Lambda \omega(x)\left(G\left.\frac{\partial \omega_c}{\partial c}\right|_{c=0} + \psi_e(x)\right). \tag{7}$$

Comparing (5) and (7), that is, if it hold that

$$\left.\frac{\partial}{\partial c}\left(\lim_{N\longrightarrow\infty}\omega_c^N\right)\right|_{c=0} = \lim_{N\longrightarrow\infty}\left(\left.\frac{\partial}{\partial c}\omega_c^N\right|_{c=0}\right), \tag{8}$$

we finally reach the relation

$$\int_\Lambda g(x,y)\omega(y)\psi_e(y)dy = \widetilde{\Omega} G\left.\frac{\partial \omega_c}{\partial c}\right|_{c=0} - \int_\Lambda \omega(x)\left(G\left.\frac{\partial \omega_c}{\partial c}\right|_{c=0} + \psi_e(x)\right).$$

Applying the linearlized operator $-\Delta + \widetilde{\beta}\widetilde{\Omega}\omega(x)$ of (3) to the both sides, finally we get the following relation:

$$\int_\Lambda (-\Delta_x + \widetilde{\beta}\widetilde{\Omega}\omega(x))\frac{g(x,y)}{-\widetilde{\beta}\widetilde{\Omega}^2}\omega(y)\psi_e(y)dy = \omega(x)\psi_e(x).$$

Since ψ_e is arbitrary, we get

$$(-\Delta_x + \widetilde{\beta}\widetilde{\Omega}\omega(x))\frac{g(x,y)}{-\widetilde{\beta}\widetilde{\Omega}^2} = \delta_y, \tag{9}$$

which might be the equation of our target function $g(x,y)$.

Almost all of the argument of this section is only an observation, but we think that the justification of this story, especially whether the commutativity of two limits (8) holds or not, seems to be an important meaning not only in mathematics but also in physics.

5 The solution of Prajapat-Tarantello

Finally we give some tiny mathematical facts concerning the solution of (9). We set the right-hand side of (7) as $-\widetilde{\beta}\widetilde{\Omega}\omega(x)\mathscr{G}$, then we get the equation concerning $\mathscr{G}$:

$$(-\Delta + \widetilde{\beta}\widetilde{\Omega}\omega(x))\mathscr{G} = -\Delta\psi_e.$$

This means that our target $g(x,y)$, the solution of (9), is the linear response to $-\Delta\psi_e = \delta_y$ (*impulse*). Indeed, we set

$$u_c(x) := -\widetilde{\beta}\left(\widetilde{\Omega}^2 G P_c(x) + \widetilde{\Omega} c \psi_e(x)\right).$$

Then u_c satisfies

$$-\Delta u_c = (-\widetilde{\beta}\widetilde{\Omega}^2)\frac{e^{u_c}}{\int_\Lambda e^{u_c}} + (-\widetilde{\beta}\widetilde{\Omega})c\delta_y. \tag{10}$$

From this equation, we are able to observe $\widetilde{\Omega}\,\frac{\partial u_c}{\partial c}\big|_{c=0} = g(\cdot, y)$. Here we should note that, strictly speaking, still we have the problem how to determine the boundary condition of $\mathscr{G}$.

Fortunately, we know one one-parameter family ω_c of the purterbed self-consistency equation (6) for the special case $\Lambda = B_1(0) := \{x \in \mathbf{R}^2 \,|\, |x| < 1\}$ with $-\Delta\psi_e(x) = \delta_0(x)$. Since $G(x,0) = \frac{1}{2\pi}\log|x|^{-1}$, the equation (6) is reduced to

$$-\Delta v_c = \lambda_c |x|^{\frac{\widetilde{\beta}\widetilde{\Omega}c}{2\pi}} e^{v_c} \quad \text{in } B_1(0), \tag{11}$$

where

$$v_c = u_c - (-\widetilde{\beta}\widetilde{\Omega}c)G(x,0), \quad \lambda_c = \frac{-\widetilde{\beta}\widetilde{\Omega}^2}{\int_{B_1(0)} e^{u_c}}.$$

Concerning this equation, we know the classification result of the solution by Prajapat-Tarantello[12]:

Fact 2 (Prajapat-Tarantello[12])**.** Let w be a solution of

$$-\Delta w = 8\pi n|x|^{2(n-1)}e^w \quad \text{in } \mathbf{R}^2, \quad \int_{\mathbf{R}^2} |x|^{2(n-1)}e^w = 1 \tag{12}$$

with the parameter $n > 0$ satisfying $0 < |n-1| \ll 1$. Then there exists $\varepsilon > 0$ such that

$$w(x) = w_*(\varepsilon x) + 2n\log\varepsilon, \tag{13}$$

where

$$w_*(x) = \log\frac{1}{(1+|x|^{2n})^2} + \log\frac{n}{\pi}.$$

Taking parameter n satisfying

$$\frac{\widetilde{\beta}\widetilde{\Omega}c}{2\pi} = 2(n-1), \tag{14}$$

the equation (12) coinside with (11) up to the multiplication of constant. On the other hand, the solution of (11) has an extra freedom represented by the parameter ε and we choose it to satisfy

$$\begin{aligned} \lambda_c = 8\pi n \quad &\Leftrightarrow \quad \frac{-\widetilde{\beta}\widetilde{\Omega}^2}{\int_{B_1(0)} e^{u_c}} = 8\pi n, \\ &\Leftrightarrow \quad -\widetilde{\beta}\widetilde{\Omega}^2 = \frac{8\pi n\varepsilon^{2n}}{1+\varepsilon^{2n}}. \end{aligned} \tag{15}$$

Then the solution of (13) gives the solution of (11), that is,

$$\begin{aligned} u_c(x) &= v_c(x) - \widetilde{\beta}\widetilde{\Omega}cG(x,0) \\ &= w_*(\varepsilon x) + 2n\log\varepsilon - \widetilde{\beta}\widetilde{\Omega}cG(x,0), \end{aligned}$$

where $n = n(c)$ and $\varepsilon = \varepsilon(c) = \varepsilon(n(c))$ are determined by (14) and (15). The solution obtained via this procedure is differentiable with respect to c and finally we get the following expression:

Theorem 3. For

$$\gamma = -\frac{\widetilde{\beta}\widetilde{\Omega}^2}{8\pi},$$

we have

$$\widetilde{\Omega}\,\frac{\partial u_c}{\partial c}\Big|_{c=0} = \frac{1-\gamma-\gamma|x|^2}{1-\gamma+\gamma|x|^2}\cdot 8\pi\gamma G(x,0) + \left(1-\frac{2|x|^2}{1-\gamma+\gamma|x|^2}\right)\frac{2\gamma^2}{1-\gamma}.$$

We think this $\widetilde{\Omega}\,\frac{\partial u_c}{\partial c}\big|_{c=0}$ would be our target $g(x,0)$ but to prove it is our future work.

References

[1] Chorin, Alexandre J., Marsden, J.E., *"A Mathematical Introduction to Fluid Mechanics," third edition*, Springer-Verlag, New York, 1993.

[2] Caglioti, E., Lions, P.L., Marchioro, C., and Pulvirenti, M., A special class of stationary flows for two-dimensional Euler equations: A statistical mechanics description, Comm. Math. Phys., 143 (1992), pp. 501-525.

[3] Eyink, G. L. and Sreenivasan, K. R., Onsager and the theory of hydrodynamic turbulence, Rev. Modern Phys. 78(2006), pp.87–135.

[4] Davidson, R. C., *" Physics of Nonneutral Plasmas" 2nd ed.*, Imperial College Press, London, 2001.

[5] Flucher, M., *" Variational Problems with Concentration"*, Birkhäuser, Basel, 1999.

[6] Kiessling, M.K.H., Statistical mechanics of classical particles with logarithmic interactions, Comm. Pure Appl. Math., 46 (1993), pp. 27-56.

[7] Le Bellac, M., Mortessagne, F., and Batrouni, G. G. , *"Equilibrium and Non-Equilibrium Statistical Thermodynamics"*, Cambridge University Press, Cambridge, 2004.

[8] Lions, P. -L., *" On Euler Equations and Statistical Physics"*, Scuola Normale Superiore, Pisa, 1997.

[9] Marchioro, C. and Pulvirenti, M., *"Mathematical Theory of Incompressible Nonviscous Fluids"*, Springer, New York, 1994.

[10] Messer, J. and Spohn, H., Statistical mechanics of the isothermal Lane - Emden equation, J. Statist. Phys. 29 (1982), pp. 561–578.

[11] Onsager, L., Statistical hydrodynamics, Nuovo Cimento Suppl. 6 (9) No.2 (1949), pp. 279–287.

[12] Prajapat, J. and Tarantello, G., On a class of elliptic problems in $\mathbf{R}^2$: symmetry and uniqueness results, Proc. Roy. Soc. Edinburgh Sect. A, 131 (2001), pp. 967–985.

[13] Sanpei, A., Kiwamoto, Y., and Ito, K., Generation of Vorticity Hole Surrounding a Point Vortex in a Nonneutral Plasma, J. Phys. Soc. Jpn., 70 (2001), pp. 2813–2816.

[14] Suzuki, T., Global analysis for a two-dimensional elliptic eigenvalue problem with the exponential nonlinearity, Ann. Inst. H. Poincaré Anal. Non Linéaire **9** (1992) 367–398.

On an evolution equation of flame/smoldering combustion propagation of a paper sheet[1]

Shigetoshi YAZAKI[2] (Meiji University[3])

Collaborators:
Kazunori KUWANA (Yamagata University),
Maika GOTO (Yamagata University),
Yasuhide UEGATA (Meiji University), and
Shunsuke KOBAYASHI (Meiji University).

This talk is divided into three parts as follows.

Part I. We propose a simple and fast numerical method for solving an evolution equation for closed flame/smoldering fronts, equivalent to the Kuramoto-Sivashinsky (KS) equation in a scale. Comparison of numerical results and an experiment suggests that our model equation is valid for not only propagating gas-phase flame fronts but also expanding smoldering fronts over thin solids.

Part II. We propose a simple and accurate procedure how to extract the values of model parameters in the KS equation from 2D movie images of real experiments. The procedure includes a novel method of image segmentation, which can detect an expanding smoldering front as a plane polygonal curve. Our results suggest a valid range of parameters in the KS equation as well as the validity of the KS equation itself.

Part III. The existence of a rotating wave solution bifurcating from a trivial solution (an expanding circle) of the KS equation is analyzed. We also give some numerical examples in which the rotating waves are visualized.

In this manuscript, Part I and Part II are described. The Part III will be explained in the Symposium.

Part I. A simple and fast numerical method for the Kuramoto-Sivashinsky equation

1 Introduction

Let $\mathcal{C}(t)$ be a flame/smoldering front or a smooth Jordan curve at time t in the plane $\mathbb{R}^2$. The front $\mathcal{C}(t)$ is parameterized by $\boldsymbol{X}(u,t)$ for $u \in [0,1]$ and moves by

$$\dot{\boldsymbol{X}}(u,t) = V(u,t)\boldsymbol{N}(u,t) + W(u,t)\boldsymbol{T}(u,t), \tag{1}$$

where $\dot{\mathsf{F}} = \partial \mathsf{F}/\partial t$. V is the normal $\boldsymbol{N}$ velocity given by

$$V = V^{(0)} + (\alpha_{\text{eff}} - 1)\kappa + \delta\kappa_{ss}, \tag{2}$$

κ_{ss} is the second derivative w.r.to the arc-length s (defined below), $V^{(0)}$ is a constant speed, and α_{eff} and δ are positive parameters. W is the tangent $\boldsymbol{T}$ velocity that controls the grid-point spacing to be uniform [10].

[1]This work is partially supported by JSPS KAKENHI Grant Numbers 15H02977, 18H01665 (KK) and 16H03953, 19H01807 (SY).

[2]syazaki@meiji.ac.jp

[3]1-1-1 Higashi-Mita, Tama-ku, Kawasaki-shi, Kanagawa 214-8571, Japan

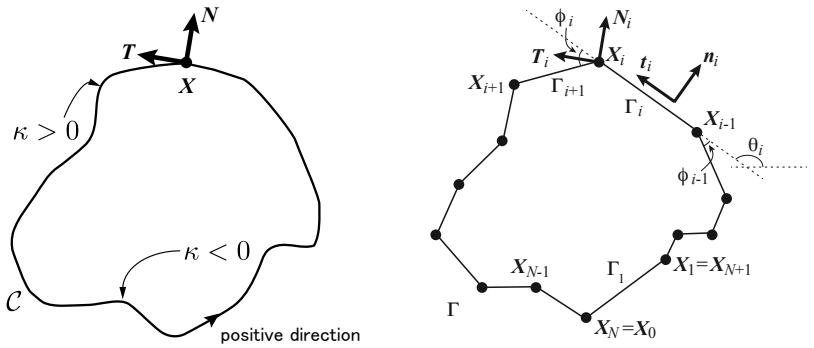

Figure 1: (a) Jordan curve $\mathcal{C}$ (b) Jordan polygonal curve Γ

As shown in the paper [6], (2), in a certain scale, is equivalent to the so-called Kuramoto-Sivashinsky (KS) equation for the graph $y = f(x,t)$ of a curved flame front when $V^{(0)} = 1$ and $\delta = 4$ [8, 11]:

$$\dot{f} + V^{(0)} f'^2/2 + (\alpha_{\text{eff}} - 1) f'' + \delta f'''' = 0, \tag{3}$$

where $f' = \partial f/\partial x$, $f'' = \partial^2 f/\partial x^2$ and $f'''' = \partial^4 f/\partial x^4$.

One of our goals of Part I is to propose a simple and fast numerical method for front tracking of (1).

2 Moving curve fronts

Time evolution of a Jordan curve $\mathcal{C}(t)$ is parameterized by $\boldsymbol{X} : [0,1] \times [0,T) \to \mathbb{R}^2$ s.t. $\mathcal{C}(t) = \{\boldsymbol{X}(u,t); u \in [0,1]\}$ and $|\boldsymbol{X}'| > 0$. Here the positive direction of u is counterclockwise, $\boldsymbol{X}' = \partial \boldsymbol{X}/\partial u$ and $g(u,t) = |\boldsymbol{X}'|$ is the local length. We denote $|\boldsymbol{a}| = \sqrt{\boldsymbol{a} \cdot \boldsymbol{a}}$ where $\boldsymbol{a} \cdot \boldsymbol{b}$ is the inner product between $\boldsymbol{a}$ and $\boldsymbol{b} \in \mathbb{R}^2$. The unit tangent vector is $\boldsymbol{T} = \boldsymbol{X}'/g = \boldsymbol{X}_s$ where s is the arc-length parameter $ds = g\,du$ and $\mathsf{F}_s = \mathsf{F}'/g$, i.e., $\partial/\partial s = g^{-1}\partial/\partial u$ is the formal definition. The unit outward normal vector is $\boldsymbol{N} = -\boldsymbol{T}^{\perp}$ where $(a,b)^{\perp} = (-b,a)$. Then the curvature κ is obtained from the Frenet formula $\boldsymbol{T}_s = -\kappa \boldsymbol{N}$ or $\kappa = \det(\boldsymbol{X}_s, \boldsymbol{X}_{ss})$ where $\mathsf{F}_{ss} = (\mathsf{F}'/g)'/g$. See Figure 1 (a).

A geometric evolution problem can be formulated as follows: For a given initial Jordan curve $\mathcal{C}^0$, find a family of curves $\{\mathcal{C}(t)\}_{0 \le t < T}$ starting from $\mathcal{C}(0) = \mathcal{C}^0$ which evolve by the normal velocity V.

A simple example of V is the Eikonal equation $V = -1$, which is the gradient flow of the enclosed area $\mathcal{A}(t) = \int_{\mathcal{C}(t)} \boldsymbol{X} \cdot \boldsymbol{N}\, ds/2$, since

$$\dot{\mathcal{A}}(t) = \int_{\mathcal{C}(t)} V\, ds. \tag{4}$$

Another typical example is the classical curvature flow equation $V = -\kappa$, which is the gradient flow of the total length $\mathcal{L}(t) = \int_{\mathcal{C}(t)} ds$, since

$$\dot{\mathcal{L}}(t) = \int_{\mathcal{C}(t)} \kappa V\, ds. \tag{5}$$

The third example is the Willmore flow equation $V = \kappa_{ss} + \kappa^3/2$, which is the gradient flow of the elastic energy or the Willmore energy $\mathcal{E}(t) = \int_{\mathcal{C}(t)} \kappa^2\, ds/2$, since

$$\dot{\mathcal{E}}(t) = -\int_{\mathcal{C}(t)} \left(\kappa_{ss} + \frac{1}{2}\kappa^3\right) V\, ds. \tag{6}$$

As the final example, we recall the surface diffusion flow equation $V = \kappa_{ss}$ which is formally obtained from the Willmore flow equation without the term $\kappa^3/2$.

In this paper we follow the so-called direct approach in which the evolution of the position vector $\boldsymbol{X} = \boldsymbol{X}(u,t)$ is governed by equation (1). The normal velocity V is a linear combination of the Eikonal, the classical curvature flow and the surface diffusion flow equations with the coefficients $V^{(0)}$, $\alpha_{\rm eff} - 1$ and δ. If $\alpha_{\rm eff} > 1$, then $(\alpha_{\rm eff} - 1)\kappa$ induces instability, and $\delta\kappa_{ss}$ plays a stabilization role of the unstable front. An alternative stabilization method is to use the Willmore flow [9]. Note that the tangential velocity W has no effect on the shape of evolving front, which is determined by the value of the normal velocity V only. Hence the impact of a suitable choice of W on the construction of robust and stable numerical schemes has been pointed out by many authors (see e.g., [10] and references therein).

3 Space discretization

In the direct approach, a moving Jordan curve is approximated by a moving Jordan polygonal curve, say $\Gamma(t)$ at time t, with N vertices labeled $\boldsymbol{X}_1, \boldsymbol{X}_2, \cdots, \boldsymbol{X}_N$ in the anti-clockwise order. Let Γ_i be the i-th edge $\Gamma_i = [\boldsymbol{X}_{i-1}, \boldsymbol{X}_i]$ $(i = 1, 2, \cdots, N;\ \boldsymbol{X}_0 = \boldsymbol{X}_N)$. Then the moving Jordan polygonal curve at time t is $\Gamma(t) = \bigcup_{i=1}^N \Gamma_i(t)$. Our goal here is to construct a discretization of (1) in space, i.e., to derive a system of ordinary differential equations (ODEs in short) for $\Gamma(t)$: for $i = 1, 2, \cdots, N$

$$\dot{\boldsymbol{X}}_i(t) = V_i(t)\boldsymbol{N}_i(t) + W_i(t)\boldsymbol{T}_i(t), \tag{7}$$

where V_i is the normal $\boldsymbol{N}_i$-component of the velocity at $\boldsymbol{X}_i$, obtained from a discretization of (2), and W_i the tangential $\boldsymbol{T}_i$-component of the velocity at $\boldsymbol{X}_i$ that controls the grid spacing to be asymptotically uniform.

The right-hand-side of (7) consists of several polygonal quantities on Γ at time t, and all of them can be constructed from $\{\boldsymbol{X}_i\}_{i=1}^N$ through the following steps. In what follows, these are regarded as functions of time t with N-periodic index, i.e., $\mathsf{F}_0 = \mathsf{F}_N$, $\mathsf{F}_{N+1} = \mathsf{F}_1$.

Step 1 $r_i = |\boldsymbol{X}_i - \boldsymbol{X}_{i-1}|$, $\boldsymbol{t}_i = (\boldsymbol{X}_i - \boldsymbol{X}_{i-1})/r_i$, $\boldsymbol{n}_i = -\boldsymbol{t}_i^{\perp}$;

Step 2 $\phi_i = \mathrm{sgn}(D_i)\arccos(\boldsymbol{t}_i \cdot \boldsymbol{t}_{i+1})$, $D_i = \det(\boldsymbol{t}_i, \boldsymbol{t}_{i+1})$,

$\mathsf{cos}_i = \cos(\phi_i/2)$, $\boldsymbol{T}_i = (\boldsymbol{t}_i + \boldsymbol{t}_{i+1})/(2\mathsf{cos}_i)$, $\boldsymbol{N}_i = -\boldsymbol{T}_i^{\perp}$;

Step 3 $L = \sum_{i=1}^N r_i$, $\mathsf{sin}_i = \sin(\phi_i/2)$, $\mathsf{tan}_i = \mathsf{sin}_i/\mathsf{cos}_i$,

$$\kappa_i = \frac{\mathsf{tan}_i + \mathsf{tan}_{i-1}}{r_i} \quad \text{on} \quad \Gamma_i; \tag{8}$$

Step 4 $(\kappa_{ss})_i = ((\kappa_{\hat{s}})_{i+1} - (\kappa_{\hat{s}})_{i-1})/(2r_i)$, where

$$(\mathsf{F}_{\hat{s}})_i = \frac{1}{r_i}\left(\frac{\mathsf{F}_{i+1} + \mathsf{F}_i}{2\mathsf{cos}_i^2} - \frac{\mathsf{F}_i + \mathsf{F}_{i-1}}{2\mathsf{cos}_{i-1}^2}\right) \quad \text{on} \quad \Gamma_i; \tag{9}$$

Step 5 $v_i = v^{(0)} + (\alpha_{\rm eff} - 1)\kappa_i + \delta(\kappa_{ss})_i$, $v^{(0)} = V^{(0)}$,

$$V_i = \frac{v_i + v_{i+1}}{2\mathsf{cos}_i} \quad \text{at} \quad \boldsymbol{X}_i; \tag{10}$$

Step 6 $W_i = (\Psi_i + c)/\mathsf{cos}_i$, where $\Psi_i = \sum_{j=1}^i \psi_j$, $c = -\left(\sum_{j=1}^N \Psi_j/\mathsf{cos}_j\right)\Big/\left(\sum_{j=1}^N 1/\mathsf{cos}_j\right)$, $\psi_1 = 0$ and

$$\psi_j = \frac{1}{N}\sum_{l=1}^N \kappa_l v_l r_l - V_j\mathsf{sin}_j - V_{j-1}\mathsf{sin}_{j-1} + \left(\frac{L}{N} - r_j\right)\omega$$

for $j = 2, 3, \cdots, N$, and ω will be defined later;

GOAL (7) can be summarized as the following ODEs:

$$\dot{\boldsymbol{X}} = \boldsymbol{F}(\boldsymbol{X}), \tag{11}$$

where $\boldsymbol{X} = (\boldsymbol{X}_1, \boldsymbol{X}_2, \cdots, \boldsymbol{X}_N) \in \mathbb{R}^{2\times N}$, and

$$\begin{cases} \boldsymbol{F} = (\boldsymbol{F}_1, \boldsymbol{F}_2, \cdots, \boldsymbol{F}_N) : \mathbb{R}^{2\times N} \to \mathbb{R}^{2\times N}; \\ \mathbb{R}^{2\times N} \ni \boldsymbol{X} \mapsto \boldsymbol{F}_i(\boldsymbol{X}) \in \mathbb{R}^2 \ (i = 1, 2, \cdots, N). \end{cases}$$

The background of the above steps are the following.

Step 1 r_i is the length of Γ_i, $\boldsymbol{t}_i$ is the unit tangent vector on Γ_i, and $\boldsymbol{n}_i$ is the outward unit normal vector on Γ_i. See Figure 1 (b).

Step 2 To define the tangent and normal vectors at $\boldsymbol{X}_i$, we use the angle ϕ_i between the adjacent edges Γ_i and Γ_{i+1} ($\boldsymbol{t}_i \cdot \boldsymbol{t}_{i+1} = \cos\phi_i$). As in Figure 1 (b), the unit tangent vector $\boldsymbol{T}_i$ at $\boldsymbol{X}_i$ are defined by an average of the adjacent corresponding vectors in the sense as in Step 2.

Step 3 To define the curvatures on Γ_i and at $\boldsymbol{X}_i$, we use (5) rather than the Frenet formulae, i.e., we recall that the curvature can be defined by the first variation of the total length $\mathcal{L}$ from (5). From (7), the total length L, and $\dot{r}_i = V_i\mathsf{sin}_i + V_{i-1}\mathsf{sin}_{i-1} + W_i\mathsf{cos}_i - W_{i-1}\mathsf{cos}_{i-1}$, we obtain $\dot{L} = \sum_{i=1}^N \hat{\kappa}_i V_i \hat{r}_i$, where $\hat{r}_i = (r_i + r_{i+1})/2$, and $\hat{\kappa}_i = 2\mathsf{sin}_i/\hat{r}_i$ is the polygonal curvature at $\boldsymbol{X}_i$. It is a natural definition since the normal velocity V_i at $\boldsymbol{X}_i$ is the average of the adjacent normal averaged velocities in the sense of (10). Then it follows that

$$\dot{L} = \sum_{i=1}^N \kappa_i v_i r_i, \tag{12}$$

which is a discretization of (5), where κ_i in (8) is the polygonal curvature on Γ_i. Note that κ_i is same as the polygonal curvature or the crystalline curvature in a prescribed class of polygonal curves [2] and v_i is not necessarily equivalent to $\dot{\boldsymbol{X}}_i \cdot \boldsymbol{n}_i$ (see Step 6 below).

Step 4 To compute $(\kappa_{ss})_i$, we calculate the gradient flow of $E = \sum_{i=1}^N \kappa_i^2 r_i/2$, which is a discrete analogue for obtaining the Willmore flow equation from (6). Under a direct calculation, we have

$$\dot{E} = -\sum_{i=1}^N \left((\kappa_{ss})_i + \frac{1}{2}\langle\kappa^3\rangle_i \right) v_i r_i + \mathrm{err}_E, \tag{13}$$

where $\langle\kappa^3\rangle_i = (\kappa_i^+\kappa_{i+1}^2 + 2\kappa_i^3 + \kappa_i^-\kappa_{i-1}^2)/4$ is an average of κ_i cubed on Γ_i ($\kappa_i^+ = 2\mathsf{tan}_i/r_i$, $\kappa_i^- = 2\mathsf{tan}_{i-1}/r_i$, n.b. $\kappa_i = (\kappa_i^+ + \kappa_i^-)/2$), and err_E is the remaining term.

The term $(\kappa_{ss})_i$ is extracted from (13), which is defined in Step 4. Note that the difference operator (9) is meaningful, since $(\boldsymbol{t}_{\hat{s}})_i = -\kappa_i \boldsymbol{n}_i$ holds, which is a discrete version of the Frenet formula $\boldsymbol{T}_s = -\kappa\boldsymbol{N}$.

Step 5 The averaged normal velocity v_i on Γ_i is given by a discrete version of (1), i.e., a linear combination of $v^{(0)} = V^{(0)}$, κ_i in (8) and $(\kappa_{ss})_i$ in Step 4. The normal velocity V_i at $\boldsymbol{X}_i$ is determined by the average (10).

Step 6 The gradient direction of the enclosed area $A = \sum_{i=1}^N \boldsymbol{X}_{i-1}^\perp \cdot \boldsymbol{X}_i/2$ is not $\boldsymbol{N}_i$ in general, and so an error term appears as follows:

$$\dot{A} = \sum_{i=1}^N v_i r_i + \mathrm{err}_A, \tag{14}$$

where $\mathrm{err}_A = \sum_{i=1}^N (W_i\mathsf{sin}_i - (v_{i+1} - v_i)/2)(r_{i+1} - r_i)/2$.

Note that if $\mathrm{err}_A = 0$,

$$\dot{A} = v^{(0)}L + 2(\alpha_{\mathrm{eff}} - 1)\pi_N \tag{15}$$

holds, where $\pi_N = \sum_{i=1}^N \mathsf{tan}_i \approx \sum_{i=1}^N \phi_i/2 = \pi$.

There are two ways to eliminate err_A: to use $W_i = (v_{i+1} - v_i)/(2\mathsf{sin}_i)$ or W_i satisfying $r_i \equiv L/N$ (the uniform distribution method (UDM in short)). The former method is equivalent to the case $v_i = \dot{\boldsymbol{X}}_i \cdot \boldsymbol{n}_i$, and in this case, Γ is restricted in a prescribed class of polygonal curves as mentioned in Step 3. In this paper, we choose the latter method. Because of numerical errors, an asymptotic UDM is utilized practically as follows.

To obtain the asymptotic UDM, $r_i \to L/N$ ($t \to T_{\max} \le \infty$), we assume that for $i = 1, 2, \cdots, N$

$$r_i - \frac{L}{N} = \eta_i e^{-\mu(t)} \quad \left(\sum_{i=1}^{N} \eta_i = 0, \ \lim_{t \to T_{\max}} \mu(t) = \infty \right).$$

Differentiating both sides of this equation and putting $\omega(t) = \dot{\mu}(t)$, we have $\dot{r}_i = U_i$ for $i = 1, 2, \cdots, N$, where

$$U_i = \frac{\dot{L}}{N} + \left(\frac{L}{N} - r_i \right) \omega(t), \quad \int_0^{T_{\max}} \omega(t)\, dt = \infty,$$

and ω is a large value if $T_{\max} = \infty$ as in this paper's case. Also, we obtain the tangential velocity equation

$$W_i \mathsf{cos}_i - W_{i-1} \mathsf{cos}_{i-1} = U_i - V_i \mathsf{sin}_i - V_{i-1} \mathsf{sin}_{i-1}$$

for $i = 1, 2, \cdots, N$. Since these N equations are linearly dependent, imposing the zero-average condition $\sum_{i=1}^{N} W_i = 0$ yields N linearly independent equations, which can be solved as in Step 6.

4 Time discretization/point insertion

To solve ODEs (11), we use the classical fourth order Runge-Kutta method for computing Γ^{m+1} from Γ^m starting from $\Gamma^0 = \Gamma(0)$, where $\Gamma^m \approx \Gamma(t_m)$ and $t_m = \sum_{j=0}^{m-1} \Delta t_j$ for $m = 1, 2, \cdots$. The time increment Δt_m is varied at every step m such that $\Delta t_m = c_0 (L^m/N)^2$, where L^m is the total length of Γ^m for $m = 0, 1, 2, \cdots$. The coefficient c_0 is computed from $\Delta t_0 = c_0 (L^0/N)^2 = 10^{-3}$ or 10^{-4} in the following computations.

In our model, the total length increases with time. Hence for an accurate computation, two approaches can be considered: the first is to begin a calculation with large N needed at the end of the calculation, whereas the second approach is to insert points during the calculation. The latter can expedite the computation but may lose the numerical accuracy. In this study, when inserting points, the number of points N is doubled when the total curve length increases two times according to the following rule: Let the fifth-order curve connecting $\boldsymbol{X}_{i-1}$ and $\boldsymbol{X}_i$ be $\boldsymbol{y}(u) = \sum_{j=0}^{5} \boldsymbol{a}_j u^j$ for $u \in [0, 1]$, where coefficients $\boldsymbol{a}_j$ are determined to satisfy

$$\begin{aligned} &\boldsymbol{y}(0) = \boldsymbol{X}_{i-1}, \ \boldsymbol{y}(1) = \boldsymbol{X}_i, \ \boldsymbol{y}'(0) = \boldsymbol{T}_{i-1}, \ \boldsymbol{y}'(1) = \boldsymbol{T}_i, \\ &\boldsymbol{y}''(0) = -\hat{\kappa}_{i-1} \boldsymbol{N}_{i-1}, \ \boldsymbol{y}''(1) = -\hat{\kappa}_i \boldsymbol{N}_i. \end{aligned}$$

We choose a new vertex as the "mid" point between $\boldsymbol{X}_{i-1}$ and $\boldsymbol{X}_i$, that is, $\boldsymbol{y}(1/2)$.

Under this point-insertion rule, our time step helps expedite computation, since if $L^{m_1} \approx 2L^{m_0}$ for $m_1 > m_0$, then N points are inserted and the new time step is $\Delta t_{m_1} = c_0 (L^{m_1}/2N) \approx c_0 (L^{m_0}/N) = \Delta t_{m_0}$. We shall compare two cases (N fixed or increased) to test the influence of inserting points in the next section. In all the following computations, the relaxation parameter ω in Step 6 is chosen such that $\omega = 0.1/\Delta t_m$.

5 Computational results

We consider the case of $\alpha_{\mathrm{eff}} = 6$ with the initial condition being an ellipse of semi axes of 5 and 6 (Figure 2 (a)). Note that $\alpha_{\mathrm{eff}} = 6$ represents a highly unstable condition, and the

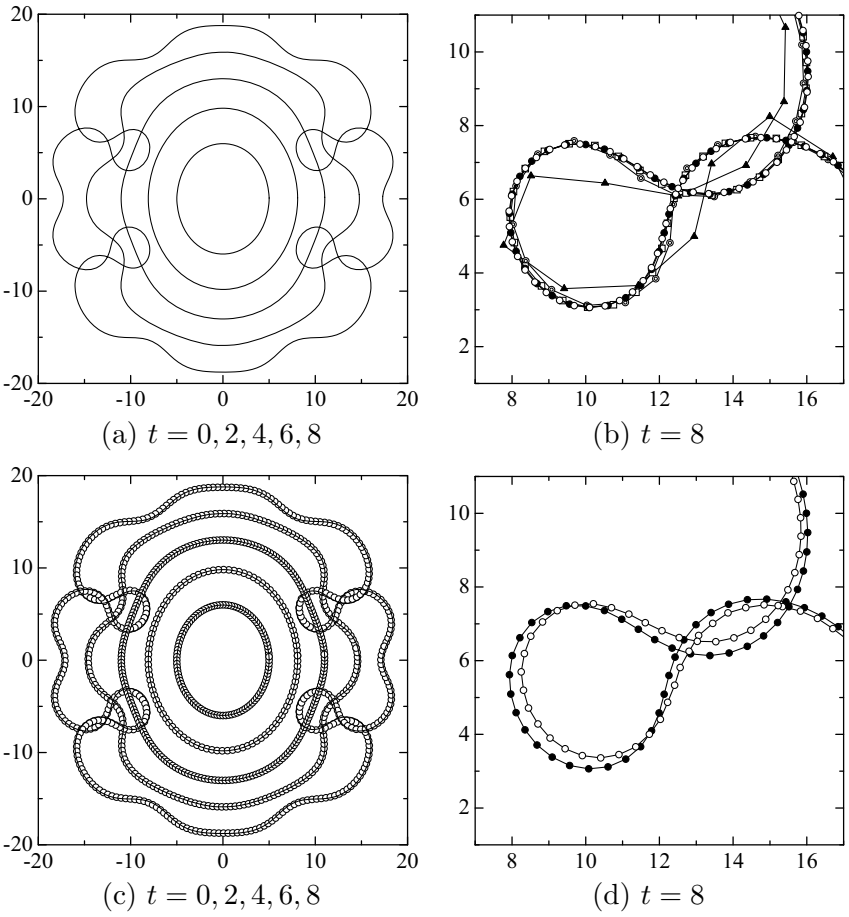

Figure 2: The time step starts from $\Delta t_0 = 10^{-4}$. (a) Evolution of curve computed with $N = 400$. (b) An enlarged view. $N = 100(\blacktriangle)$, $200(\circledcirc)$, $300(\square)$, $400(\bullet)$, $500(\circ)$. (c) Solid line: N fixed, $\circ$: N increased. (d) $\bullet$: N fixed, $\circ$: N increased.

flame front unrealistically self-intersects at $t = 8$, necessitating an algorithm to exclude flame self-intersection, which will be a topic of our future research. The discussion below is hence limited to the numerical accuracy. Computations with fixed values of N were first conducted for $t \leq 8$, revealing that results at $t = 8$ are nearly identical when $N \geq 300$ (Figure 2 (b)).

The maximal N value of 400 is therefore chosen in Figs. 2 (c) and (d), where we see the influence of inserting vertices on a polygonal curve by comparing the results obtained for $N = 400$ with those obtained by inserting points such that N increased from 100 to 400. Roughly identical results were obtained although one can observe slight differences especially in regions where instability is enhanced. Considering that the computational time was reduced to less than 1/10 by inserting points and that $\alpha_{\text{eff}} = 6$ is an extremely unstable condition, the present method has advantages for practical purposes.

Figure 3 (a) appears to be expanding circles. Indeed, if $\Gamma(t)$ is a regular N-sided polygon circumscribing a circle with radius $R(t)$, then from (15) we have $\dot{R}(t) = v^{(0)} + (\alpha_{\text{eff}} - 1)/R(t)$, since $L = 2\pi_N R$ and $A = \pi_N R^2$ with $\pi_N = N \tan(\pi/N)$. This is exactly the same as the circle-solution $\mathcal{C}(t)$ with radius $R(t)$ of (1) if $v^{(0)} = V^{(0)}$.

In Figure 3 (b), expanding circles with noise are shown. The noise is made in the following manner: From a given curve $\boldsymbol{X}(u)$, a polygonal curve with 5% noise $\{\boldsymbol{X}_i\}_{i=1}^N$ was made by $\boldsymbol{X}_i = \boldsymbol{X}(u_i) + \rho_i(\cos\theta_i, \sin\theta_i)^{\mathrm{T}}$, where $u_i = i/N$, $\rho_i = (\tilde{r}_i + \tilde{r}_{i+1})/2 \times 5\% \times \mathsf{rand}_1$, $\tilde{r}_i = |\boldsymbol{X}(u_i) - \boldsymbol{X}(u_{i-1})|$, $\theta_i = 2\pi \times \mathsf{rand}_2$, and rand_j is a random value in $[0, 1]$ $(j = 1, 2;\ i = 1, 2, \cdots, N)$. Hence $\boldsymbol{X}_i$ is in the disk with radius ρ_i and center $\boldsymbol{X}(u_i)$.

In Figs. 3 (c) and (d), expanding curve fronts are shown. Comparison between Figure 3 (d) and Figure 4 (d) in the next section suggests that our scheme can also be regarded as a model

of smoldering fronts, cf. [7].

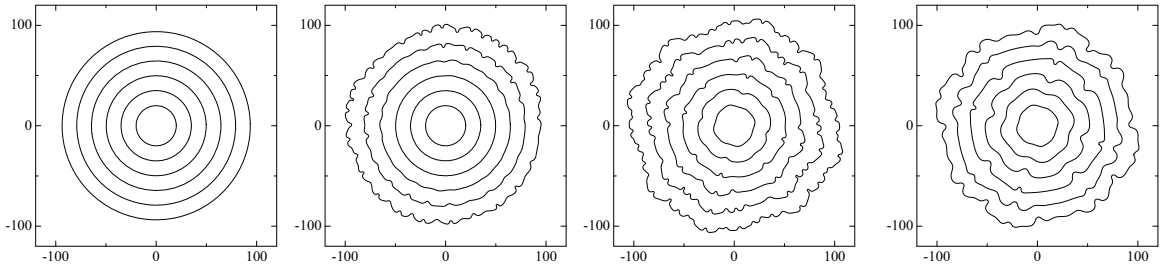

(a) $t = 0, 8, 16, \cdots, 40$ (b) $t = 0, 8, 16, \cdots, 40$ (c) $t = 0, 8, 16, \cdots, 40$ (d) $t = 0, 45, 90, \cdots, 225$

Figure 3: The time step starts from $\Delta t_0 = 10^{-3}$. Number of points increase from $N = 256$ to $N = 1024$. (a),(b) Parameters: $\alpha_{\text{eff}} = 3$, $V^{(0)} = 1.8$, $\delta = 4$. Initial curve: (a) circle ($\boldsymbol{X} = 20\boldsymbol{N}$) (b) circle ($\boldsymbol{X} = 20\boldsymbol{N}$) with 5% noise. (c),(d) Initial curve: a round square ($\boldsymbol{X} = R(u)\boldsymbol{N}$, $R(u) = 20(1 + 0.04\sin(4\pi u) + 0.02\sin(16\pi u))$) with 5% noise. Parameters: $\delta = 4$, (c) $\alpha_{\text{eff}} = 3$, $V^{(0)} = 1.8$ (d) $\alpha_{\text{eff}} = 1.7$, $V^{(0)} = 0.3$.

6 Experiment of smoldering spread

Outward smoldering spread was observed on a paper sheet of 0.2 mm thick placed above a horizontal floor. The paper sheet was inserted between two annular plates of 200 mm inner diameter, of which the lower one was 3 mm thick and thus fixed at the height of 3 mm from the floor. Because of heat loss to the floor near the paper sheet, the gas-phase flame was very weak, making the phenomenon similar to smoldering spread. The paper sheet was ignited at its center. Figure 4 shows three images of burnt area and an image of superimposed smoldering fronts at a time interval of 25 s.

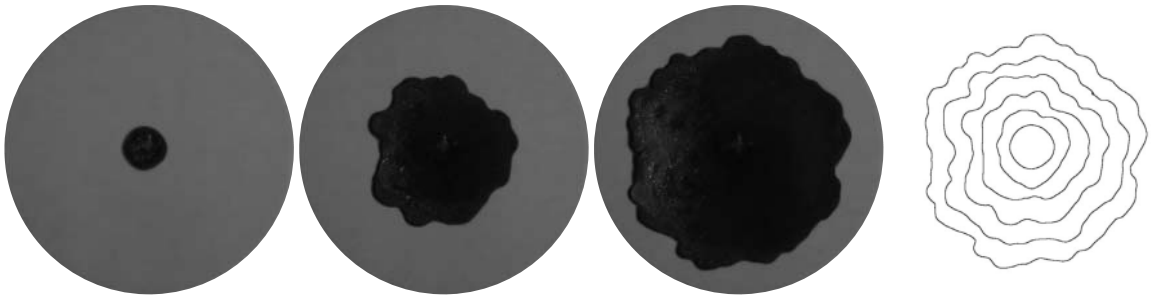

(a) $t = 0$ s (b) $t = 75$ s (c) $t = 125$ s (d)

Figure 4: The formation of corrugated reaction fronts owing to inherent instability of smoldering combustion. (a),(b),(c) Experimental images of combustion of a filter paper at each time; (d) Evolution of smoldering front segmented from experimental images at $t = 0, 25, 50, \cdots, 125$ s by the free software ImageJ.

7 Conclusion

We proposed an evolution equation for a closed curve and showed its equivalence to the KS equation in a certain scale. Our numerical method is simple and fast, and comparison between experimental and numerical results suggests that the model equation is valid for not only propagating gaseous flame fronts but also expanding smoldering fronts over thin solids.

Part II. Validity of parameters in the KS equation

8 Introduction

As shown in Part I, especially in section 6, spreading flame/smoldering fronts along a sheet of paper were tracked experimentally (see Figure 4, Figure 5 and [5]). The aim of Part II is to detect the fronts from two dimensional experimental images, and to determine the "real" values of the parameters that appear in the KS equation.

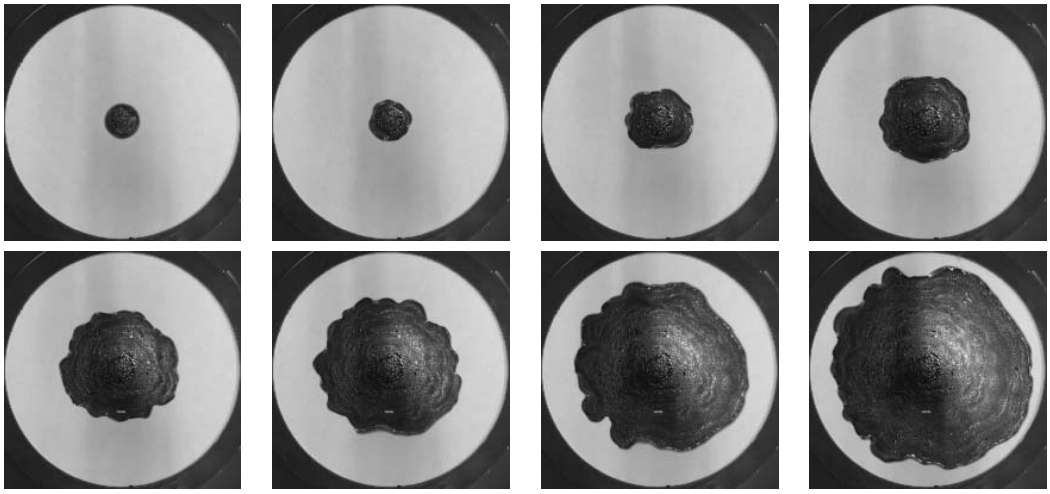

Figure 5: The photographs depict snapshots from an experimental movie of spreading flame/smoldering front along a sheet of paper placed near the floor at 200th, 400th, 1000th, 1600th,..., 4000th frames at the rate of 30 fps. Experiments were performed by the same method as [5].

The first purpose of Part II is to detect flame/smoldering fronts such as those shown in Figure 5 by means of a new method of image segmentation, which is an updated version of [1]. We will propose the new version in the next section, and here we explain basic concepts of image segmentation based on the method proposed in [1]. We define the image intensity function $I(\boldsymbol{x}) \in \{0, 255\} \subset \mathbb{Z}$ which is a piecewise constant in each pixel of the target image. When the color of the pixel is equal to the background (resp. foreground) color, we put $I(\boldsymbol{x}) = 0$ (resp. $I(\boldsymbol{x}) = 255$). Image segmentation is performed by the following normal velocity:

$$\begin{aligned} &V = -\kappa - G(\boldsymbol{x}), \\ &G(\boldsymbol{x}) = G_{\max} - (G_{\max} - G_{\min})\frac{I(\boldsymbol{x})}{255}, \end{aligned} \tag{16}$$

where $G_{\min}$ and $G_{\max}$ are given parameters satisfying $G_{\min} < 0 < G_{\max}$. In [1], several examples of image segmentation w.r.to images supplied in gray scale are shown. The method in [1] was successful except the stopping condition; it was difficult to realize $V = 0$ numerically, since images are associated with step-functions of pixel. To overcome this difficulty, we propose, say a step-function adjusted method below.

The second purpose is to determine the parameters $V^{(0)}$ and α_{eff} which appear in (2). We substitute (2) into (5) and (4), respectively, and obtain the followings:

$$\dot{\mathcal{L}} = 2\pi V^{(0)} + (\alpha_{\text{eff}} - 1)\int_{\mathcal{C}(t)} \kappa^2 ds + \delta \int_{\mathcal{C}(t)} \kappa\kappa_{ss} ds, \tag{17}$$

$$\dot{\mathcal{A}} = V^{(0)}\mathcal{L} + 2\pi(\alpha_{\text{eff}} - 1). \tag{18}$$

The parameters $V^{(0)}$ and $\alpha_{\rm eff}$ can be determined numerically by estimating κ, κ_{ss}, $\dot{\mathcal{A}}$ and $\dot{\mathcal{L}}$ from the segmentation curves of experimental images such as those shown in Figure 5, and substituting them into (17) and (18).

The organization of Part II is as follows. In section 9, we propose a image segmentation method, called the step-function adjusted method, developed from [1]. Also, to numerically evaluate the values of $V^{(0)}$ and $\alpha_{\rm eff}$ from (17) and (18), we need to calculate κ and κ_{ss} in a discrete sense, which can be obtained as the first variation of a prescribed energy such as the total length or the elastic energy. In section 10, our numerical algorithm for evaluating the "real" values of $V^{(0)}$ and $\alpha_{\rm eff}$ are presented, and some numerical experiments are performed. Future works and some remarks are summarized in the last section 11.

9 Image segmentation

As shown in Figure 5, the color of the burned region is regarded as black, whereas that of the unburned, i.e. the paper region, is regarded as white. A flame/smoldering front which is to be segmented is the interface between black and white. Experimental images are in color, so that a small flame near the interface remains as yellow- or red-colored pixels. In general, such yellowish or reddish colors are converted to gray scale by using their luminance or brightness. Therefore, it is impossible to distinguish such gray flame pixels from the burned region (black) or the unburned region (white). In our method, nevertheless, such an ambiguous region is regarded as burned if the pixel color changes appreciably as compared with its initial value. Thus, the image intensity function is given in the following manner.

(1) We choose one frame (hereafter denoted as the initial frame) among early frames of an experimental movie, e.g., frame 200 in Figure 5. The maximum difference of each component of RGB color values between $\boldsymbol{R}_{\rm ini} = (\mathcal{R}_{\rm ini}, \mathcal{G}_{\rm ini}, \mathcal{B}_{\rm ini})$ at a pixel of the initial frame and $\boldsymbol{R}_j(\boldsymbol{x}) = (\mathcal{R}_j(\boldsymbol{x}), \mathcal{G}_j(\boldsymbol{x}), \mathcal{B}_j(\boldsymbol{x}))$ at the same pixel of the jth frame to be image-segmented is defined as the intensity function $I(\boldsymbol{x})$ at the center $\boldsymbol{x}$ of the pixel. In other words, the intensity function $I(\boldsymbol{x})$ is defined by

$$I(\boldsymbol{x}) = \max\{|\mathcal{R}_{\rm ini} - \mathcal{R}_j(\boldsymbol{x})|,\ |\mathcal{G}_{\rm ini} - \mathcal{G}_j(\boldsymbol{x})|,\ |\mathcal{B}_{\rm ini} - \mathcal{B}_j(\boldsymbol{x})|\} \tag{19}$$

at the center $\boldsymbol{x}$ of each pixel.

(2) The discrete value $I(\boldsymbol{x})$ for the center $\boldsymbol{x}$ is extended to a continuous function $\hat{I}(\boldsymbol{x})$ for any position $\boldsymbol{x}$ in the image (expect within the boundary of width of a half pixel) by the standard bilinear interpolation. Hereafter, we again denote $\hat{I}(\boldsymbol{x})$ as $I(\boldsymbol{x})$.

Once $I(\boldsymbol{x})$ is determined, the following procedure will be repeated, so that a polygonal segmentation curve will evolve at the normal velocity V defined by (20) below.

We decide the threshold value I^* appropriately, and define that $\boldsymbol{x}$ is in the "inside", i.e., the burned region enclosed by the front if $I(\boldsymbol{x}) > I^*$ holds, whereas $\boldsymbol{x}$ is in the "outside" if $I(\boldsymbol{x}) < I^*$ holds. The normal velocity for image segmentation is defined as follows:

$$\begin{aligned} &V = -\gamma(\boldsymbol{x})\kappa + G(\boldsymbol{x}), \\ &\gamma(\boldsymbol{x}) = (2J(\boldsymbol{x}) - 1)^2, \quad J(\boldsymbol{x}) = \min\left\{\frac{I(\boldsymbol{x})}{2I^*}, 1\right\}, \\ &G(\boldsymbol{x}) = (2J(\boldsymbol{x}) - 1)(G_0|2J(\boldsymbol{x}) - 1| + 1), \end{aligned} \tag{20}$$

where G_0 is a positive parameter. Note that $V = 0$ if $J(\boldsymbol{x}) = 0.5$ ($I(\boldsymbol{x}) = I^*$), and $V = -4\varepsilon^2\kappa + 4G_0\varepsilon|\varepsilon| + 2\varepsilon$ if $J(\boldsymbol{x}) - 0.5 = \varepsilon$. Thus, when an evolving polygonal curve approaches sufficiently close to the front, the normal velocity V becomes very small and the speed of the curve is slowed down. The stopping condition is $I(\boldsymbol{x}) \simeq I^*$, in other words, $V \simeq 0$ at any points on the curve.

10 Evaluation of parameters $V^{(0)}$ and α_{eff}

We show the procedure for image segmentation of experimental movie and determining the values of parameters $V^{(0)}$ and α_{eff}.

Step 1 We convert an experimental movie to obtain an uncompressed color bitmap image for each frame; we can easily obtain the RGB values of its each pixel by reading the uncompressed bitmap file as a binary file. The offset, which is the distance between the beginning of file to the beginning of the data of RGB values, is stored in the first 11 to 14 bytes of the file, depending on the version the bitmap file. Therefore, it is read first, and the values after the address specified by it are used as RGB values.

Step 2 The image intensity function is computed by (19) and the standard bilinear interpolation.

Step 3 To get a segmentation curve, we solve (7) by the explicit Euler method with the normal velocity (20) and the tangential velocity defined in Step 6, section 3. The initial curve is a large circle encircling the entire burned region. The number of vertices of a polygonal curve is 2 to 4 times the total length eventually, where the unit length is the length of pixel edge. Put $I^* = 40$. The stopping condition is that the image intensity function satisfies $38 \leq I(\boldsymbol{x}) \leq 42$ at all vertices. Figure 6 is the result of our method for the image of Figure 5.

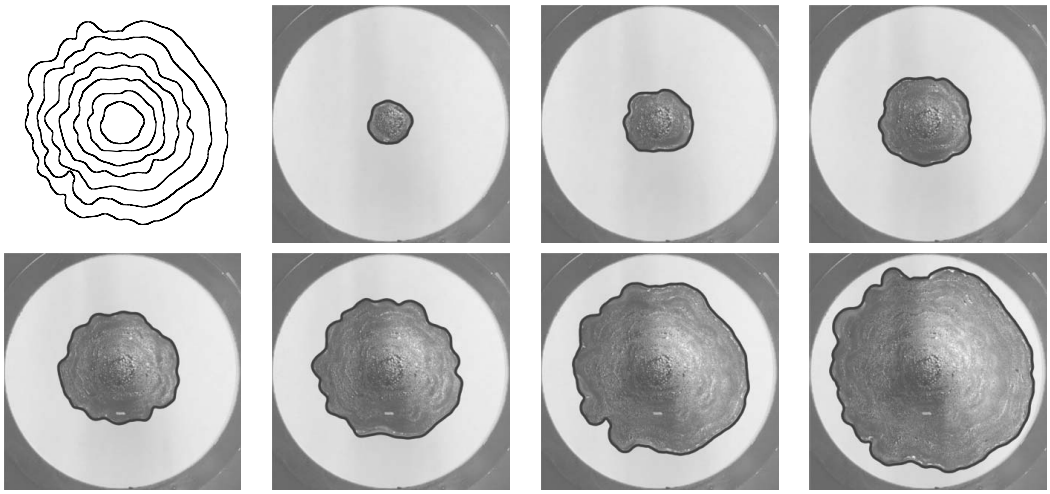

Figure 6: The upper-left figure depicts selected segmentation curves at frames: 400, 1000, 1600, 2200, 2800, 3400, 4000, summarizing the front evolution in the other photographs from left to right, upper to lower. The blue curve in each photograph is a segmentation curve, and the background vague region is the same as that in Figure 5.

Step 4 Since the segmentation curve thus obtained contains many noises, FFT is used to eliminate high frequency components. If we did not remove noises, κ_i and $(\kappa_{ss})_i$ would also contain undesired noises.

Step 5 From the segmentation curve of each frame, we can compute the values of curvature $\tilde{\kappa}$, its second derivative w.r.to the arc-length $\tilde{\kappa_{ss}}$, the total length of the front $\tilde{L}$, and the enclosed area $\tilde{A}$, each with an appropriate dimension. Assume that $\tilde{L}$ and $\tilde{A}$ are a linear and a quadratic functions of time, respectively, i.e.,

$$\tilde{L} = \tilde{L_1} t + \tilde{L_0}, \tag{21}$$

$$\tilde{A} = \tilde{A_2} t^2 + \tilde{A_1} t + \tilde{A_0}. \tag{22}$$

Then, coefficients are determined by the method of least squares:

$$\tilde{L} = 3.853295652t + 47.0874054 \text{ [mm]}, \tag{23}$$

$$\tilde{A} = 1.296716905t^2 - 15.00733847t + 1375.969254 \text{ [mm}^2\text{]}. \tag{24}$$

Figure 7 compares the actual data from segmentation curves and functions (23) and (24).

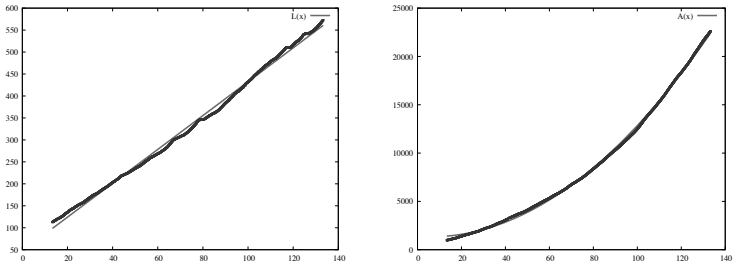

Figure 7: (Left) The total length of front $\tilde{L}$[mm] vs. the actual time [second]. (Right) The enclosed area $\tilde{A}$[mm^2] vs. the actual time [second]. Blue points indicate the actual values and red curves are the graphs of (23) and (24), respectively.

Step 6 All quantities are nondimensionalized as follows:

$$\tilde{L} = \zeta_L L, \quad \dot{\tilde{L}} = \zeta_V \dot{L}, \quad \dot{\tilde{A}} = \zeta_L \zeta_V \dot{A}, \quad \tilde{\kappa} = \frac{\kappa}{\zeta_L}, \quad \tilde{\kappa_{ss}} = \frac{\kappa_{ss}}{\zeta_L^3}, \tag{25}$$

$$\zeta_L = \frac{D_{\text{th}}}{u_{\text{r}}}, \quad \zeta_V = \frac{2u_{\text{r}}}{\beta m},$$

where $u_{\text{r}} = 1000$ [mm/s] is the reference oxidizer velocity at which the spread velocity without heat loss becomes zero, $D_{\text{th}} = 168.8808917$ [mm^2/s] is the thermal diffusivity, $\tilde{l_0} = D_{\text{th}}/u_{\text{r}}$ [mm], $\beta = 10$ is the Zel'dovich number and $m = 7.557354925776$ is the weighted density ratio of the gas to the solid phases. These data hat can be calculated from [5].

Step 7 Substituting (25) into (17) and (18), we can obtain the values of $V^{(0)}$ and α_{eff} of each frame (see Figure 8).

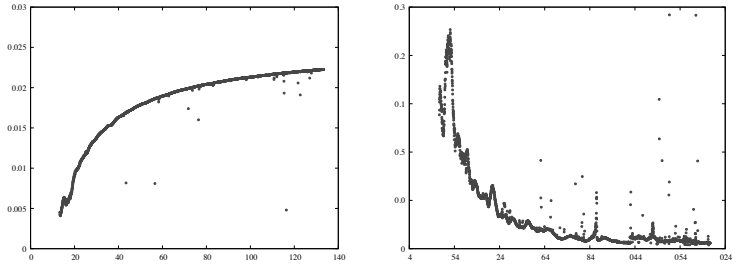

Figure 8: (Left) $V^{(0)}$ vs. time, (Right) α_{eff} vs. time.

Step 7' Another way to obtain $V^{(0)}$ and α_{eff} is to use only (18) under the assumption of (21) and (22); in other words, we substitute (21) and (22) into (18) and obtain

$$V^{(0)} = \frac{2\tilde{A}_2}{\zeta_V \zeta_L}, \quad \alpha_{\text{eff}} = 1 + \frac{1}{2\pi}\left(\frac{\tilde{A}_1}{\zeta_V} - \tilde{L_0}\right)\frac{V_0}{\zeta_L}. \tag{26}$$

In this way, we obtain the following values of parameters from (23) and (24):

$$V^{(0)} = 4.453 \times 10^{-4}, \quad \alpha_{\text{eff}} = 0.980236. \tag{27}$$

11 Conclusion

We have proposed a new method of image segmentation, called the step-function adjusted method, taking the property of pixel image into account. The method was applied to experimental image data of a spreading flame/smoldering front along a paper sheet. The parameters of a model equation (the KS equation) were determined from the actual experimental data with the actual length- and time-scale dimensions. The obtained parameters in **Step 7** and **Step 7'** were close to 1, not unreasonable values because the KS equation is valid for $\alpha_{\text{eff}} \simeq 1$. As to the future works, a new KS-like equation is desired, since in the phenomena of thin solid combustion $\alpha_{\text{eff}} > 1$ is expected. Nevertheless, we can say that our method has already indicated the application limit of the KS equation in a negative sense. Our method or strategy can be applied any experimental data to test the validity of model equations in other research fields.

References

[1] M.Beneš, M.Kimura, P.Pauš, D.Ševčovič, T.Tsujikawa and S.Yazaki, Application of a curvature adjusted method in image segmentation, *Bulletin of the Institute of Mathematics, Academia Sinica New Series* **3** (2008), 509–523.

[2] M.Beneš, M.Kimura and S.Yazaki, Second order numerical scheme for motion of polygonal curves with constant area speed, *Interfaces and Free Boundaries* **11** (2009), 515–536.

[3] C.L.Epstein & M.Gage, The curve shortening flow, Wave motion: theory, modelling, and computation (Berkeley, Calif., 1986) *Mathematical Sciences Research Institute Publications* **7** (1987), 15–59.

[4] M.L.Frankel and G.I.Sivashinsky, On the nonlinear thermal diffusive theory of curved flames, *J. Phys.* **48** (1987), 25–28.

[5] M.Goto, K.Kuwana, G.Kushida and S.Yazaki, Experimental and theoretical study on near-floor flame spread along a thin solid, *Proceedings of the Combustion Institute* **37** (2019), 3783–3791.

[6] M. Goto, K. Kuwana and S. Yazaki, A simple and fast numerical method for solving flame/smoldering evolution equations, *JSIAM Lett.* **10** (2018), 49–52.

[7] L.Kagan and G.Sivashinsky, Pattern formation in flame spread over thin solid fuels, *Comb. Theor. Model.* **12** (2008), 269–281.

[8] Y.Kuramoto and T.Tsuzuki, Persistent propagation of concentration waves in dissipative media far from thermal equilibrium, *Progress of Theoretical Physics* **55** (1976), 356–369.

[9] K.Mikula, D.Ševčovič et al., A Simple, Fast and Stabilized Flowing Finite Volume Method for Solving General Curve Evolution Equations, *Commun. Comput. Phys.* **7** (2010), 195–211.

[10] D.Ševčovič and S.Yazaki, On a gradient flow of plane curves minimizing the anisoperimetric ratio, *IAENG International Journal of Applied Mathematics* **43** (2013), 160–171.

[11] G.I.Sivashinsky, Nonlinear analysis of hydrodynamic instability in laminar flames–I, *Acta Astron.* **4** (1977), 1177–1206.

Asymptotic behavior of solutions of linear integral equations with two delays

Hideaki Matsunaga

Department of Mathematical Sciences, Osaka Prefecture University
Sakai 599-8531, Japan

E-mail: hideaki@ms.osakafu-u.ac.jp

1 Introduction

In the last half century, the theories of Volterra integral equations, Volterra integro-differential equations, and functional differential equations have been rapidly developed. It has been strongly promoted by many applications that these theories have found in physics, engineering, and biology. In mathematical demography, population dynamics in complex environment with age structure are described by use of partial differential equations and they have been studied systematically in functional analysis and infinite dimensional dynamical systems. However, limitations of a differential-equations approach have been recognized. In general, the mathematical requirement of differentiability is not necessarily essential to elucidation of the mechanism of phenomena, and it is often the case that it makes it difficult to handle strictly even for a broad meaning. To avoid such formal difficulties, various approaches based on renewal integral equation models without differential equations have recently been proposed. For the general background of Volterra integral equations, one can refer to some books [1, 2, 3].

In this paper we are concerned with a linear integral equation with two delays

$$x(t) = A\int_{t-h_2}^{t-h_1} x(s)ds, \quad t \geq 0 \tag{1}$$

with the initial condition

$$x(\xi) = \varphi(\xi), \quad -h_2 \leq \xi \leq 0, \tag{2}$$

where A is a 2×2 real constant matrix, h_1, h_2 are constants with $0 \leq h_1 < h_2$, and the initial function $\varphi : [-h_2, 0] \to \mathbb{R}^2$ is integrable. A function $x : [-h_2, b) \to \mathbb{R}^2$, $b > 0$, is called a solution of (1) with the initial function φ if x satisfies the following conditions: $x(\xi) = \varphi(\xi)$ for $\xi \in [-h_2, 0]$, x is locally integrable on $[0, b)$, and x satsifies (1) on $(0, b)$. This solution exists and is unique.

In the scalar case, Eq. (1) becomes

$$x(t) = a\int_{t-h_2}^{t-h_1} x(s)ds, \quad t \geq 0, \tag{3}$$

This work is partially supported by JSPS KAKENHI Grant Numbers JP19K03524.

where a is a real number. Eq. (3) appears as a linearized equation describing age-structured models for population dynamics under some simplifying assumptions; see, e.g. [5, 8, 9, 10]. In [8], Messina et al. studied asymptotic behavior of solutions of integral equations including (3) and gave the following result.

Theorem A. *If $|a| < 1/(h_2 - h_1)$, then every solution of* (3) *converges to* 0 *as $t \to \infty$.*

Note that, to the best of our knowledge, even the stability problem of (3) has not been solved yet.

Also, when $h_1 = 0$, Himoto and the author ([4]) have recently shown the following result by using analysis of characteristic roots. Here we say that the zero solution of (1) is *exponentially stable* if every solution of (1) converges to 0 exponentially as $t \to \infty$.

Theorem B. *Let $h_1 = 0$, $h_2 = h$ and let a_1, a_2 be real eigenvalues of A. Then the zero solution of* (1) *is exponentially stable if and only if $a_1 h < 1$ and $a_2 h < 1$.*

Theorem C. *Let $h_1 = 0$, $h_2 = h$ and let $\rho e^{\pm i\theta}$ be complex eigenvalues of A where ρ and θ are real numbers with $0 < |\theta| \leq \pi/2$. Then the zero solution of* (1) *is exponentially stable if and only if $(|\theta| - \pi)/\sin|\theta| < \rho h < \theta/\sin\theta$.*

The purpose of this paper is to present some necessary and sufficient conditions for the zero solution of (1) with two delays to be exponentially stable. It is an extension of the previous results above. We also investigate the limit of solutions of (1) in the critical case where (1) loses its exponential stability. More precisely, if the solution tends to an equilibrium point or a periodic orbit, we establish the explicit expressions depending on given initial functions

The asymptotic behavior of the solutions of (1) is determined by the roots of the associated characteristic equation

$$\det\left(E - A\int_{h_1}^{h_2} e^{-\lambda t}dt\right) = 0 \tag{4}$$

where E denotes the 2×2 unit matrix. It is well known that the zero solution of (1) is exponentially stable if and only if all roots of (4) have negative real parts. Eq. (4) is a transcendental equation and is too complicated to analyze. Also, root analysis becomes more difficult under multiple delays than one delay. For this reason, some careful root analysis is needed. We have investigated the distribution of the roots of (4) on the imaginary axis or in the right-half of the complex plane by developing further analysis based on the method under one delay which was studied by Himoto and the author ([4]). In particular, by virtue of our new results, the stability problem of (3) has just been solved. Furthermore, to establish the explicit asymptotic formulae of the solutions of (1), we utilize the formal adjoint theory for integral equations with delay which is developed in a work of Matsunaga et al. ([7]).

2 Preliminaries

In this section we will introduce the decomposition theory and the formal adjoint theory for linear autonomous integral equations with delay developed in [6, 7].

Let ρ be a fixed positive constant. Denote by X the function space defined by

$$X = \{\varphi : \mathbb{R}^- \to \mathbb{C}^m \mid \varphi(\xi)e^{\rho\xi} \text{ is intergrable on } \mathbb{R}^- = (-\infty, 0]\}$$

with norm $\|\varphi\| = \int_{-\infty}^{0} |\varphi(\xi)|e^{\rho\xi}d\xi$ for $\varphi \in X$. For any function $x : (-\infty, b) \to \mathbb{C}^m$ and $t < b$, we define a function $x_t : \mathbb{R}^- \to \mathbb{C}^m$ by $x_t(\xi) = x(t + \xi)$ for $\xi \in \mathbb{R}^-$.

Let us consider the linear integral equation with infinite delay

$$x(t) = \int_{-\infty}^{t} K(t - s)x(s)ds, \tag{5}$$

where the kernel K is a measurable $m \times m$ matrix valued function on $\mathbb{R}^+ = [0, \infty)$ with complex components satisfying the conditions

$$\int_0^\infty \|K(t)\|e^{\rho t}dt < \infty \quad \text{and} \quad \operatorname{ess\,sup}\{\|K(t)\|e^{\rho t} \mid t \geq 0\} < \infty.$$

Eq. (5) can be formulated as an autonomous equation on X of the form

$$x(t) = L(x_t), \tag{6}$$

where L is a bounded linear operator defined by $L(\varphi) = \int_{-\infty}^{0} K(-\xi)\varphi(\xi)d\xi$ for $\varphi \in X$. It is known that there exists a unique global solution $x : \mathbb{R} \to \mathbb{C}^m$ of (6) such that $x_0 = \varphi$ on $\mathbb{R}^-$, which is called the solution of (6) through $(0, \varphi)$, and denoted by $x(t; \varphi)$.

For any $t \geq 0$ and $\varphi \in X$, the solution operator $T(t) : X \to X$ is defined by $T(t)\varphi = x_t(\cdot; \varphi)$. Since the family $\{T(t)\}_{t\geq 0}$ is a strongly continuous semigroup of linear operators on X, the generator A_0 of $\{T(t)\}_{t\geq 0}$ is characterized as follows:

$$\begin{aligned} \mathcal{D}(A_0) &= \{\varphi \in X \mid \varphi(\xi) = \tilde{\varphi}(\xi) \text{ a.e. } \xi \in \mathbb{R}^- \text{ for some } \tilde{\varphi} \in \tilde{X}\}, \\ A_0\varphi &= (d/d\xi)\tilde{\varphi}, \qquad \varphi \in \mathcal{D}(A_0), \end{aligned}$$

where $\tilde{X} = \{\tilde{\varphi} \in X \mid \tilde{\varphi} \text{ is locally absolutely continuous on } \mathbb{R}^-,\ (d/d\xi)\tilde{\varphi} \in X \text{ and } \tilde{\varphi}(0) = L(\tilde{\varphi})\}$. Let us introduce the characteristic equation for (5) defined by

$$\det \Delta(z) = 0, \quad \Delta(z) = E_m - \int_0^\infty K(t)e^{-zt}dt, \tag{7}$$

where E_m is the $m \times m$ unit matrix. We call $\lambda \in \mathbb{C}_{-\rho} = \{z \in \mathbb{C} \mid \operatorname{Re} z > -\rho\}$ such that $\det \Delta(\lambda) = 0$ a *characteristic root* of (5). Then the spectra of A_0 are characterized as

$$\sigma(A_0) \cap \mathbb{C}_{-\rho} = P_\sigma(A_0) \cap \mathbb{C}_{-\rho} = \{\lambda \in \mathbb{C}_{-\rho} \mid \det \Delta(\lambda) = 0\} \quad \text{and} \quad \sup_{\lambda \in \operatorname{ess}(A_0)} \operatorname{Re} \lambda \leq -\rho,$$

where $\sigma(A_0)$, $P_\sigma(A_0)$ and $\operatorname{ess}(A_0)$ are the spectrum, the point spectrum and the essential spectrum of A_0, respectively.

Let $\Sigma^{cu} = \{\lambda \in \sigma(A_0) \mid \operatorname{Re}\lambda \geq 0\}$ and $\Sigma^s = \sigma(A_0) \setminus \Sigma^{cu}$. Then $\Sigma^{cu} \cap \operatorname{ess}(A_0) = \emptyset$ and Σ^{cu} is a finite set, and hence X is decomposed as a direct sum $X = X^{cu} \oplus X^s$, where X^{cu} and X^s are closed subspaces satisfying the following properties:

$$\dim X^{cu} < \infty, \quad \sigma(A_0|_{X^{cu}}) = \Sigma^{cu} \quad \text{and} \quad \sigma(A_0|_{X^s \cap \mathcal{D}(A_0)}) = \Sigma^s.$$

Denote by Π^{cu} the projection from X onto X^{cu}. Then we have the following result on the asymptotic behavior of solutions of (5).

Proposition 1. *([7, Corollary 2.1]) Let $x(t;\varphi)$ be a solution of (5) with the initial function $\varphi \in X$. Then the following statements hold:*

(i) *If $\Sigma^{cu} = \emptyset$, then the zero solution of (5) is exponentially stable.*

(ii) *If $\Sigma^{cu} \neq \emptyset$, then the solution $x(t;\varphi)$ tends to $x(t;\Pi^{cu}\varphi)$ exponentially as $t \to \infty$. More precisely, there exist positive constants K_1 and β with $K_1 \geq 1$ such that*

$$|x(t;\varphi) - x(t;\Pi^{cu}\varphi)| \leq K_1 e^{-\beta t}\|\varphi\|, \quad t > 0, \ \ \varphi \in X.$$

Next we introduce the formal adjoint theory to obtain the explicit form of $x(t;\Pi^{cu}\varphi)$. Let $\mathbb{C}^{m*}$ be the space of all m-dimensional row vectors. Consider the function space $X^\sharp$ defined by

$$X^\sharp = \{\psi : \mathbb{R}^+ \to \mathbb{C}^{m*} \mid \psi(s)e^{-\rho s} \text{ is integrable on } \mathbb{R}^+\}$$

with the norm $\|\psi\| = \int_0^\infty |\psi(s)|e^{-\rho s}ds$ for $\psi \in X^\sharp$. Also we set

$$\begin{aligned} \mathcal{D}(A_0^\sharp) &= \{\psi \in X^\sharp \mid \psi(s) = \tilde{\psi}(s) \text{ a.e. } s \in \mathbb{R}^+ \text{ for some } \tilde{\psi} \in \tilde{X}^\sharp\}, \\ A_0^\sharp\psi &= -(d/ds)\tilde{\psi}, \qquad \psi \in \mathcal{D}(A_0^\sharp), \end{aligned}$$

where $\tilde{X}^\sharp = \{\tilde{\psi} \in X^\sharp \mid \tilde{\psi}$ is locally absolutely continuous on $\mathbb{R}^+$, $(d/ds)\tilde{\psi} \in X^\sharp$ and $\tilde{\psi}(0) = \int_0^\infty \tilde{\psi}(s)K(s)ds\}$. We call the operator $A_0^\sharp$ the *formal adjoint operator* of A_0. Furthermore, let us consider the bilinear form $\langle\langle \cdot, \cdot \rangle\rangle$ on $X^\sharp \times X$ defined by

$$\langle\langle \psi, \varphi \rangle\rangle = \int_{-\infty}^0 \int_\xi^0 \psi(\tau - \xi)K(-\xi)\varphi(\tau)d\tau d\xi, \quad \varphi \in X, \ \psi \in X^\sharp. \tag{8}$$

Then for $\varphi \in \mathcal{D}(A_0)$ and $\psi \in \mathcal{D}(A_0^\sharp)$, the dual relation $\langle\langle \psi, A_0\varphi \rangle\rangle = \langle\langle A_0^\sharp\psi, \varphi \rangle\rangle$ is satisfied. For $\lambda \in \mathbb{C}_{-\rho}$ and $k \in \mathbb{N}$, the function φ belongs to $\mathcal{R}((A_0 - \lambda I)^k)$ if and only if $\langle\langle \psi, \varphi \rangle\rangle = 0$ for all $\psi \in \mathcal{N}((A_0^\sharp - \lambda I)^k)$.

Let $\Sigma^{cu} = \{\lambda_1, \ldots, \lambda_r\}$, and denote by p_i the ascent of λ_i for each $i = 1, \ldots, r$. Then

$$X^{cu} = \mathcal{N}((A_0 - \lambda_1 I)^{p_1}) \oplus \cdots \oplus \mathcal{N}((A_0 - \lambda_r I)^{p_r}).$$

We consider the subspace X^{cu} of X as well as the subspace $\mathcal{N}^\sharp$ of $X^\sharp$ defined by

$$\mathcal{N}^\sharp = \mathcal{N}((A_0^\sharp - \lambda_1 I)^{p_1}) \oplus \cdots \oplus \mathcal{N}((A_0^\sharp - \lambda_r I)^{p_r}).$$

Let $\{\varphi_1, \dots, \varphi_d\}$ be a basis for X^{cu}, and set $\Phi = (\varphi_1, \dots, \varphi_d)$. Similarly, let $\{\psi_1, \dots, \psi_d\}$ be a basis for $\mathcal{N}^\sharp$, and set $\Psi = \mathrm{col}(\psi_1, \dots, \psi_d)$. We call Φ and Ψ a *basis vector* for X^{cu} and $\mathcal{N}^\sharp$, respectively. Let $\langle\!\langle \Psi, \Phi \rangle\!\rangle$ be the $d \times d$ matrix $(\langle\!\langle \psi_i, \varphi_j \rangle\!\rangle)$ $i, j = 1, 2, \dots, d$, and denote by $\langle\!\langle \Psi, \phi \rangle\!\rangle$ the column vector $\mathrm{col}\,(\langle\!\langle \psi_1, \varphi \rangle\!\rangle, \dots, \langle\!\langle \psi_d, \varphi \rangle\!\rangle)$ for $\varphi \in X$. In addition, let $\tilde{\Phi}$ be the canonical prolongation of Φ defined on $\mathbb{R}$ such that $\tilde{\Phi}(\xi) = \Phi(\xi)$ for $\xi \in \mathbb{R}^-$. Then we have the following result on the projection $\Pi^{cu} : X \to X^{cu}$ and an asymptotic formula for solutions of (5).

Proposition 2. (*[7, Theorems 3.1 and 3.2]*) *Let Φ and Ψ be a basis vector for X^{cu} and $\mathcal{N}^\sharp$, respectively. Let $\tilde{\Phi}$ be the canonical prolongation of Φ defined on $\mathbb{R}$. Then the matrix $\langle\!\langle \Psi, \Phi \rangle\!\rangle$ is nonsingular, and the projection Π^{cu} is given by*

$$\Pi^{cu}\varphi = \Phi \langle\!\langle \Psi, \Phi \rangle\!\rangle^{-1} \langle\!\langle \Psi, \varphi \rangle\!\rangle, \quad \varphi \in X.$$

Moreover, the solution $x_*(t)$ of (5) through $(0, \Pi^{cu}\varphi)$ is expressed as

$$x_*(t) = \tilde{\Phi}(t) \langle\!\langle \Psi, \Phi \rangle\!\rangle^{-1} \langle\!\langle \Psi, \varphi \rangle\!\rangle, \quad t > 0.$$

In particular, for any $\varphi \in X$, the solution $x(t; \varphi)$ of (5) satisfies the relation

$$\lim_{t \to \infty} |x(t; \varphi) - \tilde{\Phi}(t) \langle\!\langle \Psi, \Phi \rangle\!\rangle^{-1} \langle\!\langle \Psi, \varphi \rangle\!\rangle| = 0 \quad (\textit{exponentially}).$$

To compute a basis for null spaces $\mathcal{N}((A_0 - \lambda I)^k)$ and $\mathcal{N}((A_0^\sharp - \lambda I)^k)$, the following result is useful. To this end, for $\lambda \in \mathbb{C}_{-\rho}$ and $k \in \mathbb{N}$, we introduce functions $w_k(\lambda) : \mathbb{R}^- \to \mathbb{C}$, $w_k^\sharp(\lambda) : \mathbb{R}^+ \to \mathbb{C}$ and a $(km) \times (km)$ matrix $D_k(\lambda)$ defined by

$$\begin{aligned}
&[w_k(\lambda)](\xi) = \frac{\xi^{k-1}}{(k-1)!} e^{\lambda \xi}, \quad \xi \in \mathbb{R}^-, \\
&[w_k^\sharp(\lambda)](s) = [w_k(\lambda)](-s), \quad s \in \mathbb{R}^+, \\
&D_k(\lambda) = \begin{pmatrix}
\Delta(\lambda) & \Delta'(\lambda) & \cdots & \Delta^{(k-1)}(\lambda)/(k-1)! \\
0 & \Delta(\lambda) & \cdots & \Delta^{(k-2)}(\lambda)/(k-2)! \\
\vdots & \vdots & \ddots & \vdots \\
0 & \cdots & 0 & \Delta(\lambda)
\end{pmatrix},
\end{aligned}$$

respectively, where $\Delta^{(n)}(z) = (d^n/dz^n)\Delta(z)$ for $n \in \mathbb{N}$.

Proposition 3. (*[7, Propositions 3.1 and 3.4]*) *Let $\lambda \in \mathbb{C}_{-\rho}$ and $k \in \mathbb{N}$. Then the following statements hold:*

(i) *$\varphi \in \mathcal{N}((A_0 - \lambda I)^k)$ if and only if it is written as $\varphi = \sum_{j=1}^k w_j(\lambda)\eta_j$, where $\eta_1, \dots, \eta_k \in \mathbb{C}^m$ with the relation $D_k(\lambda)\mathrm{col}(\eta_1, \dots, \eta_k) = \mathrm{col}(0, \dots, 0)$.*

(ii) *$\psi \in \mathcal{N}((A_0^\sharp - \lambda I)^k)$ if and only if it is written as $\psi = \sum_{j=1}^k w_j^\sharp(\lambda)\zeta_{k+1-j}$, where $\zeta_1, \dots, \zeta_k \in \mathbb{C}^{m*}$ with the relation $(\zeta_1, \dots, \zeta_k)D_k(\lambda) = (0, \dots, 0)$.*

3 Main Results

First we will consider the scalar equation (3). For simplicity, we put

$$a^* = -\frac{\pi}{(h_1+h_2)\sin\dfrac{(h_2-h_1)\pi}{h_1+h_2}}.$$

Theorem 1. *Let $x(t;\varphi)$ be a solution of (3) with the initial condition (2) where $\varphi \in L^1([-h_2,0],\mathbb{R})$. Then the following statements hold:*

(i) *If $a^* < a < 1/(h_2-h_1)$, then $x(t;\varphi)$ converges to 0 exponentially as $t\to\infty$.*

(ii) *If $a = 1/(h_2-h_1)$, then $x(t;\varphi)$ converges to c exponentially as $t\to\infty$.*

(iii) *If $a = a^*$, then $|x(t;\varphi) - \tilde{\Phi}_1(t)c_1|$ converges to 0 exponentially as $t\to\infty$.*

(iv) *If $a > 1/(h_2-h_1)$ or $a < a^*$, there exists an unbounded solution of (3).*

Here $c = c(\varphi)$, $\tilde{\Phi}_1(t)$ and $c_1 = c_1(\varphi)$ are expressed as

$$c = \frac{2}{h_2^2-h_1^2}\int_{-h_2}^{-h_1}\int_{\theta}^{0}\varphi(\xi)d\xi d\theta,$$

$$\tilde{\Phi}_1(t) = \begin{pmatrix}\cos\omega_1 t & \sin\omega_1 t\end{pmatrix}, \quad \omega_1 = \frac{2\pi}{h_1+h_2},$$

$$c_1 = \left(\int_{-h_2}^{-h_1}\int_{\theta}^{0}\tilde{\Phi}_1^T(\xi-\theta)\tilde{\Phi}_1(\xi)d\xi d\theta\right)^{-1}\int_{-h_2}^{-h_1}\left(\int_{\theta}^{0}\tilde{\Phi}_1^T(\xi-\theta)\varphi(\xi)d\xi\right)d\theta.$$

Corollary 1. *The zero solution of (3) is exponentially stable if and only if $a^* < a < 1/(h_2-h_1)$.*

The characteristic equation of (3) becomes

$$f(\lambda) := 1 - a\int_{h_1}^{h_2} e^{-\lambda t}dt = 0.$$

Theorem 1 is proved by the following key lemma on the distribution of characteristic roots together with Propositions 2 and 3.

Lemma 1. *Let $\omega_1 = 2\pi/(h_1+h_2)$. Then for $a \neq 0$ the following statements hold:*

(i) *If $a^* < a < 1/(h_2-h_1)$, then all the roots of $f(\lambda)=0$ have negative real parts.*

(ii) *If $a = 1/(h_2-h_1)$, then $f(\lambda)=0$ has a simple root 0 and the remaining roots have negative real parts.*

(iii) *If $a = a^*$, then $f(\lambda)=0$ has simple roots $\pm i\omega_1$ and the remaining roots have negative real parts.*

(iv) *If $a < a^*$ or $a > 1/(h_2-h_1)$, there exists a root of $f(\lambda)=0$ with a positive real part.*

Next we will consider Eq. (1) where the matrix A has complex eigenvalues, that is,

$$A = \rho \begin{pmatrix} \cos\theta & -\sin\theta \\ \sin\theta & \cos\theta \end{pmatrix}. \tag{9}$$

Here ρ and θ are real numbers with $0 < |\theta| \le \pi/2$. For brevity, we set

$$\rho_{-1} = -\frac{\pi - |\theta|}{(h_1+h_2)\sin\dfrac{(h_2-h_1)(\pi-|\theta|)}{h_1+h_2}}, \quad \rho_0 = \frac{\theta}{(h_1+h_2)\sin\dfrac{(h_2-h_1)\theta}{h_1+h_2}}.$$

Theorem 2. *Suppose that the matrix A is given by* (9). *Let $x(t;\varphi)$ be a solution of* (1) *with the initial condition* (2). *Then the following statements hold:*

(i) *If $\rho_{-1} < \rho < \rho_0$, then $x(t;\varphi)$ converges to 0 exponentially as $t \to \infty$.*

(ii) *If $\rho = \rho_0$, then $|x(t;\varphi) - \tilde{\Phi}_2(t)c_2|$ converges to 0 exponentially as $t \to \infty$.*

(iii) *If $\rho = \rho_{-1}$, then $|x(t;\varphi) - \tilde{\Phi}_3(t)c_3|$ converges to 0 exponentially as $t \to \infty$.*

(iv) *If $\rho > \rho_0$ or $\rho < \rho_{-1}$, there exists an unbounded solution of* (1).

Here $c_2 = c_2(\varphi)$, $\tilde{\Phi}_2(t)$, $c_3 = c_3(\varphi)$ and $\tilde{\Phi}_3(t)$ are expressed as

$$\tilde{\Phi}_2(t) = \begin{pmatrix} \cos\omega_0 t & \sin\omega_0 t \\ -\sin\omega_0 t & \cos\omega_0 t \end{pmatrix}, \quad \omega_0 = \frac{2|\theta|}{h_1+h_2},$$

$$c_2 = \left(\int_{h_1}^{h_2} s\tilde{\Phi}_2(-s)ds\right)^{-1} \int_{-h_2}^{-h_1}\int_{\xi}^{0} \tilde{\Phi}_2(\xi-\tau)\varphi(\tau)d\tau d\xi,$$

$$\tilde{\Phi}_3(t) = \begin{pmatrix} \cos\omega_{-1}^* t & \sin\omega_{-1}^* t \\ -\sin\omega_{-1}^* t & \cos\omega_{-1}^* t \end{pmatrix}, \quad \omega_{-1}^* = \frac{2(|\theta|-\pi)}{h_1+h_2}\mathrm{sgn}(\theta),$$

$$c_3 = \left(\int_{h_1}^{h_2} s\tilde{\Phi}_3(-s)ds\right)^{-1} \int_{-h_2}^{-h_1}\int_{\xi}^{0} \tilde{\Phi}_3(\xi-\tau)\varphi(\tau)d\tau d\xi.$$

Corollary 2. *Let $\rho e^{\pm i\theta}$ be complex eigenvalues of A where ρ and θ are real numbers with $0 < |\theta| \le \pi/2$. The zero solution of* (1) *is exponentially stable if and only if $\rho_{-1} < \rho < \rho_0$.*

Lemma 2. *Suppose that the matrix A is given by* (9). *Let $\omega_0 = 2\theta/(h_1+h_2)$ and $\omega_{-1} = 2(|\theta|-\pi)/(h_1+h_2)$. Then for $\rho \neq 0$ the following statements hold:*

(i) *If $\rho_{-1} < \rho < \rho_0$, then all the roots of* (4) *have negative real parts.*

(ii) *If $\rho = \rho_0$, then Eq.* (4) *has simple roots $\pm i\omega_0$ and the remaining roots have negative real parts.*

(iii) *If $\rho = \rho_{-1}$, then Eq.* (4) *has simple roots $\pm i\omega_{-1}$ and the remaining roots have negative real parts.*

(iv) *If $\rho > \rho_0$ or $\rho < \rho_{-1}$, there exists a root of* (4) *with a positive real part.*

References

[1] T. A. Burton, *Volterra Integral and Differential Equations, 2nd ed.*, Elsevier, Amsterdam, 2005.

[2] C. Corduneanu, *Integral Equations and Applications*, Cambridge Univ. Press, Cambridge, 1991.

[3] G. Gripenberg, S.-O. Londen and O. Staffans, *Volterra Integral and Functional Equations*, Cambridge Univ. Press, Cambridge, 1990.

[4] K. Himoto and H. Matsunaga, *The limits of solutions of a linear delay integral equation*, submitted.

[5] M. Iannelli, H. Inaba and T. Kuniya, *Mathematical Theory of Age-Structured Population Dynamics (Japanese)*, Tokyo Univ. Press, Tokyo, 2014.

[6] H. Matsunaga, S. Murakami and Nguyen Van Minh, Decomposition and variation-of-constants formula in the phase space for integral equations, *Funkcial. Ekvac.*, **55** (2012), 479–520.

[7] H. Matsunaga, S. Murakami and Y. Nagabuchi, Formal adjoint operators and asymptotic formula for solutions of autonomous linear integral equations, *J. Math. Anal. Appl.*, **410** (2014), 807–826.

[8] E. Messina, E. Russo and A. Vecchio, A stable numerical method for Volterra integral equations with discontinuous kernel, *J. Math. Anal. Appl.*, **337** (2008), 1383–1393.

[9] E. Messina, E. Russo, A. Vecchio, A convolution test equation for double delay integral equations, *J. Comput. Appl. Math.*, **228** (2009), 589–599.

[10] E. Messina, E. Russo and A. Vecchio, Comparing analytical and numerical solution of a nonlinear two-delay integral equations, *Math. Comput. Simulation*, **81** (2011), 1017–1026.

Stability analysis for the system of linear differential equations

Yoshihiro UEDA (Kobe University)*

1. Introduction and main results

In this talk, we consider the symmetric hyperbolic system with relaxation

$$A^0 u_t + \sum_{j=1}^{n} A^j u_{x_j} + Lu = 0, \tag{1}$$

where $u = u(t,x)$ over $t > 0$ and $x = (x_1, \cdots, x_n) \in \mathbb{R}^n$ is an unknown vector function, and A^0, A^j and L are $m \times m$ constant matrices for $1 \le j, k \le n$ and $m \ge 2$. Then, we assume the following condition for the coefficient matrices of (1).

Condition (A): A^0 is real symmetric and positive definite, A^j $(1 \le j \le n)$ are real symmetric, while L are not necessarily real symmetric but are non-negative definite with the non-trivial kernel.

To analyze the dissipative structure of (1), we apply the Fourier transform to (1). This yields

$$A^0 \hat{u}_t + i|\xi| A(\omega)\hat{u} + L\hat{u} = 0. \tag{2}$$

Here, we used a notation that

$$A(\omega) := \sum_{j=1}^{n} A^j \omega_j,$$

where $\omega = (\omega_1, \cdots, \omega_n)$ is a unit vector in $\mathbb{R}^n$, which means $\omega \in S^{n-1}$. Then the corresponding eigenvalue problem is

$$\lambda A^0 \varphi + (irA(\omega) + L)\varphi = 0 \tag{3}$$

for $r \ge 0$ and $\omega \in S^{n-1}$, and we look for the eigenvalue $\lambda = \lambda(r,\omega) \in \mathbb{C}$ and the corresponding eigenvector $\varphi = \varphi(r,\omega) \in \mathbb{C}^m \backslash \{0\}$.

Under the symmetric property of L, Beauchard-Zuazua [1], Shizuta-Kawashima [6] and Umeda-Kawashima-Shizuta [12] introduced the following conditions for (1) to get the stability of solutions.

Classical Stability Condition (CSC): For each $(\mu, \omega) \in \mathbb{R} \times S^{n-1}$,

$$\mathrm{Ker}(\mu I + (A^0)^{-1} A(\omega)) \cap \mathrm{Ker}(L) = \{0\}.$$

Classical Craftsmanship Condition Condition (CK): There is a real compensating matrix $K(\omega) \in C^\infty(S^{n-1})$ with the following properties: $K(-\omega) = -K(\omega)$, $(K(\omega)A^0)^T = -K(\omega)A^0$ and

$$(K(\omega)A(\omega))^\sharp > 0 \quad \text{on} \quad \ker(L)$$

* e-mail: ueda@maritime.kobe-u.ac.jp

for each $\omega \in S^{n-1}$.

Classical Kalman Rank Condition (CR): For each $\omega \in S^{n-1}$, the $m^2 \times m$ Kalman matrix has rank m, that is

$$\operatorname{rank} \begin{pmatrix} L \\ L(A^0)^{-1}A(\omega) \\ \vdots \\ L((A^0)^{-1}A(\omega))^{m-1} \end{pmatrix} = m.$$

Here and in the sequel, the superscript * stands for the adjoint, and $X^\sharp$ and $X^\flat$ denote the Hermitian and skew-Hermitian part of the matrix X, respectively. Under this situation, the following theorem was obtained.

Theorem 1. ([1, 6, 12]) *Suppose that the system* (1) *satisfies Condition* (A) *with*

$$\ker(L) = \ker(L^\sharp). \tag{4}$$

Then, for the system (1) (*and* (3)), *the following conditions are equivalent.*

(i) *Classical Stability Condition* (CSC) *holds.*
(ii) *Classical Kalman Rank Condition* (CR) *holds.*
(iii) *Classical Craftsmanship Condition Condition* (CK) *holds.*
(iv) *All eigenvalues of* (3) *satisfy* $\mathrm{Re}\lambda(r,\omega) < 0$ *for each* $(r,\omega) \in \mathbb{R}_+ \times S^{n-1}$.
(v) *All eigenvalues of* (3) *satisfy* $\mathrm{Re}\lambda(r,\omega) \lesssim -\dfrac{r^2}{1+r^2}$ *for each* $(r,\omega) \in \mathbb{R}_+ \times S^{n-1}$.

We remark that the typical feature of (v) in Theorem 1 is that the high-frequency part decays exponentially while the low-frequency part decays polynomially with the rate of the heat kernel.

In recent 10 years, some complicated physical models which do not satisfy (4) are appeared. For example, the dissipative Timoshenko system was discussed in [2, 3, 5], the Euler-Maxwell system was studied in [10, 11], and the thermoelastic plate equation with Cattaneo's law was also considered in [4]. These models have the weak dissipative structure called the regularity-loss structure. Under this situation, our purpose is to extend the classical stability conditions and get the weak dissipative structure.

We introduce notations that $\mathbb{R}_+ := (0,\infty)$, $\mathbb{S}^{m-1} := \{\sigma \in \mathbb{C}^m\,;\, |\sigma| = 0\}$ and $\mathcal{A}(\nu,\omega) := (A^0)^{-1}(\nu A(\omega) - iL^\flat)$ to state our new conditions.

Stability Condition (SC): For each $(\mu,\nu,\omega) \in \mathbb{R} \times \mathbb{R}_+ \times S^{n-1}$,

$$\mathrm{Ker}(\mu I + \mathcal{A}(\nu,\omega)) \cap \mathrm{Ker}(L^\sharp) = \{0\}.$$

Craftsmanship Condition (K): There is a $m \times m$ complex compensating matrix $\mathcal{K}(\nu,\omega) \in C(\mathbb{R}_+ \times S^{n-1})$ with the following properties:

$$\bar{\mathcal{K}}(\nu,-\omega) = -\mathcal{K}(\nu,\omega), \qquad \mathcal{K}(\nu,\omega)^* = -\mathcal{K}(\nu,\omega)$$

for each $(\nu,\omega) \in \mathbb{R}_+ \times S^{n-1}$, and there exists c_K and C_K such that

$$\langle (L^\sharp + (\mathcal{K}(\nu,\omega)\mathcal{A}(\nu,\omega))^\sharp)\sigma,\sigma\rangle > \frac{c_K\nu^2}{1+\nu^2}|\mathcal{K}(\nu,\omega)\sigma|^2, \qquad \|\mathcal{K}(\nu,\omega)\| \le C_K$$

for each $(\nu,\omega,\sigma) \in \mathbb{R}_+ \times S^{n-1} \times \mathbb{S}^{m-1}$.

Kalman Rank Condition (R): For each $(\nu,\omega)\in\mathbb{R}_+\times S^{n-1}$, the $2m^2\times m$ Kalman matrix has rank m, that is

$$\operatorname{rank}\begin{pmatrix} L^\sharp \\ L^\sharp\mathcal{A}(\nu,\omega) \\ \vdots \\ L^\sharp\mathcal{A}(\nu,\omega)^{m-1}\end{pmatrix}=m.$$

Theorem 2. *Suppose that the system* (1) *satisfies Condition* (A)*. Then, for the system* (1) (*and* (3))*, the following conditions are equivalent.*

(i) *Stability Condition* (SC) *holds.*
(ii) *Kalman Rank Condition* (R) *holds.*
(iii) *Craftsmanship Condition* (K) *holds.*
(iv) *All eigenvalues of* (3) *satisfy* $\mathrm{Re}\lambda(r,\omega)<0$ *for each* $(r,\omega)\in\mathbb{R}_+\times S^{n-1}$.

Furthermore, if $n=1$*, the above four conditions are equivalent to the following.*

(v) *All eigenvalues of* (3) *satisfy* $\mathrm{Re}\lambda(r,\omega)\lesssim -\dfrac{r^{2(m-1)}}{(1+r^2)^{2(m-1)}}$ *for each* $(r,\omega)\in\mathbb{R}_+\times S^{n-1}$.

We remark that the same result is obtained in the case $n\geq 2$ when we suppose the additional assumption. The cndition (v) in Theorem 2 gives the following pointwise estimates for solutions in Fourier space.

Theorem 3. *Suppose the same assumptions as in Theorem 2 and Condition* (R)*. Then the solutions to* (2) *with the intial data satisfy the following pointwise estimate in Fourier space.*

$$|\hat{u}(t,\xi)|\leq Ce^{-c\rho(\xi)t}|\hat{u}_0(\xi)| \tag{5}$$

with

$$\rho(\xi):=\begin{cases}\dfrac{|\xi|^{2(m-1)}}{(1+|\xi|^2)^{2(m-1)}} & \text{if} \quad A(\omega)\not\equiv O,\quad L^\flat\neq O,\\ \dfrac{|\xi|^2}{1+|\xi|^2} & \text{if} \quad A(\omega)\not\equiv O,\quad L^\flat= O,\\ 1 & \text{if} \quad A(\omega)\equiv O,\quad L^\flat\neq O,\end{cases} \tag{6}$$

where c *and* C *are certain positive constants, and* $\hat{u}_0$ *denotes the initial data of* (2) *in Fourier space.*

Furthermore, using the standard argument, Theorem 3 gives the following decay estimates for soltuions.

Corollary 4. *Suppose that the solutions satisfy the pointwise estimate* (5) *with* (6) *in Fourier space. Then the corresponding solutions to* (1) *with the initial data satisfy the following decay estimates.*

$$\begin{aligned}\|\partial_x^k u(t)\|_{L^2}&\leq C(1+t)^{-\frac{n}{4(m-1)}-\frac{k}{2(m-1)}}\|u_0\|_{L^1}\\ &\quad + C(1+t)^{-\frac{\ell}{2(m-1)}}\|\partial_x^{k+\ell}u_0\|_{L^2} \quad \text{if } A(\omega)\not\equiv O,\ L^\flat\neq O,\\ \|\partial_x^k u(t)\|_{L^2}&\leq C(1+t)^{-\frac{n}{4}-\frac{k}{2}}\|u_0\|_{L^1}+Ce^{-ct}\|\partial_x^k u_0\|_{L^2} \quad \text{if } A(\omega)\not\equiv O,\ L^\flat= O,\\ |u(t,x)|&\leq Ce^{-ct}|u_0(x)| \quad \text{if } A(\omega)\equiv O,\ L^\flat\neq O\end{aligned}$$

for $k \geq 0$ and $\ell \geq 0$, where c and C are certain positive constants.

The equivalences of (i), (ii) and (iv) in Theorem 2 are obtained by the Cayley–Hamilton theorem and the contradiction argument discussed in Ueda [7]. The key condition is Kalman Rank Condition (R) to obtain (v) in Theorem 2. More precisely, we construct the Lyapunov function for (2) and employ Condition (R) to derive (v), which is explained later. On the other hand, we will construct the compensating matrix $\mathcal{K}$ from Condition (R) and lead to (iv) in Theorem 2 by using the energy method.

Ueda-Duan-Kawashima [8, 9] studied the dissipaitve structure for the system (1) and introduced the compensating matrices concerned with $\mathcal{K}$. Their argument is different from the argument of this talk. However, their results and argument will help to derive the optimality of the condition in Theorem 2.

2. Lyapnov function

In this section, we state the key lemma to prove Theorem 2. Precisely, we introduce the Lyapunov function for (2). To this end, we give a preparation. Let κ be a small positive number. Then we introduce κ_k for $k = 0, 1, \cdots, m$ such that

$$\begin{aligned} &0 = \kappa_0 < \kappa_1 < \cdots < \kappa_m, \\ &\kappa_k - \frac{1}{2}(\kappa_{k-1} + \kappa_{k+1}) \geq \kappa > 0, \quad k = 0, 1, \cdots, m-1. \end{aligned} \tag{7}$$

Then we construct the useful Lyapunov function as follows.

Lemma 5. *Define the Lyapnov function for the system* (2) *that*

$$\mathcal{E}(\hat{u}) := \langle A^0 \hat{u}, \hat{u} \rangle + \delta h(|\xi|, \omega) \sum_{k=1}^{m-1} \varepsilon^{\kappa_k} \frac{\mathrm{Im} \langle L^\sharp \mathcal{A}(|\xi|, \omega)^{k-1} \hat{u}, L^\sharp \mathcal{A}(|\xi|, \omega)^k \hat{u} \rangle}{\|\mathcal{A}(|\xi|, \omega)\|^{2k}}$$

for $\delta > 0$ and $\varepsilon > 0$, where κ_k is introduced in (7) *and*

$$h(|\xi|, \omega) := \frac{\|\mathcal{A}(|\xi|, \omega)\|^2}{(\|\mathcal{A}(|\xi|, \omega)\| + \|(A^0)^{-1}\| \|L^\sharp\|)^2}.$$

Then, under Condition (A), *there exist positive constants δ_0 and ε_0 such that*

$$\frac{d}{dt}\mathcal{E}(\hat{u}) + c_0 |L^\sharp \hat{u}|^2 + c_1 h(|\xi|, \omega) \sum_{k=1}^{m-1} \varepsilon^{\kappa_k} \frac{|L^\sharp \mathcal{A}(|\xi|, \omega)^k \hat{u}|^2}{\|\mathcal{A}(|\xi|, \omega)\|^{2k}} \leq 0$$

and

$$c_* |\hat{u}|^2 \leq \mathcal{E}(\hat{u}) \leq C_* |\hat{u}|^2,$$

provided by $\delta = \delta_0$ and $0 < \varepsilon \leq \varepsilon_0$, where c_0, c_1, c_* and C_* are certain positive constants.

Remark 6. *In Lemma 5, the constants are defined explicitly. More precisely, we can take*

$$\delta_0 = \frac{1}{(1 + C_m)\|L^\sharp\|}, \quad \varepsilon_0 = \min\left\{1, \left(\frac{1}{2(m - 1 + C_m)}\right)^{1/\kappa}, \left(\frac{1 + C_m}{m - 1}\right)^{1/\kappa}\right\},$$

$$c_0 = \frac{1}{\|L^\sharp\|}, \ c_1 = \frac{1}{2(1 + C_m)\|L^\sharp\|}, \ c_* = \frac{1}{2\|(A^0)^{-1}\|}, \ C_* = \|A^0\| + \frac{1}{2\|(A^0)^{-1}\|}$$

to get the estimates in Lemma 5, where C_m is defined by

$$C_m := 1 + \frac{m}{2} \max_{0 \le k \le m-1} \left\{ \binom{m}{m-k}^2 \|A^0\|^{m-k} \|(A^0)^{-1}\|^{m-k} \right\}.$$

The proof of Lemma 5 is based on the Cayley–Hamilton theorem. Remark that we do not need to use Condition (R) to derive Lemma 5. We can derive Theorem 3 by using Condition (R) and Lemma 5.

References

[1] K. Beauchard and E. Zuazua, *Large time asymptotics for partially dissipative hyperbolic systems*, Arch. Rational Mech. Anal., **199** (2011), 177–227.

[2] K. Ide, K. Haramoto and S. Kawashima, *Decay property of regularity-loss type for dissipative Timoshenko system*, Math. Models Meth. Appl. Sci., **18** (2008), 647–667.

[3] K. Ide and S. Kawashima, *Decay property of regularity-loss type and nonlinear effects for dissipative Timoshenko system*, Math. Models Meth. Appl. Sci., **18** (2008), 1001–1025.

[4] R. Racke and Y. Ueda, *Dissipative structures for thermoelastic plate equations in $\mathbb{R}^n$*, Adv. Differential Equations, **21** (2016), no.7-8, 601–630.

[5] J.E. Muñoz Rivera and R. Racke, *Global stability for damped Timoshenko systems*, Discrete Contin. Dyn. Syst., **9** (2003), 1625–1639.

[6] Y. Shizuta and S. Kawashima, *Systems of equations of hyperbolic-parabolic type with applications to the discrete Boltzmann equation*, Hokkaido Math. J., **14** (1985), 249–275.

[7] Y. Ueda: *New stability criterion for the dissipative linear system and analysis of Bresse system*, Symmetry **10** (2018), no.11, 542.

[8] Y. Ueda, R. Duan, and S. Kawashima, *Decay structure for symmetric hyperbolic systems with non-symmetric relaxation and its application*, Arch. Rational Mech. Anal. **205** (2012), 239–266.

[9] Y. Ueda, R. Duan, and S. Kawashima, *New structural conditions on decay property with regularity-loss for symmetric hyperbolic systems with non-symmetric relaxation*, J. Hyperbolic Differ. Equ. **15**(1) (2018), 149–174.

[10] Y. Ueda and S. Kawashima, *Decay property of regularity-loss type for the Euler-Maxwell system*, Methods Appl. Anal., **18** (2011), no.3, 245–267.

[11] Y. Ueda, S. Wang and S. Kawashima, *Dissipative structure of the regularity-loss type and time asymptotic decay of solutions for the Euler-Maxwell system*, SIAM J. Math. Anal., **44** (2012), no.3, 2002–2017.

[12] T. Umeda, S. Kawashima and Y. Shizuta, *On the decay of solutions to the linearized equations of electro-magneto-fluid dynamics*, Japan J. Appl. Math., **1** (1984), 435–457.

Blow-up analysis for nodal radial solutions in Trudinger-Moser critical equations in $\mathbb{R}^2$

Daisuke Naimen (Muroran Institute of Technology)

1 Introduction

We consider the following elliptic problem.

$$\begin{cases} -\Delta u = \lambda u e^{u^2+|u|^{1+\varepsilon}} & \text{in } B, \\ u = 0 & \text{on } \partial B, \end{cases} \tag{1.1}$$

where $B \subset \mathbb{R}^2$ is a ball centered at the origin with radius 1. Moreover we assume $\lambda > 0$ and $\varepsilon \in (0,1)$. Due to the nonlinearity with exponential growth of the form e^{u^2}, we can regard (1.1) as a critical equation in dimension two. Our aim is to investigate the blow up behaviour of radial nodal (i.e., sign-changing) solutions of (1.1) as $\varepsilon \to 0$.

(1.1) relates to the critical embedding of the Sobolev space $H_0^1(\Omega)$ where $\Omega \subset \mathbb{R}^2$ is a smooth bounded domain. From earlier works by Pohozaev [15] and Trudinger [17], we know that for any $u \in H_0^1(\Omega)$, $\int_\Omega e^{u^2} dx < \infty$ and the exponential growth e^{u^2} is sharp. After that, Moser [13] sharpened the result above by proving that

$$\sup_{\|u\|_{H_0^1(\Omega)} \le 1} \int_\Omega e^{\alpha u^2} dx \begin{cases} < \infty & \alpha \le 4\pi, \\ = \infty & \alpha > 4\pi. \end{cases}$$

This is called the Trudinger-Moser inequality. Here we note that in the critical case $\alpha = 4\pi$, this maximization problem lacks the compactness and thus, to consider the existence of the maximizer is very interesting question. For the answer, we refer the readers to previous works by Carlson-Chang [6] when Ω is ball and Flucher [7] for general bounded domain case. An

interesting point is that they prove the existence of a maximizer. This fact is very different from that in the critical embedding in higher dimension.

Now, we focus our attention to a critical equation in dimension two. By the results noted above, a critical equation in dimension two is given by the problem of the form

$$\begin{cases} -\Delta u = f(u)e^{u^2} & \text{in } \Omega, \\ u = 0 & \text{on } \partial\Omega, \end{cases} \tag{1.2}$$

where $f : \mathbb{R} \to \mathbb{R}$ is a subcritical perturbation, that is, it satisfies that for all $\beta > 0$, $\lim_{|t|\to\infty} f(t)/e^{\beta t^2} = 0$. For a while, we assume $f(u) = \lambda u$ with a parameter $\lambda > 0$ for simplicity. In view of the lack of the compactness of the Trudinger-Moser inequality, to study the existence and asymptotic behaviour of solutions of (1.2) is nontrivial and interesting. First, Adimurthi [1] proves that for any $\lambda \in (0, \lambda_1)$ there exists a (least energy) positive solution u_λ of (1.2) where $\lambda_1 > 0$ is the first eigenvalue of $-\Delta$ on Ω. Furthermore by the works by [14], [3] and [2], we get that u_λ exhibits the concentration phenomenon as $\lambda \to 0$ and, after a suitable scaling, its asymptotic profile is given by the solution of the Liouville problem

$$-\Delta u = e^u \text{ in } \mathbb{R}^2, \quad \int_{\mathbb{R}^2} e^u dx < +\infty.$$

Moreover, Druet [9] shows that the energy of any $H_0^1(\Omega)$–bounded sequence of solutions must converge to a sum of $2\pi k$ with some number $k \in \mathbb{N} \cup \{0\}$ and the energy of the weak limit. Hence, we observe the energy quantization phenomenon as was observed in higher dimensional critical problem [16]. After that, for any $k \in \mathbb{N}$, delPino-Musso-Ruf [8] obtain a sufficient condition under which (1.2) admits a positive solution u_λ whose energy converges to $2\pi k$ as $\lambda \to 0$. In particular, by their result, if Ω is not simply connected, we can get a positive solution u_λ whose energy converges to 4π as $\lambda \to 0$. This gives a specific example of the result by [9] noted above with $k = 2$. More recently, Druet-Thizy [10] consider any $H_0^1(\Omega)$–bounded solution u_λ as $\lambda \to \lambda^* \geq 0$ and sharpened the result by [9] by showing that if $\lambda^* > 0$, $u_\lambda \to u_{\lambda^*} \neq 0$ in $C^2(\overline{\Omega})$ and if $\lambda^* = 0$, $k \neq 0$ and the weak limit u_{λ^*} of u_λ is trivial. In particular, they show that the concentration can not appear with the nontrivial weak limit.

2 Main result

Since the results above are mainly given for only positive solutions, we want to extend them to the sign-changing case. To do this, let us assume $f(u) = \lambda u e^{u^2+|u|^{1+\varepsilon}}$ in (1.2). Notice that we multiply the standard nonlinearity $\lambda u e^{u^2}$ by a subcritical perturbation $e^{|u|^{1+\varepsilon}}$. This is natural and essential if we want to consider the sing-changing solutions. Indeed, Adimurthi-Yadava [4] obtain a sing–changing solution of (1.2) for all $\lambda \in (0, \lambda_1)$ and $\varepsilon \in (0, 1)$. Furthermore, they also prove that if Ω is a ball, for any $\varepsilon \in [-1, 0]$, there exists a constant $\lambda_* = \lambda_*(\varepsilon)$ such that (1.2) does not admit any nodal radial solution for all $\lambda \in (0, \lambda_*)$ [5]. Now, we can find a natural and interesting question as follows. We fix $\lambda \in (0, \lambda_*(0))$. Then let us investigate the asymptotic behaviour of the nodal radial solution u_ε of (1.1) with $\varepsilon \in (0, 1)$ as $\varepsilon \to 0$. Since no nodal radial solution exists for $\varepsilon = 0$, we should observe a concentration phenomenon. We are interested in the energy and the asymptotic profile of them. Our main result is the following. We first show the global behaviour.

Theorem 2.1 (Global behavior [12]). *Let $\lambda \in (0, \min\{\lambda_*(0), \lambda_1\})$ and u_ε be a nodal radial solution to (1.1) with $\varepsilon \in (0, 1)$ obtained by [4] which changes the sign exactly k times, i.e. there exist values $0 = r_{0,\varepsilon} < r_{1,\varepsilon} < r_{2,\varepsilon} < \cdots < r_{k,\varepsilon} < r_{k+1,\varepsilon} = 1$ such that $u_\varepsilon(x) = 0$ if and only if $|x| = r_{i,\varepsilon}$ $(i = 1, \cdots, k+1)$. Moreover assume $u_0 > 0$ is the least energy solution of (1.1) with $\varepsilon = 0$. Then we have $\|u_\varepsilon\|_\infty \to \infty$ and further*

$$u_\varepsilon \to (-1)^k u_0 \quad \text{in } C^2_{loc}(B \setminus \{0\}),$$

and

$$I_\varepsilon(u_\varepsilon) \to 2\pi k + I_0(u_0)$$

as $\varepsilon \to 0$ where $f_\varepsilon(t) := \lambda t e^{t^2+|t|^{1+\varepsilon}}$, $F_\varepsilon(t) := \int_0^t f_\varepsilon(s)ds$ and

$$I_\varepsilon(u) := \frac{1}{2}\int_B |\nabla u|^2 dx - \int_B F_\varepsilon(u)dx \quad \left(u \in H^1_0(B)\right).$$

Note that u_ε exhibits the energy quantization phenomenon as is observed for the positive solutions [9]. An interesting point is that, it concentrates with the nontrivial weak limit. It is a very different point from the fact on positive solutions by [10] noted above. Next let us check the local behaviour.

Theorem 2.2 (Local behavior [12]). *Assume as in Theorem 2.1 and let* $u_\varepsilon = u_\varepsilon(r)$ $(r \in [0,1])$. *Moreover, for* $i = 1, \dots, k$, *let* $u_{i,\varepsilon} = u_\varepsilon|_{(r_{i-1,\varepsilon}, r_{i,\varepsilon})}$ *and* $r^*_{i,\varepsilon} \in [r_{i-1,\varepsilon}, r_{i,\varepsilon})$ *be such that* $|u_{i,\varepsilon}(r^*_{i,\varepsilon})| = ||u_{i,\varepsilon}||_{L^\infty((r_{i-1,\varepsilon}, r_{i,\varepsilon}))}$. *Then if we set* $\delta_{i,\varepsilon} = r_{i,\varepsilon}\gamma_{i,\varepsilon}$ *where* $\gamma_{i,\varepsilon} > 0$ *is defined by*

$$2\lambda r^2_{i,\varepsilon} e^{||u_{i,\varepsilon}||^2_{L^\infty((r_{i-1,\varepsilon}, r_{i,\varepsilon}))} + ||u_{i,\varepsilon}||^{1+\varepsilon}_{L^\infty((r_{i-1,\varepsilon}, r_{i,\varepsilon}))}} ||u_{i,\varepsilon}||_{L^\infty((r_{i-1,\varepsilon}, r_{i,\varepsilon}))} \gamma^2_{i,\varepsilon} = 1,$$

we have that $r_{i,\varepsilon} \to 0$, $||u_{i,\varepsilon}||_{L^\infty((r_{i-1,\varepsilon}, r_{i,\varepsilon}))} \to \infty$, $\delta_{i,\varepsilon} \to 0$ *and*

$$2\|u_{i,\varepsilon}\|_{L^\infty((r_{i-1,\varepsilon}, r_{i,\varepsilon}))}(|u_{i,\varepsilon}\left(r^*_{i,\varepsilon} + \delta_{i,\varepsilon} r\right)| - \|u_{i,\varepsilon}\|_{L^\infty((r_{i-1,\varepsilon}, r_{i,\varepsilon}))}) \\ \to \log \frac{1}{\left(1 + \frac{r^2}{8}\right)^2} \quad \text{in } C^2_{loc}(0, +\infty).$$

as $\varepsilon \to 0$ *for any* $i = 1, \dots, k$. *Furthermore, for* $u_{k+1,\varepsilon} := u_\varepsilon|_{(r_{k,\varepsilon}, 1)}$ *with zero extension, we get* $u_{k+1,\varepsilon} \in H^1_0(B)$ *and* $u_{k+1,\varepsilon} \to (-1)^k u_0$ *in* $H^1_0(B)$ *as* $\varepsilon \to 0$.

We observe that the limit profile of each concentration part is described by the solution of the Liouville problem. This is the same phenomenon with that for the positive solutions. An interesting point is that $u_{k+1,\varepsilon}$, the solution on outer annulus, exhibits a compactness phenomenon. It implies that u_ε is decomposed by k concentration parts with a compactness part. We here observe the "mixed" behaviour on u_ε. Finally we check the outline of the proof.

3 Outline of the proof

Here we give a key energy estimate. Noting the variational characterization for u_ε by [4] and using the Moser function [A], a concentrating test function whose energy converges to 2π, we can show the following.

Lemma 3.1. *We have*

$$\limsup_{\varepsilon \to 0} I_\varepsilon(u_\varepsilon) \le 2\pi k + I_0(u_0).$$

Note that we know $I_0(u_0) \in (0, 2\pi)$ by [1]. Then, since each concentration part should use the energy 2π, we can expect that u_ε can have k concentration parts but can not have $k+1$ concentration parts. This gives a reason why we can observe the compact phenomenon. Now, since the energy of u_ε is bounded, we can prove the following by noting the nonexistence result by [5].

Lemma 3.2. *We see*

$$r_{i,\varepsilon} \to 0 \ \textit{as} \ \varepsilon \to 0$$

and

$$|u_{i,\varepsilon}(r^*_{i,\varepsilon})| \to \infty.$$

for all $i = 1, 2, \cdots, k$.

Moreover, based on lemmas above, by the concentration compactness argument, we can get the next precise energy estimate.

Lemma 3.3. *We get for all* $i = 1, 2, \cdots, k$,

$$\lim_{\varepsilon \to 0} I_\varepsilon(u_{i,\varepsilon}) = 2\pi$$

and

$$\lim_{\varepsilon \to 0} I_\varepsilon(u_{k+1,\varepsilon}) = I_0(u_0)(< 2\pi).$$

In particular, we find that the energy of $u_{k+1,\varepsilon}$ does not attain the standard blow up level 2π. Based on this fact, we can prove the compactness of $u_{k+1,\varepsilon}$ by the standard concentration compactness argument. Hence the rest of the proof is to show the limit profile of each concentration part. Here, notice that $u_{1,\varepsilon}$ can be regarded as a positive solution on a (shrinking) ball. Hence we can easily reduce the proof to that in the previous work on positive solutions [2]. The important step is to consider $u_{i,\varepsilon}$ for $i = 2, \cdots, k$ which is defined on shrinking annulus. In this case, we need to avoid a possibility for the concentration part to converge to the singular Liouville equation observed in [11]. The proof is based on a blow–up argument in [11] and our energy estimate (Lemma 3.3). Then we finally deduce that the limit profile is given by the classical Liouville problem.

References

[1] Adimurthi, Existence of positive solutions of the semilinear Dirichlet problem with critical growth for the n-Laplacian, Ann. Scuola Norm. Sup. Pisa Cl. Sci. (4) 17 (1990) 393-413.

[2] Adimurthi and O. Druet, Blow-up analysis in dimension 2 and a sharp form of Trudinger-Moser inequality, Comm. in PDE. 29 (2004) 295-322.

[3] Adimurthi and M. Struwe, Global compactness properties of semilinear elliptic equations with critical exponential growth, J. Funct. Anal. 175 (2000) 125-167.

[4] Adimurthi and S.L. Yadava, Multiplicity results for semilinear elliptic equations in a bounded domain of $\mathbb{R}^2$ involving critical exponents. Ann. Scuola Norm. Sup. Pisa Cl. Sci. (4) 17 (1990) 481-504.

[5] Adimurthi and S.L. Yadava, Nonexistence of Nodal Solutions of Elliptic Equations with Critical Growth in $\mathbb{R}^2$, Trans. Amer. Math. Soc. 332 (1992) 449-458.

[6] L. Carleson, A. Chang, On the existence of an extremal function for an inequality of J. Moser, Bull. Sci. Math. 110 (1986) 113-127.

[7] M. Flucher, Extremal functions for the Trudinger-Moser inequality in 2 dimensions, Comment. Math. Helv. 67 (1992) 471-497.

[8] M. del Pino, M. Musso and B. Ruf, New solutions for Trudinger-Moser critical equations in $\mathbb{R}^2$, J. Funct. Anal. 258 (2010) 421-457.

[9] O. Druet, Multibumps analysis in dimention 2: quantification of blow-up levels, Duke Math. J. 132 (2006) 217-269.

[10] O. Druet and P. T. Thizy, Multi-bumps analysis for Trudinger-Moses nonlinearities I-Quantification and location of concentration points, to appear in J. Eur. Math. Soc.

[11] M. Grossi, C. Grumiau and F. Pacella, Lane Emden problems with large exponents and singular Liouville equations, Jour. Math. Pures Appl. (2014) 101 735-754.

[12] M. Grossi and D. Naimen, Blow-up analysis for nodal radial solutions in Moser-Trudinger critical equations in $\mathbb{R}^2$, to appear in Ann. Scuola Norm. Sup. Pisa Cl. Sci.

[13] J.K. Moser, A sharp form of an inequality by N. Trudinger, Indiana Univ. Math. J. 20 (1971) 1077-1092.

[14] T. Ogawa and T. Suzuki, Two-dimensional elliptic equation with critical nonlinear growth, Trans. Amer. Math. Soc. 350 (1998) 4897-4918.

[15] S. I. Pohozaev, The Sobolev embedding in the case $pl = n$, Proc. of the Technical Scientific Conference on Advances of Scientific Research 1964-1965, Mathematics Section (Moskov. Energet. Inst., Moscow) (1965) 158-170.

[16] M. Struwe, A global compactness result for elliptic boundary value problems involving limiting nonlinearities, Math. Z. 18 (1984) 511-517.

[17] N.S. Trudinger, On imbeddings into Orlicz spaces and some applications, J. Math. Mech. 17 (1967) 473-483.

Graph Ginzburg–Landau: discrete dynamics, continuum limits, and applications. An overview

Yves van Gennip
Delft Institute of Applied Mathematics (DIAM)
Technische Universiteit Delft
Delft, The Netherlands

1 Introduction

In [BF12, BF16] the graph Ginzburg–Landau functional,

$$F_\varepsilon(u) := \frac{\varepsilon}{2}\sum_{i,j\in V}\omega_{ij}(u_i-u_j)^2 + \frac{1}{\varepsilon}\sum_{i\in V}W(u_i), \tag{1}$$

was introduced. Here u is a real-valued function on the node set V of a simple[1], undirected graph (with u_i its value at node i), $\omega_{ij}\geq 0$ are edge weights which are assumed to be positive on all edges in the graph and zero between non-neighbouring nodes i and j, ε is a positive parameter, and W is a double well potential with wells of equal depth. A typical choice is the quartic polynomial $W(x)=x^2(x-1)^2$ which has wells of depth 0 at $x=0$ and $x=1$, but we will encounter some situations where other choices are useful or even necessary.

This introduction of this graph-based functional was inspired by its continuum counterpart,

$$\mathcal{F}_\varepsilon(u) := \varepsilon\int_\Omega |\nabla u|^2\,dx + \frac{1}{\varepsilon}\int_\Omega W(u)\,dx, \tag{2}$$

which was introduced into the materials science literature to model phase separation (such as the separation of oil and water) [CH58], but has since been extensively used in the image processing literature as well, because of its intimate connection to the total variation functional, which we will explore further below. In $\mathcal{F}_\varepsilon(u)$ above, u is a real-valued function on a domain $\Omega\subset\mathbb{R}^n$ and ε and W are as before. For small positive values of ε, minimization of $\mathcal{F}_\varepsilon$ will lead to functions u which take values close to the wells of W (say 0 and 1) while keeping the L^2 norm of the gradient small. Minimizers of $\mathcal{F}_\varepsilon$[2] tend to have regions where $u\approx 0$ and regions where $u\approx 1$, with transition regions in between whose length is (approximately) minimal and whose thickness is of order ε.

The study of a graph-based version of the Ginzburg–Landau functional in [BF12] was motivated by the translation of the phase separating behaviour of its continuum counterpart $\mathcal{F}_\varepsilon$ into node clustering behaviour on a graph. Forcing the double well potential term to have a small value has the same effect as before: It drives u to take values close to 0 or 1. The term $\sum_{i,j}\omega_{ij}(u_i-u_j)^2$ encourages u to take similar values on those nodes which are connected by a highly weighted edge. These two effects together result in a function u which can be interpreted as a labelling function which indicates which of two clusters a node in the graph belongs to, based on the (weighted) structure of the graph. Combined with either an additional fidelity term in the functional, which weakly enforces compatibility of the final result with a priori known

[1] We call a graph simple if it has no self-loops and at most one edge between each pair of nodes.

[2] Careful readers will have noted that minimizers of $\mathcal{F}_\varepsilon$ are given by constant functions which take value 0 everywhere or value 1 everywhere. In practice $\mathcal{F}_\varepsilon$ is always minimized with some additional term or constraint present as we will see shortly.

data, or a hard mass constraint (if the desired cluster sizes are known), the graph Ginzburg–Landau functional was sucessfully used in [BF12] for various data clustering and classification[3] and image segmentation[4] tasks.

The method used in [BF12] to minimize the graph Ginzburg–Landau functional again took its inspiration from a practice which is common in the world of continuum variational methods[5]: using a gradient flow. This approach consists of introducing an artificial time parameter and computing a solution to $u_t = -\operatorname{grad} F_\varepsilon$. For the graph Ginzburg–Landau functional, this leads to the graph Allen–Cahn equation,

$$\frac{d}{dt}u_i = -\varepsilon(\Delta u)_i - \frac{1}{\varepsilon}W'(u_i) \tag{3}$$

which earns its name due to its great similarity to the (continuum) Allen–Cahn equation[6], which is the L^2 gradient flow of $\mathcal{F}_\varepsilon$ [AC79]. In the equation above we have used the suggestive notation

$$(\Delta u)_i := \sum_j \omega_{ij}(u_i - u_j). \tag{4}$$

In fact, the object in (4) has been extensively studied by the field of spectral graph theory [Chu97] and is known as the (combinatorial) graph Laplacian.

In [MKB13] a second method was devised for (approximately) minimizing the graph Ginzburg–Landau functional: the graph Merriman–Bence–Osher (MBO) scheme. Also this method took its inspiration from an existing continuum method. The MBO scheme (or threshold dynamics scheme) was originally introduced as a method for approximating flow by mean curvature [MBO92, MBO93]. It consists of alternatively diffusing the indicator function of a set and thresholding the diffused result back to an indicator function. On a graph, this gives rise to the following iterative scheme:

$$\begin{aligned}
u_i^0 = (\chi_S)_i &:= \begin{cases} 1, & \text{if } i \in S, \\ 0, & \text{if } i \in S^c, \end{cases} \\
u^{n+\frac{1}{2}} &\text{ solves} \\
&\begin{cases} u(0) = u^n, \\ \frac{d}{dt}u_i = -(\Delta u)_i, \quad \text{on } (0,\tau], \end{cases} \\
u^{n+1} &= \begin{cases} 1, & \text{if } u^{n+\frac{1}{2}}(\tau) \geq \frac{1}{2}, \\ 0, & \text{if } u^{n+\frac{1}{2}}(\tau) < \frac{1}{2}. \end{cases}
\end{aligned} \tag{5}$$

On an intuitive level, one can think of the thresholding step (going from $u^{n+\frac{1}{2}}$ to u^n) as (approximately) mimicking the effect of the nonlinear term $-\frac{1}{\varepsilon}W'(u_i)$ in the Allen–Cahn equation. The MBO scheme is usually easier to implement than the nonlinear Allen–Cahn equation.

Both the Allen–Cahn and MBO approach have been used successfully for various applications in later papers, e.g. [HLPB13, MKB13, GCMB+14, HSB15, CvGS+17, MBC18], and for the former convergence has been proven [LB17]. At the end of this overview paper we will

[3] Data clustering refers to the process of grouping data points together without a priori knowledge of the classes —except perhaps class size– while data classification refers to that process using such prior knowlwedge.

[4] Image segmentation is the process of extracting specific structures from an image. For a digital image this can be interpreted to mean clustering or classification of the image's pixels.

[5] Variational methods broadly refer to the practice of modelling a system as the minimizer of a given function(al).

[6] Note that the minus sign in the Laplacian term is not a mistake: Different from the continuum Laplacian, the graph Laplacian is positive semi-definite.

discuss some of these applications, but first we will dive deeper into the theoretical understanding of the Ginzburg–Landau functional and its related dynamics that has been built since the functional's introduction in [BF12]. These theoretical studies can roughly be divided into two categories: those that are concerned with the functional or the dynamics on the discrete graph level and those that try to bridge the gap between the discrete and continuum worlds. In Section 2 we take a look at the former and in Section 3 we discuss the latter. In Section 4 we give an overview of some applications of these methods.

2 Discrete dynamics

The graph Laplacian which we discussed above is an important operator when studying discrete dynamics on graphs. As is well known from spectral graph theory [Chu97], the spectral properties of the graph Laplacian tell us important information about the properties of the underlying graph (such as its number of connected components). Conversely, any graph dynamics driven by the graph Laplacian will be highly dependent on the graph structure.

It is somewhat misleading to talk about *the* graph Laplacian, as there are different versions of the discrete Laplacian that appear in the literature. To understand their differences, we need to consider the node degree

$$d_i := \sum_{j \in V} \omega_{ij}.$$

The three most commonly encountered graph Laplacians are the combinatorial graph Laplacian defined above, the random walk graph Laplacian, which has an additional factor d_i^{-1} on the right hand side compared to the combinatorial graph Laplacian in (4), and the symmetrically normalised graph Laplacian $d_i^{-1/2} \sum_j \omega_{ij} \left(d_i^{-1/2} u_i - d_j^{-1/2} u_j \right)$.

Where we encountered the combinatorial graph Laplacian in the dynamics above, we can also consider versions which use the random walk or symmetrically normalised graph Laplacian. In fact, by introducing the parameter r, we can capture both the combinatorial ($r = 0$) and random walk Laplacians ($r = 1$) in the same definition:

$$(\Delta u)_i := d_i^{-r} \sum_j \omega_{ij}(u_i - u_j). \tag{6}$$

Taking the gradient flow of the graph Ginzburg–Landau functional with respect to the topology generated by the inner product

$$\langle u, v \rangle_{\mathcal{V}} := \sum_{i \in V} u_i v_i d_i^r$$

on the space of real-valued node functions $\mathcal{V} := \{u : V \to \mathbb{R}\}$, naturally leads to an Allen–Cahn equation which uses the generalised definition of the graph Laplacian from (6)[7]. The symmetrically normalised Laplacian cannot be incorporated in this framework and we will not consider it further here.

The two main discrete dynamics that are studied in the context of the graph Ginzburg–Landau functional are those generated by the graph Allen–Cahn equation and the graph MBO scheme which are explained in the previous section. For both of their continuum counterparts it is known that they approximate flow by mean curvature in a sense that can be made precise in the form of various limiting arguments. In its geometric formulation, (continuum) flow by

[7] Using this inner product, the Allen–Cahn gradient flow also picks up a factor d_i^{-r} in the $\frac{1}{\varepsilon} W'(u_i)$ term. Alternatively, we can redefine the double well potential term in F_ε to be $\frac{1}{\varepsilon} \langle W \circ u, \chi_V \rangle_{\mathcal{V}}$, in which case the gradient flow remains unchanged as in (3). Both choices appear in the literature.

mean curvature of a Euclidean subset is obtained by letting its boundary evolve with a normal velocity at each point proportional to the boundary's curvature at that point [Bra78, AC79]. The possibility of singularity formation during this process has given rise to different formulations of continuum flow by mean curvature, such as the level set description [CGG91, ES91, ES92a, ES92b, ES95]. In [BK91] and [ESS92] it was proven that solutions of the continuum Allen–Cahn equation converge (when $\varepsilon \to 0$) to solutions of the continuum flow by mean curvature. The first paper does this in the radial case (where flow by mean curvature is well understood), while the second shows that the Allen–Cahn solutions converge to viscosity solutions of the level set equation for continuum flow by mean curvature. Also solutions of the continuum MBO scheme converge to solutions of the continuum flow by mean curvature (in some appropriate senses) when $\tau \to 0$ [Eva93, BG95].

It is therefore reasonable to ask if similar connections can be found between the various discrete dynamics. In particular the following questions have been considered: (a) Are the graph Allen–Cahn equation and MBO scheme related and if so, how? (b) Can a graph-based flow by mean curvature be defined in a way that preserves important properties of its continuum counterpart? Specifically, (c) are the graph Allen–Cahn equation and MBO scheme approximations of graph based flow by mean curvature in any rigorous sense?

In [vGGOB14] these questions were first asked and, in the case of question (b), partly answered. In [vGGOB14] (and its sequel [vG19]) a graph-based version of the variational formulation for flow by mean curvature, which was originally given by [ATW93, LS95] in the continuum, was introduced[8]: Given an initial node set S_0, a discrete time step ($\Delta t > 0$) sequence of node sets evolving by graph-based mean curvature flow is defined by

$$S_n \in \operatorname*{argmin}_{S \subset V} \mathrm{TV}(\chi_S) + \frac{1}{\Delta t}\langle \chi_S, \mathrm{sd}_{n-1}\rangle_{\mathcal{V}}. \tag{7}$$

Here sd_{n-1} is a signed distance to the set S_{n-1} from the previous iteration and the graph total variation is defined as

$$\mathrm{TV}(u) := \frac{1}{2}\sum_{i,j \in V} \omega_{ij}|u_i - u_j|.$$

In particular, we note that

$$\mathrm{TV}(\chi_S) = \sum_{\substack{i \in S \\ j \in S^c}} \omega_{ij} \tag{8}$$

is the graph cut between the node subset S and its complement (a concept known from graph theory).

Above we have been a bit vague in defining the signed distance sd_{n-1}. This was done on purpose, as it is still a topic of ongoing research what influence the choice of distance has on the resulting flow. In [vGGOB14] the signed distance was taken to the boundary of the set S_{n-1}, which was defined to be the union of the set of nodes in S which have a neighbour in S^c and the set of nodes in S^c which have a neighbour in S. While this definition gives rise to a well-defined flow on a given graph and is an obvious discretisation of the continuum distance used in [ATW93, LS95], it is unstable with respect to small perturbations in the graph structure. Consider 'completing' a given graph by adding an edge with a very small positive

[8] In the same paper, also a graph-based (mean) curvature,

$$(\kappa_S)_i := d_i^{-r} \begin{cases} \sum_{j \in S^c} \omega_{ij}, & \text{if } i \in S, \\ -\sum_{j \in S} \omega_{ij}, & \text{if } i \in S^c, \end{cases}$$

was introduced, with the property that $\mathrm{TV}(\chi_S) = \langle \kappa_S, \chi_S \rangle_{\mathcal{V}}$.

weight between every pair of non-neighbouring nodes. If we expect flow by mean curvature to resemble a diffusion generated process, as per our question (c) above, such a small perturbation of the edge weights should not have a large impact on the resulting flow. This perturbation however, does have a major impact on the boundaries of node subsets: For any nonempty proper subset of V, every node in the graph is now in its boundary. This suggests that to be able to answer question (c) positively, a different notion of distance needs to be employed in the definition of graph flow by mean curvature. This is a subject of current research by the author and coauthors.

It should also be noted that the variational approach to flow by mean curvature on graphs is different from the 'partial difference equation on graphs' approach in [ECED14].

Most progress has been made on question (a): How are the graph MBO scheme and Allen–Cahn equation related? The answer, as given in [BvGepa], is that MBO corresponds to a specific time discretisation of Allen–Cahn, with some important caveats which we will address below.

First we will redefine the graph Allen–Cahn equation slightly:

$$\frac{d}{dt}u = -\Delta u - \frac{1}{\varepsilon}W' \circ u.$$

Comparing this with (3) we see that ε is lacking from the Laplacian term. The ε has been removed with an eye to the limiting behaviour for $\varepsilon \to 0$ which we will discuss in more detail below. From the point of view of the discrete dynamics, we can simply interpret this as a rescaling of time.

We partly discretise the Allen–Cahn equation above with a time step τ: We treat the diffusion term continuously in time, while using an implicit Euler discretisation for the potential term:

$$u^{k+1} = e^{-\tau\Delta}u^k - \frac{\tau}{\varepsilon}W' \circ u^{k+1}. \tag{9}$$

We note that $e^{-\tau\Delta}u_k$ is the solution at time τ of the graph diffusion equation $\frac{d}{dt}u = -\Delta u$ with initial condition u^k. This time discretisation addresses one obvious difference between the Allen–Cahn equation and MBO scheme: The former is continuous in time, while each iteration of the latter generates outputs at discrete times. The second immediately noticeable discrepancy between these two dynamics, is that MBO produces binary ($\{0,1\}$-valued) results at a given node in each iteration, while solutions of the Allen–Cahn equation a priori can have any real value at a node. To deal with this, we change the (discretised) Allen–Cahn equation further: Instead of using a continuous function W as double well potential, such as the quartic polynomial given above, we use the double obstacle potential:

$$W(x) := \begin{cases} \frac{1}{2}x(1-x), & \text{if } x \in [0,1], \\ +\infty, & \text{otherwise.} \end{cases}$$

The non-smoothness of this potential requires us to interpret W' in a subdifferential way. This is done rigorously in [BvGepa], where it is concluded that for $\lambda := \frac{\tau}{\varepsilon} = 1$, the iterates of (9) are the same as the iterates of the graph MBO scheme (5). Moreover, every sequence $\tau_n \to 0$ has a subsequence whose corresponding sequence of solutions to (9) converges pointwise to a solution of the graph Allen–Cahn equation (3). If $0 < \lambda < 1$ the iterates of (9) correspond to an MBO-like scheme with a relaxed thresholding step, in which the hard thresholding step function is replaced by a piecewise linear continuous approximation. This allows the semi-discrete scheme to avoid pinning[9] in certain situations, which can be of practical interest.

[9] In this context, pinning describes the trivial dynamics which can occur in the MBO scheme when τ is so small that at every node the value of $u^{n+\frac{1}{2}}$ is on the same side of $\frac{1}{2}$ as in u^n and thus $u^{n+1} = u^n$ and no more changes occur. For more information, see [vGGOB14, vG19].

In [BvGepb] the above procedure, which relates the graph Allen–Cahn equation to the graph MBO scheme, is applied to a version of the Allen–Cahn equation with an additional term which assures that mass is conserved along iterates (where the mass of a node function is defined to be $\mathcal{M}(u) := \sum_{i\in V} d_i^r u_i$). The resulting mass preserving MBO scheme corresponds to a version of the one introduced in [vG18] for (approximately) minimizing the pattern forming Ohta–Kawasaki functional on graphs.

We close this section with a quick return to question (c). Even though the search for an explicit relationship between the graph Allen–Cahn equation and MBO scheme on the one hand and graph flow by mean curvature on the other is still open, there are some preliminary results worth mentioning in this context. These results are also of interest in their own right and are formulated in the language of Γ-convergence.

The notion of Γ-convergence is specifically tailored to minimization problems. Its precise definition can be found in any of the standard works on the topic [Bra02, DM93] and we will not repeat it here. For our present purposes it is enough to remember the main result which makes this a worthwhile concept: If a sequence of function(al)s (f_n) Γ-converges to a limit function f_∞ and (x_n) is a sequence such that x_n minimizes f_n, then every limit point of (x_n) is a minimizer of f_∞.

In [vGB12] it was proven that the graph Ginzburg–Landau functionals $\frac{1}{\sqrt{\varepsilon}}F_{\sqrt{\varepsilon}}$[10] Γ-converge (when $\varepsilon \to 0$) to a limit functional that takes the value $\mathrm{TV}(u)$ when $u = \chi_S$ for some node set S and $+\infty$ otherwise. This mirrors a well-known result from [MM77, Mod87] which states that in the continuum the functionals $\mathcal{F}_\varepsilon$ Γ-converge (when $\varepsilon \to 0$) to a limit functional that is equal to the total variation on indicator functions and $+\infty$ otherwise.

Because flow by mean curvature is defined in (7) via (approximate) minimization of total variation (and because the first variation of total variation is graph curvature in the sense of footnote 8), this limiting result which connects the functional which generates the Allen–Cahn equation as a gradient flow to the total variation teases a connection between Allen–Cahn and flow by mean curvature on graphs.

A similarly promising Γ-convergence result is formulated for the graph MBO scheme in [vG18]. To understand this result, we need to consider the Lyapunov functional for the graph MBO scheme, introduced in [vGGOB14] (following the introduction of a similar functional for the continuum MBO scheme in [EO15]):

$$J_\tau(u) := \langle 1 - u, e^{\tau\Delta} u\rangle_{\mathcal{V}}.$$

This is a Lyapunov functional for the graph MBO scheme, in the sense that $k \mapsto J(u^k)$ is non-increasing if (u^k) is a sequence of iterates generated by the graph MBO scheme in (5). Moreover, these iterates can also be obtained as minimizers of the first variation of J_τ:

$$u^{k+1} \in \operatorname*{argmin}_v dJ_\tau(v; u^k), \quad \text{where} \quad dJ_\tau(v; u^k) = \langle 1 - 2e^{-\tau\Delta u^k}, v\rangle_{\mathcal{V}}.$$

The minimization is over $[0,1]$-valued node functions v. We thus see that, at nodes where $1-2^{-\tau\Delta u^k} < 0$, minimization of $dJ_\tau(v; u^{k+1})$ forces v to take the value 1 at that node. Similarly, at nodes where $1 - 2^{-\tau\Delta u^k} > 0$ the function v will take value 0. Hence, we recover the MBO scheme (up to the underdetermined value at nodes where $1 - 2^{-\tau\Delta u^k} = 0$).

In [vG18] it was proven that $\frac{1}{\tau}J_\tau$ Γ-converges to the same limit functional we encountered as Γ-limit of $\frac{1}{\sqrt{\varepsilon}}F_{\sqrt{\varepsilon}}$ (when $\varepsilon \to 0$), i.e. the functional which is equal to $\mathrm{TV}(u)$ when $u = \chi_S$ for some node set S and $+\infty$ otherwise. For the same reasons as above, this is a promising sign that also the graph MBO scheme has links to flow by mean curvature.

[10] The rescaling $\frac{1}{\sqrt{\varepsilon}}F_{\sqrt{\varepsilon}}$ amounts to removing the ε prefactor from the first term in (1). The reason for this is that, contrary to the corresponding term in the continuum functional $\mathcal{F}_\varepsilon$, this discrete gradient term is finite even for binary functions u and so no rescaling with ε is needed to keep this term finite in the limit $\varepsilon \to 0$.

3 Continuum limits

In the previous section we discussed dynamics and some Γ-convergence results at a discrete level: All the dynamics and convergence results happened against the fixed background of a given finite graph. We can also consider the question what happens if we let the graphs change in such a way that we can reasonably talk about continuum limits.

We will discuss here three different ways to consider graph limits: Γ-convergence along a sequence of graphs generated through mesh refinements; Γ-convergence along a sequence of graphs generated through sampling; and graphon limits. The results and papers discussed in this section typically consider W to be a smooth double well potential, such as the quartic polynomial given in Section 1[11].

In [vGB12] a sequence of 4-regular graphs is generated by refining a regular mesh on the flat torus. Identifying the torus with $[0,1]^2$ (with periodic boundary conditions) it can be discretised by a square grid with horizontal and vertical spacing $\frac{1}{N}$, such that the resulting graph will have N^2 points. Choosing the edge weights $\omega_{ij} = \frac{1}{N}$ on all edges of this square grid, we denote the resulting graph Ginzburg–Landau functional (obtained from $\frac{1}{\sqrt{\varepsilon}} F_{\sqrt{\varepsilon}}$ in (1); see footnote 10) by $F_{\varepsilon,N}$. By choosing $\varepsilon = N^{-\alpha}$ for $\alpha > 0$ large enough (depending on the growth rate of W near its wells) and letting $N \to \infty$, $F_{\varepsilon,N}$ is shown to Γ-converge to a functional which is equal to the anistropic total variation for $\{0,1\}$-valued functions of bounded variation (and $+\infty$ otherwise), with the anisotropies aligned with the horizontal and vertical directions of the grid: $\int |u_x| + |u_y| \, dx$.

The paper [vGB12] also considers a second sequence of discrete Ginzburg–Landau functionals generated by directly discretising the continuum Ginzburg–Landau functional in (2) using forward finite differences for the gradient and equidistant Riemann sums for the integrals. This leads to a different scaling in the discrete functional: The gradient term has a factor ε (where this was N^{-1} in $F_{\varepsilon,N}$) and the potential term a factor $\varepsilon^{-1}N^{-2}$ (which was ε^{-1} in $F_{\varepsilon,N}$). Again setting $\varepsilon = N^{-\alpha}$, but this time with $\alpha > 0$ small enough (depending on the polynomial growth of W') a different Γ-limit is recovered: a functional which is proportional[12] to the standard isotropic total variation $\int |\nabla u| \, dx$ for $\{0,1\}$-valued functions of bounded variation (and $+\infty$ otherwise). We see that the graph functional $F_{\varepsilon,N}$ retains information about the structure of the graph (the horizontal and vertical directions of its grid) even in the limit, while the discrete functional which is obtained using standard discretisation techniques from numerical analysis does not retain this information (as one would want for consistency of a numerical method).

An important step in deriving the discrete-to-continuum results in [vGB12] discussed above is the identification of the graph-based functions with continuum-based functions, as the setup of Γ-convergence requires the domain of the functionals along the sequence, $F_{\varepsilon,N}$, to agree with the domain of the limit functional. This is done by identifying the graph-based functions with their piecewise constant extensions, which is possible because the grid structure of the graph gives a tesselation of $[0,1]^2$. The next type of discrete-to-continuum Γ-convergence results we discuss here use a different technique which can be used in less regularly structured situations.

In [GTS16], the authors consider a sequence of graphs constructed by sampling ever more points X_i (which serve as the graphs' vertices) from $D \subset \mathbb{R}^d$ according to some measure ν and constructing an edge structure via the weights $\omega_{ij} := \varepsilon^{-d}\eta(|X_i - X_j|/\varepsilon)$, where η is some given kernel (which can be taken to have compact support if complete graphs are to be avoided). The identification of functions defined on such graphs with functions defined on D is accomplished using ideas from optimal transport theory. The key idea is not to consider graph-based functions

[11] Which is not to say these result could not be generalised to include non-smooth potentials such as the double obstacle potential considered in Section 2.

[12] With proportionality factor depending on the explicit form of W.

u_n and continuum-based functions u by themselves, but look at function-measure pairs (μ_n, u_n), (μ, u), with $u_n \in L^p(D, \mu_n)$ and $u \in L^p(D, \mu)$ and express convergence using a transportation distance between such pairs:

$$d_{TL^p}((\mu_n, u_n), (\mu, u))^p := \inf_{\pi \in \Gamma(\mu_n, \mu)} \int_D \int_D (|x - y|^p + |u_n(x) - u(y)|^p) \, d\pi(x, y),$$

where $\Gamma(\mu_n, \mu)$ denotes the set of all Borel measures on $D \times D$ whose marginal on the first variable is μ_n and whose marginal on the second variable is μ. By letting $\mu_n := \frac{1}{n} \sum_{i=1}^n \delta_{X_i}$, the empirical measure supported at the sampled points, this provides the discrete-to-continuum identification needed to make sense of Γ-convergence statements.

This tool was used in [GTS16] to prove that a rescaled graph total variation, $\varepsilon^{-1} n^{-2} \mathrm{TV}$, on such sampled graphs as described above, Γ-converges[13] to a constant (depending on η) times a weighted continuum total variation, with the weight depending on the sampling measure ρ:

$$\mathrm{TV}(u; \rho^2) := \sup \left\{ \int_D u \operatorname{div} \phi \, dx : \forall x \in D \ |\phi(x)| \leq \rho^2(x), \phi \in C_c^\infty(D, \mathbb{R}^d) \right\}.$$

These discrete-to-continuum indentification methods have since been used in a series of papers to prove discrete-to-continuum Γ-convergence results for many different functionals, including the Ginzburg–Landau functional [TSVB$^+$16, TKSSA17, TS18, ST19, TvG].

A third and final approach to discrete-to-continuum graph limits that should be mentioned here, is that of graphons [LS06, BCL$^+$08, BCL$^+$11, BCL$^+$12, Gla15] (see [BCCL18] and references therein for recent generalisations), as applied in various recent papers [Med14, HFE18b, HFE18a]. A graphon is a measurable symmetric function K on $[0, 1]^2$. By partitioning $[0, 1]$ into n intervals of length $\frac{1}{n}$ and defining edge weights $w_{ij}^n := n^2 \int_{[\frac{i}{n}, \frac{i+1}{n}) \times [\frac{j}{n}, \frac{j+1}{n})} K(x, y) \, dx \, dy$, every graphon gives rise to a sequence of simple unweighted graphs. Conversely, any simple unweighted graph $G = (V(G), E(G))$ with $|V(G)| = n$ can be identified with a graphon by setting

$$K(x, y) := \begin{cases} 1, & \text{if } (i, j) \in E(G) \text{ and } (x, y) \in [\frac{i}{n}, \frac{i+1}{n}) \times [\frac{j}{n}, \frac{j+1}{n}), \\ 0, & \text{otherwise.} \end{cases}$$

A sequence of simple graphs (G_n) is called convergent if $t(F, G_n)$ is convergent for all simple graphs F, where

$$t(F, G_n) := \frac{\hom(F, G_n)}{|V(G_n)|^{|V(F)|}}$$

is the density of homomorphisms (i.e. adjacency preserving maps from $V(F)$, the vertex set of F, to $V(G_n)$, the vertex set of G_n). It is a fundamental result in the study of graphons that for each convergent sequence of simple graphs (G_n) there exists a graphon K such that, for all simple graphs F,

$$t(F, G_n) \to t(F, K) := \int_{[0,1]^{|V(F)|}} \prod_{(i,j) \in E(F)} K(x_i, x_j) \, dx.$$

In [HFE18a] convergence (with error estimates) of minimizers is proved for a discrete functional consisting of an ℓ^2 fidelity term plus the discrete gradient term from F_ε[14]. These minimizers are

[13] Where $\varepsilon \to 0$ slow enough as $n \to \infty$ for the sampled graphs to be connected with high probability.

[14] The paper considers the more general case where the gradient term has a power $p \in [1, \infty)$ instead of 2.

shown to converge to the minimizer of a continuum functional with a similar L^2 fidelity term and the L^2 norm[15] of the nonlocal gradient[16]

$$\nabla_K u(x,y) := K(x,y)^{1/2}(u(y) - u(x)),$$

where the kernel K is determined as graphon limit of the graphs determined by the edge weight matrices in the gradient term along the discrete sequence. To the best knowledge of the author, the graphon approach has not yet been applied to the graph Ginzburg–Landau functional.

4 Applications

The applications of PDE-inspired methods on graphs are numerous, even when we restrict ourselves to those which directly use (variants of) the graph Ginzburg–Landau functional. In this section we present a short selection of such applications.

One of the applications studied in [BF12, BF16] is image segmentation in the presence of some a priori information. A graph is constructed from a digital image in the following way: Each pixel in the image is represented by a node in the graph. A weighted edge structure is created via $\omega_{ij} := e^{||z_i - z_j||^2/\sigma^2}$, where z_i is a feature vector associated with pixel i. In simple cases, such a feature vector consists of the nine grey values of the pixels in the three by three window around the pixel (or the values from a larger window; or, in the case of colour images or hyperspectral images, the $9c$ intensity values, where c is the number of colour/spectral channels in the image), but it can also incorporate, say, texture filters. In principle such an edge weight is computed for each pair of pixels (i, j) in the graph, but since this is computationally unfeasible in practice, [BF12, BF16] proposes to use the Nyström matrix completion technique [Nys28, Nys29, BFCM02, FBCM04] which approximates the full weight matrix based on a sampled subset of pairs. The a priori known pixel assignments are incorporated into the functional via a fidelity term. The resulting Allen–Cahn equation with fidelity term is solved by combining a convex splitting method with a projection onto the top eigenvectors of the graph Laplacian (which in turn makes the Nyström method even more valuable, as it allows for a quick computation of the top eigenvectors and eigenvalues, without the need to compute the full weight matrix). In [BF12, BF16] the same method is also applied to other data classification and clustering methods, which each require their own context specific graph construction (and fidelity terms or mass constraints), but can all be tackled with the same general Allen–Cahn/Nyström approach. In [CvGS+17] this same method was incorporated into an image segmentation and measurement method developed to be employed in zoological research (specifically for the automated detection and measurement of the blaze (white spot) on a bird's head in pictures). It should also be mentioned here that image segmentation can be achieved through other PDE-inspired graph-based methods as well, see for example [ELT16] and references therein.

The Ginzburg–Landau based method for image segmentation and data clustering and classification has been adapted and extended to allow for multiple phases [GCMB+13, GCFP13, MGCB+14, GCMB+14, GCFP15], high-dimensional data (such as hyperspectral images) [HLB12, HSB15, MMK17], and computation with the MBO scheme instead of the Allen–Cahn equation [MKB13]. It has also proven useful for clustering signed graphs, i.e. graphs in which the edge weights can have negative, as well as non-negative, values, with the (highly) negatively weighted edges connecting pairs of nodes that should not be clustered together [CPvG]. In this case the MBO scheme uses a signed graph Laplacian, which is the sum of a regular graph Laplacian on the graph induced by the positively weighted edges and a signless Laplacian (see (10) below) on the graph induced by the negatively weighted edges.

[15] Or L^p norm.

[16] Or $Ku(x,y) := K(x,y)^{1/p}(u(y) - u(x))$.

We end with an application which uses a variant of the graph Ginzburg–Landau functional: (approximate) computation of the maximum cut of a graph. A classic task in graph theory [Kar72, GJS74, PT95] (with some applications in physics and engineering [BGJR88, DL94a, DL94b, EJR03, MM06, GM19]) is to find the maximum value the graph cut from (8) can have, if we allow S to be any subset of the graph's vertex set. To tackle this task, in [KvG] the signless graph Ginzburg–Landau functional is introduced:

$$F_\varepsilon^+(u) := \frac{\varepsilon}{2} \sum_{i,j \in V} \omega_{ij}(u_i + u_j)^2 + \frac{1}{\varepsilon} \sum_{i \in V} W(u_i).$$

Note that the only apparent difference between F_ε^+ and F_ε is the plus sign instead of the minus sign in (what in F_ε was) the discrete gradient term of the functional. There is, however, a significant second difference: While in F_ε the specific placement of the two wells of W was not very important (we chose the well locations to be at 0 and 1 to make their connection to indicator functions of node sets more immediate), in F_ε^+ it is important that the wells are placed symmetrically with respect to the origin, e.g. $W(x) := (x-1)^2(x+1)^2$ with wells located at ± 1. The reason for this is that we want minimizers of F_ε^+ (without any further constraints imposed) to be (approximately) binary and not just constant functions equal to, say, 0.

Heuristically it quickly can be seen that in minimizing F_ε^+, the first term encourages u to take different values in strongly connected nodes, thereby leading to high graph cut values. While any hard guarantees of this kind (which are unlikely, given that accurately solving the maximum cut problem is NP-hard [TSSW00]) or even lower bound guarantees on the performance of the method (how close are minimizers to a maximum cut?) are lacking, in practice the method gives results that are competitive with those of the well-established Goemans–Williamson method [GW95].

The practical (approximate) minimization of F_ε^+ is achieved via a variant of the MBO scheme, which uses a signless graph Laplacian [DR94, HS04, CRS07, JC$^+$10, BH11],

$$(\Delta^+ u)_i := d_i^{-r} \sum_j \omega_{ij}(u_i + u_j), \tag{10}$$

instead of one of the usual graph Laplacians. This method is faster and scales to much larger graphs than the Goeman–Williamsion method on the same hardware. An extension of these methods to mulitple phases is in development by the authors of [KvG].

5 Conclusions

In this overview article we have looked at multiple appearances of the graph Ginzburg–Landau functional (and related concepts) in both theoretical studies and applications in recent literature. It is a paradigmatic example of a variational method on graphs which is inspired by ideas, concepts, and results from the area of continuum variational methods, and which has been very successfully applied in various practical contexts, yet is also still a central object in an area of active study.

Acknowledgements Thanks to Jeremy Budd for his feedback and comments on an earlier draft of this document.

References

[AC79] Samuel M. Allen and John W. Cahn, *A microscopic theory for antiphase boundary motion and its application to antiphase domain coarsening*, Acta Metallurgica **27** (1979), no. 6, 1085–1095.

[ATW93] Fred Almgren, Jean E. Taylor, and Lihe Wang, *Curvature-driven flows: a variational approach*, SIAM J. Control Optim. **31** (1993), no. 2, 387–438. MR 1205983 (94h:58067)

[BCCL18] Christian Borgs, Jennifer T Chayes, Henry Cohn, and László Miklós Lovász, *Identifiability for graphexes and the weak kernel metric*, preprint arXiv:1804.03277 (2018).

[BCL+08] Christian Borgs, Jennifer T Chayes, László Lovász, Vera T Sós, and Katalin Vesztergombi, *Convergent sequences of dense graphs i: Subgraph frequencies, metric properties and testing*, Advances in Mathematics **219** (2008), no. 6, 1801–1851.

[BCL+11] Christian Borgs, Jennifer Chayes, László Lovász, Vera Sós, and Katalin Vesztergombi, *Limits of randomly grown graph sequences*, European Journal of Combinatorics **32** (2011), no. 7, 985–999.

[BCL+12] Christian Borgs, Jennifer T Chayes, László Lovász, Vera T Sós, and Katalin Vesztergombi, *Convergent sequences of dense graphs ii. multiway cuts and statistical physics*, Annals of Mathematics **176** (2012), no. 1, 151–219.

[BF12] Andrea L. Bertozzi and Arjuna Flenner, *Diffuse interface models on graphs for analysis of high dimensional data*, Multiscale Modeling and Simulation **10** (2012), no. 3, 1090–1118.

[BF16] ———, *Diffuse interface models on graphs for classification of high dimensional data*, SIAM Review **58** (2016), no. 2, 293–328.

[BFCM02] Serge Belongie, Charless Fowlkes, Fan Chung, and Jitendra Malik, *Spectral partitioning with indefinite kernels using the nyström extension*, European conference on computer vision, Springer, 2002, pp. 531–542.

[BG95] Guy Barles and Christine Georgelin, *A simple proof of convergence for an approximation scheme for computing motions by mean curvature*, SIAM J. Numer. Anal. **32** (1995), no. 2, 484–500.

[BGJR88] Francisco Barahona, Martin Grötschel, Michael Jünger, and Gerhard Reinelt, *An application of combinatorial optimization to statistical physics and circuit layout design*, Operations Research **36** (1988), no. 3, 493–513.

[BH11] Andries E. Brouwer and Willem H. Haemers, *Spectra of graphs*, Springer Science & Business Media, 2011.

[BK91] Lia Bronsard and Robert V. Kohn, *Motion by mean curvature as the singular limit of Ginzburg-Landau dynamics*, J. Differential Equations **90** (1991), no. 2, 211–237. MR 1101239 (92d:35037)

[Bra78] Kenneth A. Brakke, *The motion of a surface by its mean curvature*, Mathematical Notes, vol. 20, Princeton University Press, Princeton, N.J., 1978. MR 485012 (82c:49035)

[Bra02] A. Braides, Γ*-convergence for beginners*, first ed., Oxford Lecture Series in Mathematics and its Applications, vol. 22, Oxford University Press, Oxford, 2002.

[BvGepa] Jeremy Budd and Yves van Gennip, *Deriving graph MBO as a semi-discrete implicit euler scheme for graph allen–cahn.*

[BvGepb] ———, *Mass preserving diffusion-based dynamics on graphs.*

[CGG91] Yun Gang Chen, Yoshikazu Giga, and Shun'ichi Goto, *Uniqueness and existence of viscosity solutions of generalized mean curvature flow equations*, Journal of differential geometry **33** (1991), no. 3, 749–786.

[CH58] John W. Cahn and John E. Hilliard, *Free energy of a nonuniform system. i. interfacial free energy*, The Journal of chemical physics **28** (1958), no. 2, 258–267.

[Chu97] Fan R. K. Chung, *Spectral graph theory*, CBMS Regional Conference Series in Mathematics, vol. 92, Published for the Conference Board of the Mathematical Sciences, Washington, DC, by the American Mathematical Society, Providence, Rhode Island, 1997. MR 1421568 (97k:58183)

[CPvG] Mihai Cucuringu, Andrea Pizzoferrato, and Yves van Gennip, *An MBO scheme for clustering and semi-supervised clustering of signed networks*, preprint arXiv 1901.03091.

[CRS07] Dragoš Cvetković, Peter Rowlinson, and Slobodan K Simić, *Signless Laplacians of finite graphs*, Linear Algebra and its applications **423** (2007), no. 1, 155–171.

[CvGS+17] Luca Calatroni, Yves van Gennip, Carola-Bibiane Schönlieb, Hannah M. Rowland, and Arjuna Flenner, *Graph clustering, variational image segmentation methods and hough transform scale detection for object measurement in images*, Journal of Mathematical Imaging and Vision **57** (2017), no. 2, 269–291.

[DL94a] Michel Deza and Monique Laurent, *Applications of cut polyhedra—I*, Journal of Computational and Applied Mathematics **55** (1994), no. 2, 191–216.

[DL94b] ———, *Applications of cut polyhedra—II*, Journal of Computational and Applied Mathematics **55** (1994), no. 2, 217–247.

[DM93] G. Dal Maso, *An introduction to Γ-convergence*, first ed., Progress in Nonlinear Differential Equations and Their Applications, vol. 8, Birkhäuser, Boston, 1993.

[DR94] Madhav Desai and Vasant Rao, *A characterization of the smallest eigenvalue of a graph*, Journal of Graph Theory **18** (1994), no. 2, 181–194.

[ECED14] Abdallah El Chakik, Abdderahim Elmoataz, and Xavier Desquesnes, *Mean curvature flow on graphs for image and manifold restoration and enhancement*, Signal Processing **105** (2014), 449–463.

[EJR03] Matthias Elf, Michael Jünger, and Giovanni Rinaldi, *Minimizing breaks by maximizing cuts*, Operations Research Letters **31** (2003), no. 5, 343–349.

[ELT16] Abderrahim Elmoataz, François Lozes, and Hugues Talbot, *Morphological pdes on graphs for analyzing unorganized data in 3d and higher*, 2016 IEEE Global Conference on Signal and Information Processing (GlobalSIP), IEEE, 2016, pp. 361–364.

[EO15] Selim Esedoḡlu and Felix Otto, *Threshold dynamics for networks with arbitrary surface tensions*, Communications on Pure and Applied Mathematics **68** (2015), no. 5, 808–864.

[ES91] L. C. Evans and J. Spruck, *Motion of level sets by mean curvature. I*, J. Differential Geom. **33** (1991), no. 3, 635–681. MR 1100206 (92h:35097)

[ES92a] ———, *Motion of level sets by mean curvature. II*, Trans. Amer. Math. Soc. **330** (1992), no. 1, 321–332. MR 1068927 (92f:58050)

[ES92b] ———, *Motion of level sets by mean curvature. III*, J. Geom. Anal. **2** (1992), no. 2, 121–150. MR 1151756 (93d:58044)

[ES95] Lawrence C. Evans and Joel Spruck, *Motion of level sets by mean curvature. IV*, J. Geom. Anal. **5** (1995), no. 1, 77–114. MR 1315658 (96a:35077)

[ESS92] Lawrence C Evans, H Mete Soner, and Panagiotis E Souganidis, *Phase transitions and generalized motion by mean curvature*, Communications on Pure and Applied Mathematics **45** (1992), no. 9, 1097–1123.

[Eva93] Lawrence C. Evans, *Convergence of an algorithm for mean curvature motion*, Indiana Univ. Math. J. **42** (1993), no. 2, 533–557.

[FBCM04] Charless Fowlkes, Serge Belongie, Fan Chung, and Jitendra Malik, *Spectral grouping using the Nyström method*, IEEE transactions on pattern analysis and machine intelligence **26** (2004), no. 2, 214–225.

[GCFP13] Cristina Garcia-Cardona, Arjuna Flenner, and Allon G. Percus, *Multiclass diffuse interface models for semi-supervised learning on graphs*, Proceedings of the 2nd International Conference on Pattern Recognition Applications and Methods (ICPRAM 2013), 2013, pp. 78–86.

[GCFP15] ———, *Multiclass semi-supervised learning on graphs using ginzburg-landau functional minimization*, Advances in Intelligent Systems and Computing **318** (2015), 119–135.

[GCMB+13] Cristina Garcia-Cardona, Ekaterina Merkurjev, Andrea L. Bertozzi, Arjuna Flenner, and Allon G. Percus, *Fast multiclass segmentation using diffuse interface methods on graphs*, Tech. report, DTIC Document, 2013.

[GCMB+14] Cristina Garcia-Cardona, Ekaterina Merkurjev, Andrea L. Bertozzi, Arjuna Flenner, and Allon Percus, *Multiclass data segmentation using diffuse interface methods on graphs*, IEEE Transactions on Pattern Analysis and Machine Intelligence **36** (2014), no. 8, 1600–1613.

[GJS74] Michael R Garey, David S Johnson, and Larry Stockmeyer, *Some simplified np-complete problems*, Proceedings of the sixth annual ACM symposium on Theory of computing, ACM, 1974, pp. 47–63.

[Gla15] Daniel Glasscock, *What is ... a graphon?*, Notices of the AMS **62** (2015), no. 1.

[GM19] Gian Giacomo Guerreschi and A. Y. Matsuura, *QAOA for Max-Cut requires hundreds of qubits for quantum speed-up*, Scientific reports **9** (2019), no. 1, 6903.

[GTS16] Nicolas García Trillos and Dejan Slepčev, *Continuum limit of total variation on point clouds*, Archive for Rational Mechanics and Analysis **220** (2016), 193–241.

[GW95] Michel X Goemans and David P Williamson, *Improved approximation algorithms for maximum cut and satisfiability problems using semidefinite programming*, Journal of the ACM (JACM) **42** (1995), no. 6, 1115–1145.

[HFE18a] Yosra Hafiene, Jalal Fadili, and Abderrahim Elmoataz, *Nonlocal p-Laplacian variational problems on graphs*, preprint arXiv:1810.12817 (2018).

[HFE18b] ———, *Nonlocal p-Laplacian evolution problems on graphs*, SIAM Journal on Numerical Analysis **56** (2018), no. 2, 1064–1090.

[HLB12] Blake Hunter, Yifei Lou, and Andrea L Bertozzi, *A spectral graph based approach to analyze hyperspectral data*, Proc. IEEE Appl. Imagery Pattern Recognit., 2012.

[HLPB13] Huiyi Hu, Thomas Laurent, Mason A Porter, and Andrea L Bertozzi, *A method based on total variation for network modularity optimization using the MBO scheme*, SIAM Journal on Applied Mathematics **73** (2013), no. 6, 2224–2246.

[HS04] Willem H. Haemers and Edward Spence, *Enumeration of cospectral graphs*, European Journal of Combinatorics **25** (2004), no. 2, 199–211.

[HSB15] Huiyi Hu, Justin Sunu, and Andrea L Bertozzi, *Multi-class graph Mumford-Shah model for plume detection using the MBO scheme*, Energy Minimization Methods in Computer Vision and Pattern Recognition, 2015, pp. 209–222.

[JC+10] Bao Jiao, Yang Chun, et al., *Signless Laplacians of finite graphs*, The 2010 International Conference on Apperceiving Computing and Intelligence Analysis Proceeding, IEEE, 2010, pp. 440–443.

[Kar72] Richard M Karp, *Reducibility among combinatorial problems*, Complexity of computer computations, Springer, 1972, pp. 85–103.

[KvG] Blaine Keetch and Yves van Gennip, *A Max-Cut approximation using a graph based MBO scheme*, to appear; preprint arXiv:1711.02419.

[LB17] Xiyang Luo and Andrea L. Bertozzi, *Convergence of the graph Allen-Cahn scheme*, Journal of Statistical Physics **167** (2017), no. 3, 934–958.

[LS95] Stephan Luckhaus and Thomas Sturzenhecker, *Implicit time discretization for the mean curvature flow equation*, Calc. Var. Partial Differential Equations **3** (1995), no. 2, 253–271. MR 1386964 (97e:65085)

[LS06] László Lovász and Balázs Szegedy, *Limits of dense graph sequences*, Journal of Combinatorial Theory, Series B **96** (2006), no. 6, 933–957.

[MBC18] Ekaterina Merkurjev, Andrea L Bertozzi, and Fan Chung, *A semi-supervised heat kernel pagerank MBO algorithm for data classification*.

[MBO92] B. Merriman, J. K. Bence, and S. Osher, *Diffusion generated motion by mean curvature*, UCLA Department of Mathematics CAM report CAM 06–32 (1992).

[MBO93] B. Merriman, J.K. Bence, and S. Osher, *Diffusion generated motion by mean curvature*, AMS Selected Letters, Crystal Grower's Workshop (1993), 73–83.

[Med14] Georgi S. Medvedev, *The nonlinear heat equation on dense graphs and graph limits*, SIAM Journal on Mathematical Analysis **46** (2014), no. 4, 2743–2766.

[MGCB+14] Ekaterina Merkurjev, Cristina Garcia-Cardona, Andrea L. Bertozzi, Arjuna Flenner, and Allon G. Percus, *Diffuse interface methods for multiclass segmentation of high-dimensional data*, Applied Mathematics Letters **33** (2014), 29–34.

[MKB13] E. Merkurjev, T. Kostic, and A. Bertozzi, *An MBO scheme on graphs for segmentation and image processing*, SIAM J. Imaging Sci. **6** (2013), no. 4, 1903–1930.

[MM77] L. Modica and S. Mortola, *Un esempio di Γ^--convergenza*, Bollettino U.M.I. **5** (1977), no. 14-B, 285–299.

[MM06] Ryuhei Miyashiro and Tomomi Matsui, *Semidefinite programming based approaches to the break minimization problem*, Computers & Operations Research **33** (2006), no. 7, 1975–1982.

[MMK17] Zhaoyi Meng, Ekaterina Merkurjev, Alice Koniges, and Andrea L. , *Hyperspectral Image Classification Using Graph Clustering Methods*, Image Processing On Line **7** (2017), 218–245.

[Mod87] Luciano Modica, *The gradient theory of phase transitions and the minimal interface criterion*, Arch. Rational Mech. Anal. **98** (1987), no. 2, 123–142. MR 866718 (88f:76038)

[Nys28] Evert Johannes Nyström, *Über die praktische Auflösung von linearen Integralgleichungen mit Anwendungen auf Randwertaufgaben der Potentialtheorie*, Commentationes Physico-Mathematicae **4** (1928), no. 15, 1–52.

[Nys29] ———, *Über die praktische Auflösung von linearen Integralgleichungen mit Anwendungen auf Randwertaufgaben der Potentialtheorie*, Akademische Buchhandlung, 1929.

[PT95] Svatopluk Poljak and Zsolt Tuza, *Maximum cuts and large bipartite subgraphs*, DIMACS Series **20** (1995), 181–244.

[ST19] Dejan Slepčev and Matthew Thorpe, *Analysis of p-Laplacian regularization in semisupervised learning*, SIAM Journal on Mathematical Analysis **51** (2019), no. 3, 2085–2120.

[TKSSA17] Nicolás Garcia Trillos, Zachary Kaplan, Thabo Samakhoana, and Daniel Sanz-Alonso, *On the consistency of graph-based bayesian learning and the scalability of sampling algorithms*, preprint arXiv:1710.07702 (2017).

[TS18] Nicolás Garcia Trillos and Dejan Slepčev, *A variational approach to the consistency of spectral clustering*, Applied and Computational Harmonic Analysis **45** (2018), no. 2, 239–281.

[TSSW00] Luca Trevisan, Gregory B. Sorkin, Madhu Sudan, and David P. Williamson, *Gadgets, approximation, and linear programming*, SIAM Journal on Computing **29** (2000), no. 6, 2074–2097.

[TSVB+16] Nicolás Garcia Trillos, Dejan Slepčev, James Von Brecht, Thomas Laurent, and Xavier Bresson, *Consistency of cheeger and ratio graph cuts*, The Journal of Machine Learning Research **17** (2016), no. 1, 6268–6313.

[TvG] Matthew Thorpe and Yves van Gennip, *Deep limits of residual neural networks*, preprint arXiv 1810.11741.

[vG18] Yves van Gennip, *An MBO scheme for minimizing the graph Ohta–Kawasaki functional*, Journal of Nonlinear Science (2018), 1–49.

[vG19] ———, *Graph MBO on star graphs and regular trees. With corrections to DOI 10.1007/s00032-014-0216-8*, Milan Journal of Mathematics **87** (2019), no. 1, 141–168.

[vGB12] Y. van Gennip and A. L. Bertozzi, *Γ-convergence of graph Ginzburg-Landau functionals*, Adv. Differential Equations **17** (2012), no. 11–12, 1115–1180.

[vGGOB14] Y. van Gennip, N. Guillen, B. Osting, and A. L. Bertozzi, *Mean curvature, threshold dynamics, and phase field theory on finite graphs*, Milan Journal of Mathematics **82** (2014), no. 1, 3–65.

Blowup of solutions to a system related to chemotaxis systems

Takasi Senba (Fukuoka University, Japan)

In this talk, we will consider solutions to parabolic systems related to Keller-Segel system.

First, we describe Keller-Segel system and some properties of solutions to the system. Keller-Segel system is the following system.

$$(KS)\begin{cases} u_t = \Delta u - \chi\nabla\cdot(u\nabla v) & \text{in } \Omega\times(0,T),\\ \tau v_t = \Delta v - v + u & \text{in } \Omega\times(0,T),\\ \dfrac{\partial u}{\partial \nu} - \chi u\dfrac{\partial v}{\partial \nu} = 0,\ v = 0 & \text{on } \partial\Omega\times(0,T),\\ u(\cdot,0) = u_0,\ v(\cdot,0) = v_0 & \text{in } \Omega. \end{cases}$$

Here, we assume the following.

- χ and τ are positive constants.
- $\Omega \subset \mathbf{R}^n$ $(n \geq 1)$ is bounded. The boundary $\partial\Omega$ is smooth.
- u_0 and v_0 are smooth and non-negative.
- T is the maximal existence time of the classical solution.

In this talk, we treat only classical solutions.

Keller-Segel system was introduced to describe the aggregation of living things. In the system, u represents the density of living thing, and v represents chemical concentration produced by the living thing, and the chemical substance is an attractant. That is to say, the relation between living thing and chemoattractant is direct. Then, we regard chemotaxis mentioned by classical Keller-Segel system as direct process.

Keller-Segel system has a critical number in two dimensional case. That is to say, the following properties hold.

Known properties on solutions to Keller-Segel system.

- $u \geq 0$, $v \geq 0$ in $\Omega\times(0,T)$.
- $\|u(t)\|_{L^1(\Omega)} = \|u_0\|_{L^1(\Omega)}$ in $[0,T)$.
- If $n = 1$ or "$n = 2$ and $\|u_0\|_{L^1(\Omega)} < 8\pi/\chi$", solutions exist globally in time and are uniformly bounded.
- If $n \geq 3$ or "$n = 2$ and $\|u_0\|_{L^1(\Omega)} > 8\pi/\chi$", there exist solutions blowing up.

Definition of blowup.
We say that a solution blows up at a time $T \in (0, \infty]$, if

$$\limsup_{t \to T} (\|u(t)\|_{L^\infty(\Omega)} + \|v(t)\|_{L^\infty(\Omega)}) = \infty.$$

In this talk, we consider the following system.

$$(PPP) \begin{cases} u_t = \Delta u - \chi \nabla \cdot (u \nabla v) & \text{in } \Omega \times (0,T), \\ \tau_1 v_t = \Delta v - v + w & \text{in } \Omega \times (0,T), \\ \tau_2 w_t = \Delta w - w + u & \text{in } \Omega \times (0,T), \\ \dfrac{\partial u}{\partial \nu} - \chi u \dfrac{\partial v}{\partial \nu} = 0, \ v = w = 0 & \text{on } \partial\Omega \times (0,T), \\ u(\cdot,0) = u_0, \ v(\cdot,0) = v_0, \ w(\cdot,0) = w_0 & \text{in } \Omega. \end{cases}$$

We assume the following.

- χ, τ_1 and τ_2 are positive constants.
- $\Omega \subset \mathbf{R}^n$ $(n \geq 1)$ is bounded. The boundary $\partial\Omega$ is smooth.
- u_0, v_0 and w_0 are smooth and nonnegative.
- T is the maximal existence time of the classical solution.

Then, we consider only classical solution also to our system.

This system is one of chemotaxis systems. u represents density of living thing, w represents chemical concentration and the chemical substance is produced by the living thing, and v also represents chemical concentration, the chemical substance is produced by reaction of chemical substance w, and the substance is attractant.

That is to say, u produces w, w produces v, and v stimulus u. Then, we consider chemotaxis mentioned by our system as indirect process.

Since our system is a parabolic system, then the following properties hold.

Fundamental properties on solutions to (PPP).
- $w \geq 0$, $w \geq 0$, $w \geq 0$ in $\Omega \times (0,T)$.
- $\|u(t)\|_{L^1(\Omega)} = \|u_0\|_{L^1(\Omega)}$ in $[0,T)$.
- There exists a unique time-local classical solution (u,v,w) to (P).

Definition of blowup to solutions to (PPP)
We say that a solution (u,v,w) to (P) blows up at a time $T \in (0, \infty]$, if

$$\limsup_{t \to T} (\|u(t)\|_{L^\infty(\Omega)} + \|v(t)\|_{L^\infty(\Omega)} + \|w(t)\|_{L^\infty(\Omega)}) = \infty.$$

Our system is a simplified version of the following system.

$$(FIWY)\begin{cases} u_t = \Delta u - \chi\nabla\cdot(u\nabla v) & \text{in } \Omega\times(0,\infty),\\ v_t = \Delta v + wz,\ z_t = \Delta z - z + u & \text{in } \Omega\times(0,\infty),\\ w_t = -\gamma wz & \text{in } \Omega\times(0,\infty),\\ \dfrac{\partial u}{\partial\nu} = \dfrac{\partial v}{\partial\nu} = \dfrac{\partial z}{\partial\nu} = 0 & \text{on } \partial\Omega\times(0,T),\\ u(0)=u_0, v(0)=v_0,\\ \qquad w(0)=w_0, z(0)=z_0 & \text{in } \Omega. \end{cases}$$

Here, we assume the following.
• χ and γ are positive constants.
• $\Omega\subset\mathbf{R}^n$ $(n\geq 1)$ is bounded. The boundary $\partial\Omega$ is smooth.
• u_0, v_0, w_0 and z_0 are nonnegative and smooth.

This system is one of tumor invasion models. Fujie, Ito, Winkler, Yokota (DCDS, '16) show that solutions to (FIWY) exist globally in time and are bounded, if $n\geq 3$.

Our aim is the construction of blowup solutions. However, it was shown that solutions are uniformly bounded in time, if $n\leq 3$. Then, we consider high dimensional case to find blowup solutions. Moreover, (FIWY) has a ordinal differential equation. The equation makes construction of blowup solutions difficult. Our system (PPP) is equal to (FIWY), if $\gamma = 0$. Then, we regard our system (PPP) as a simplified version of (FIWY).

Then, our problem is as follows.
Our problem. Find blowup solutions to (PPP).

A partial answer for this problem is as follows.

Theorem 1. [Fujie-S.(JDE, '17) (JDE, '19)]
(1) If Ω is a bounded domain of $\mathbf{R}^n$ and one of the following assumptions holds:

· "$n\leq 3$" or "$n=4$ and $\|u_0\|_{L^1(\Omega)} < (8\pi)^2/\chi$".

Then, solutions to our system (P) exist globally in time and are uniformly bounded in time.
(2) If Ω is a bounded and convex domain of $\mathbf{R}^4$, then there exist blowup solutions to our system (P) satisfying $\|u_0\|_{L^1(\Omega)} > (8\pi)^2/\chi$.

There exist blowup solutions in four dimensional case, and that in four dimensional case the number $(8\pi)^2/\chi$ is threshold. In this sense, the number $(8\pi)^2/\chi$ in four dimensional our system corresponds to the number $8\pi/\chi$ appearing in two dimensional Keller-Segel system.

We think that the assumption of convexity of domain is technical.

In the above results, we can not judge whether the blowup time is finite. However, we can construct solutions blowing up at a finite time.

Theorem 2.
If Ω is a bounded ball of $\mathbf{R}^4$, there exist radial solutions blowing up at a finite time T. Moreover, the solutions satisfy that

$$u(t) \to m(0)\delta_0 + f \quad \text{as } t \to T,$$

where $m(0) \geq (8\pi)^2/\chi$, $f \in L^1(\Omega)$ and δ_0 is the delta function whose support is the origin.

Our next problem is the investigation of blowup rate. In two dimensional Keller-Segel system, it is shown that any finite time blowup solution is of Type II.

Theorem (Mizoguchi (JFA, '16))
Let Ω be a bounded ball in $\mathbf{R}^2$. If radial solutions blow up at a finite time, the blowup is of Type II.

Here, we define Type I blowup and Type II blowup as follows.

Definition of Type I blowup and Type II blowup.
Let Ω be a bounded domain in $\mathbf{R}^n$ and let a solutions to (KS) or (PPP) blow up at a finite time T.

We say that a solution exhibits Type I blowup, if the solution satisfies that

$$\sup_{0<t<T} (T-t)^{n/2} \|u(t)\|_{L^\infty} < \infty.$$

We say that a solution exhibits Type II blowup, if the solution satisfies that

$$\limsup_{t \to T} (T-t)^{n/2} \|u(t)\|_{L^\infty} = \infty.$$

However, it is difficult for us to investigate the blowup rate for all blowup solutions to (PPP). Then, we consider the following parabolic-elliptic system, which is a simplified version of (PPP).

$$(PEE)\begin{cases} u_t = \Delta u - \chi\nabla\cdot(u\nabla v) & \text{in } \Omega\times(0,T),\\ 0 = \Delta v - v + w & \text{in } \Omega\times(0,T),\\ 0 = \Delta w - w + u & \text{in } \Omega\times(0,T),\\ \dfrac{\partial u}{\partial \nu} - \chi u\dfrac{\partial v}{\partial \nu} = 0,\ v = w = 0 & \text{on } \partial\Omega\times(0,T),\\ u(\cdot,0) = u_0 & \text{in } \Omega. \end{cases}$$

Here, we assume the following.

- χ is a positive constant.
- $\Omega \subset \mathbf{R}^4$ is a bounded ball.
- u_0 is smooth and nonnegative.

This system is equal to (PPP) with $\tau_1 = \tau_2 = 0$.

For radial solutions to (PEE), we get the following result, which is a partial answer for our problem.

Theorem 3. Let Ω be a bounded domain of $\mathbf{R}^4$ and let u_0 be nonnegative and smooth. Then, there exist solutions to (PEE) blowing up at a finite time and satisfying $\|u_0\|_{L^1(\Omega)} > (8\pi)^2/\chi$.

Furthermore, if Ω is a bounded ball in $\mathbf{R}^4$ and a radial solution blows up at a finite time T, the solution satisfies

$$u(\cdot,t) \to \frac{(8\pi)^2}{\chi}\delta_0 + f \quad \text{as } t\to T,$$
$$\limsup_{t\to T}(T-t)^2\|u(t)\|_{L^\infty(\Omega)} = \infty.$$

Here, δ_0 is the delta function at the origin, and f is a radial and nonnegative L^1 function.

Then, this result says that the blowup is of Type II, if radial solutions to the four dimensional simplified system blow up at a finite time.